Technical Report No. 12

July 1972

Water Quality in the Lower Colorado River and the Effect of Reservoirs

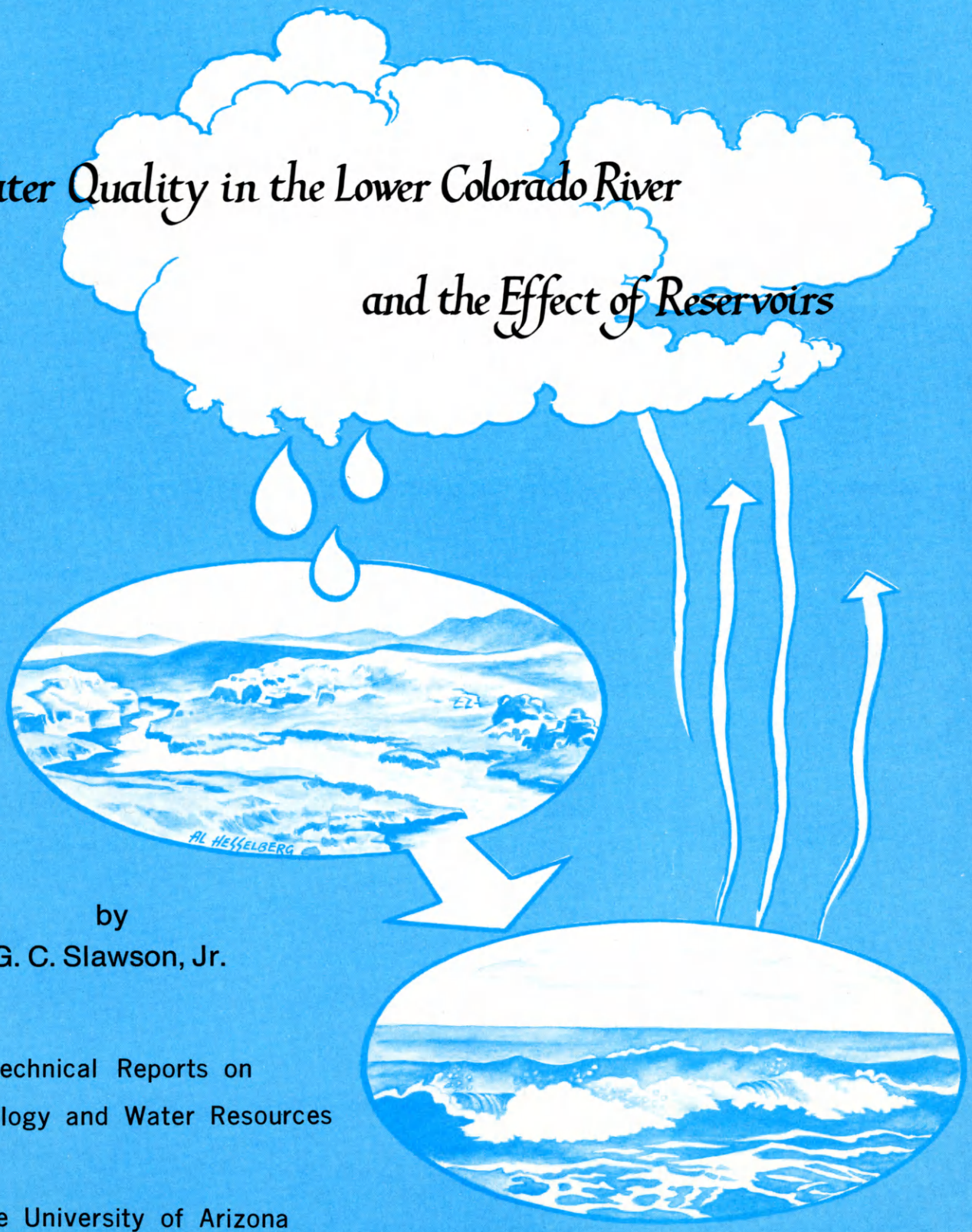

by

G. C. Slawson, Jr.

Technical Reports on
Hydrology and Water Resources

The University of Arizona
Tucson, Arizona 85721

WATER QUALITY IN THE LOWER COLORADO RIVER AND THE EFFECT OF RESERVOIRS

by

G. C. Slawson, Jr.

Report No. 12
July 1972

Reports on Natural Resource Systems
Department of Hydrology and Water Resources

University of Arizona
Tucson, Arizona 85721

PREFACE

This report constitutes the Master's thesis of the same title completed by the author in June, 1972. The thesis was written under the direction of Hasan K. Qashu, Associate Professor of Hydrology and Water Resources.

This study is a preliminary effort in evaluating the utility of time series analysis for estimating the impacts of developmental activities on salinity. It is part of a program which includes analytic and validation studies in cooperation with several agencies seeking to develop models for diagnosing water quality changes in the river and their relation to biotic and abiotic interactions.

The work upon which this report is based was supported by funds provided by the United States Bureau of Reclamation, Region 3, and by an Allotment Grant from the Water Resources Research Center of the University of Arizona.

ACKNOWLEDGMENTS

I wish to acknowledge the United States Bureau of Reclamation, Region 3, and the United States Geological Survey, Water Resources Division, Tucson, for making the data available; Dr. Hasan K. Qashu for the discussions and dialogues leading to this report; Dr. Chester C. Kisiel for providing help for more efficient use of the methodology; Dr. Simon Ince for revising the manuscript; and Dr. Lorne G. Everett whose studies on Lake Mead helped in better interpretation of some physical characteristics.

TABLE OF CONTENTS

TABLE OF CONTENTS--Continued

LIST OF ILLUSTRATIONS

LIST OF ILLUSTRATIONS--Continued

LIST OF ILLUSTRATIONS--Continued

LIST OF TABLES

ABSTRACT

Comparison of the power spectra of TDS time series from different locations on the Lower Colorado River is useful in showing changes in salinity and for indicating physical factors influencing salinity. Similarities between the power spectra of the Lee Ferry and Grand Canyon time series indicated that lateral inputs and evaporation are not greatly influencing the salinity cycle. The salinity change within this reach was approximated by a constant concentration change of 66.6 ppm. A similar model form was used for the Hoover Dam to Parker Dam reach. Dissimilarities between power spectra indicated that additional inputs are significant and must be accounted for in any model of such reaches. The model for Lake Mead required compensation for evaporation and for the inputs of the Virgin River and Las Vegas Wash. The modeled salinity increase between Parker Dam and Yuma contained a trend factor to allow for the effect of irrigation return flows and seepage. The crosscovariance function was used to approximate the time lag between data stations. Time series statistics, including coherence, response function spectra, and overall unit response, were used and are of utility in estimating salinity in a river system.

CHAPTER I

INTRODUCTION

Goals

Salt concentrations in the Colorado River System increase from Lake Powell to the Mexican border. This trend has been documented in several reports either for or by the U.S. Department of the Interior (1971) and the U.S. Environmental Protection Agency (1971).

The effect of reservoirs and other inputs on the system has been studied in parts (Anderson and Pritchard 1951, Qashu and Everett 1971, Everett 1971) but as yet no effort has been made to trace the course and changes in water quality in the entire system. The goal of this study is to examine the changes in water quality from Lee Ferry* to Yuma. Knowledge of these changes and their causes is necessary for the successful management of the water resources of the Colorado River Basin.

Historical salinity data will be evaluated using time series analysis techniques. The specific objectives of the study are:

1. To determine effects of reservoirs and river transit in relation to space and time distribution of salinity.
2. To analyze effects of reservoir characteristics (depth/volume, depth/surface area, etc.) on water quality of inputs and outputs.

---

* Spelling of Lee Ferry taken from Lower Colorado Region Comprehensive Framework Study by State-Federal Interagency Group, 1971.

3. To develop a method for detecting salt loading effects in some reaches and reservoirs.

Description of Study Area

The Lower Colorado River Basin (Figure 1), defined here as the reach between Lee Ferry and the Mexican border, has a drainage area of about 75,100 square miles. Flow is controlled by a series of storage and diversion dams. The data stations to be used in this study are Lee Ferry, Grand Canyon, below Hoover Dam, Parker Dam, and Yuma. A detailed description of the location of each station is given in Appendix A.

Tributaries between Glen Canyon Dam and Lake Mead have erratic inflow into the Colorado River but add almost enough water to offset evaporation losses from Lake Mead (U.S. Department of the Interior 1971). Unfortunately, these tributaries also contribute relatively large amounts of dissolved solids to the river flow. According to the Water Quality Chart prepared by the Hydrographic Engineering Branch of the Metropolitan Water District of Southern California (1971), the mean TDS concentration for the period 1941 to 1968 was 552 ppm at Lee Ferry and 614 ppm at the Grand Canyon sampling station. This increase has been attributed mainly to inflow from the several tributaries in the Grand Canyon reach. Of the approximately one million tons of dissolved solids added in this reach, half is from the Little Colorado River (U.S. Department of the Interior 1970). Using 1941 to 1968 average discharges, contributions from Grand Canyon tributaries (Paria River,

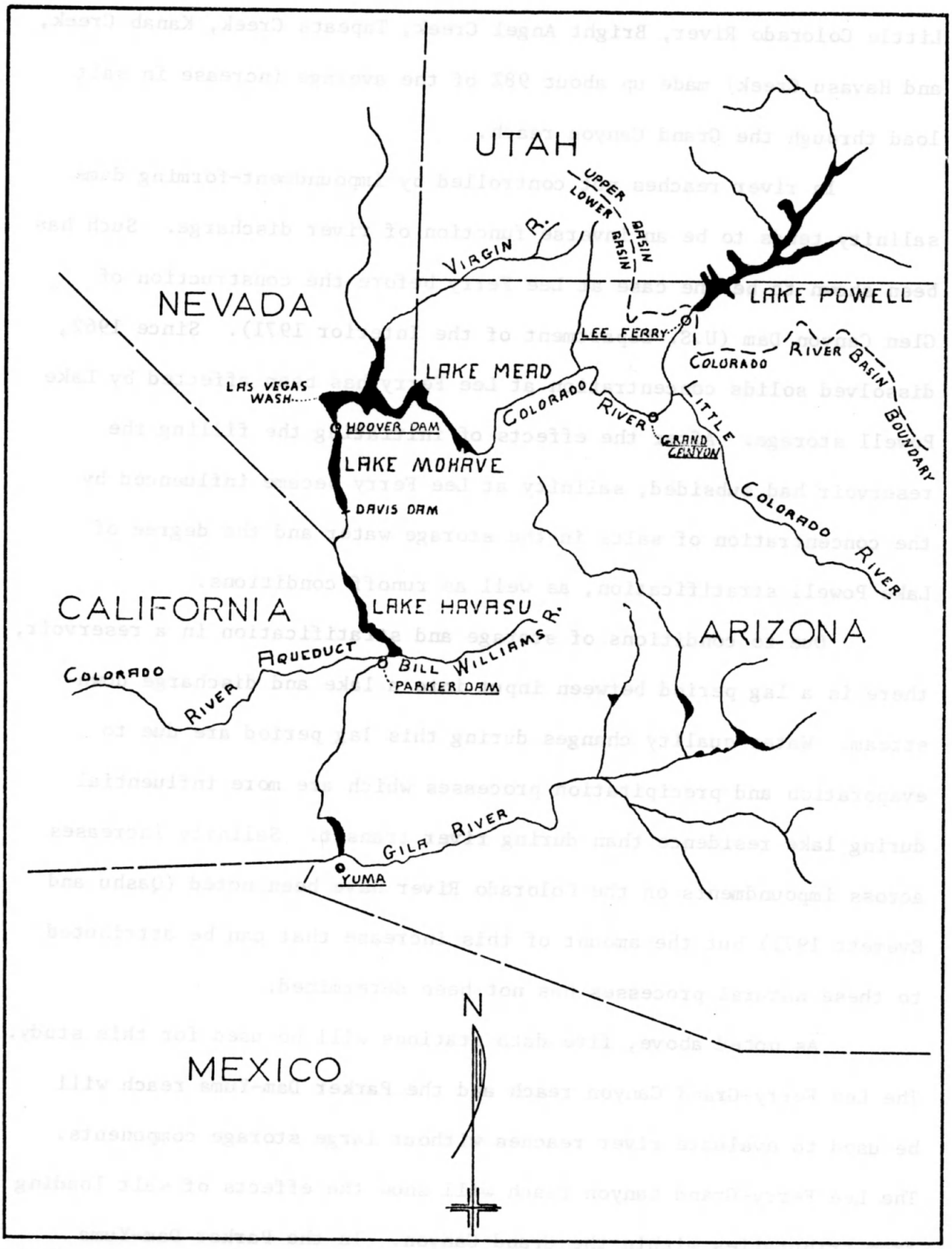

Figure 1. Map of Lower Colorado River Basin.

Little Colorado River, Bright Angel Creek, Tapeats Creek, Kanab Creek, and Havasu Creek) made up about 98% of the average increase in salt load through the Grand Canyon reach.

In river reaches not controlled by impoundment-forming dams salinity tends to be an inverse function of river discharge. Such has been shown to be the case at Lee Ferry before the construction of Glen Canyon Dam (U.S. Department of the Interior 1971). Since 1962, dissolved solids concentration at Lee Ferry has been affected by Lake Powell storage. After the effects of initiating the filling the reservoir had subsided, salinity at Lee Ferry became influenced by the concentration of salts in the storage water and the degree of Lake Powell stratification, as well as runoff conditions.

Due to conditions of storage and stratification in a reservoir, there is a lag period between input into a lake and discharge downstream. Water quality changes during this lag period are due to evaporation and precipitation processes which are more influential during lake residence than during river transit. Salinity increases across impoundments on the Colorado River have been noted (Qashu and Everett 1971) but the amount of this increase that can be attributed to these natural processes has not been determined.

As noted above, five data stations will be used for this study. The Lee Ferry-Grand Canyon reach and the Parker Dam-Yuma reach will be used to evaluate river reaches without large storage components. The Lee Ferry-Grand Canyon reach will show the effects of salt loading from tributaries within the Grand Canyon. In the Parker Dam-Yuma

reach there are several diversion structures (Imperial Dam, Headgate Rock Dam, and Palo Verde Diversion Dam) that create only small storage volumes. Analysis of this river reach should yield information concerning salt loading from agricultural runoff.

Data from river runs through the Grand Canyon (Qashu, Everett, and Staker 1971) indicated that little salinity change occurs in the Colorado main channel downstream from Bright Angel Creek for at least 150 miles. Thus the Grand Canyon-below Hoover Dam station set will be used to assess the effect of flow through Lake Mead on water quality. Salinity has been found to increase by about 100 ppm from South Cove on Lake Mead to Hoover Dam (Qashu and Everett 1971).

Since the data from Davis Dam is not sufficient for time series analysis, Lake Mohave cannot be evaluated as a separate unit. Data from Parker Dam and the Lake Havasu Intake Pumping Station will be used to evaluate the effects of the Lake Mohave-Lake Havasu chain on water quality. Since only a short river reach divides these two reservoirs, their combination does not seem unjustified.

CHAPTER II

METHODOLOGY

Description of Statistical Parameters

The purpose of this study was to examine the salinity changes that occur in the Colorado River between Lee Ferry and Yuma. The approach to evaluating the magnitude and nature of these changes was to examine the salinity time series at five river stations using time series analysis. The results of this statistical analysis (power spectra, autocovariance function, crosscovariance function, coherence, and response function spectrum) were used to describe the nature of the salinity cycles at each location, to indicate the changes in cyclic patterns between data stations, to show changes in salinity with respect to time, and to indicate cause-and-effect relationships between salinity time series at different locations. This information was used in models to describe the changes in salinity both with respect to time and distance.

Normally, different segments of a time series resemble one another only in their average behavior. The possible values of a time series are thus described by a random variable X(t). Associated with each value, $x(t)$, of X(t) is a probability distribution which attaches a probability of occurrence to each possible value of the random variable at time t. In the general case any time series can be

described as a set of random variables {X(t)} where t is time and $-\infty<t<+\infty$. The statistical properties of the series are described by the probability distributions associated with each random variable. This ordered set of random variables and the associated probability distributions is called a stochastic process.

The number of time series which might be generated by such a process is doubly infinite because there are an infinite number of possible values at any time t and an infinite number of time values. Because description of an infinite time series and the probability distributions associated with each time point is impossible, simplifications or assumptions are made in time series analysis to make possible the analysis of practically attainable time series.

One assumption is that the time series is stationary. A stationary time series is one in which sequential sections "look alike," i.e., the properties of the time series do not change with time or the process is origin-independent. The statistical properties of a stationary time series do not change with time and thus the properties of the entire series can be described by computation of statistical functions using a non-infinite set of time series points.

The assumption of stationarity is probably not met by any of the five time series used in this study. The discussions in the following chapters dealing with trends and other changes in the series with respect to time indicate that the time series are at least partically non-stationary. The Lee Ferry and Grand Canyon time series show a great change in the pattern of the time series after the

construction of Glen Canyon Dam. The stations below Hoover Dam show the effects of increased discharge from Las Vegas Wash and the Yuma Station time series shows changes due to agricultural development. Thus the time series change with respect to time and are not stationary. The form of the power spectrum is affected by such changes in the characteristics of the system. The proposed use of the power spectra (see below) was to compare the salinity cycles at different locations on the river. The study indicates that this technique makes the interpretation of the data possible in spite of the violations of the steady-state assumptions.

The approach taken in this study was to use the TDS concentration at some time and place on the river to predict the salinity at a downstream location. Time series analysis was used to show similarities (or dissimilarities) in the time series of upstream-downstream station pairs. Comparison of autocovariance functions and power spectra was used to demonstrate statistical similarities between station pairs. The degree of this indicated similarity demonstrated the complexity of the salinity change occurring between the two data stations.

The autocovariance function, $R_x(p)$, is written

$$R_x(p) = E[(X(t) - m)(X(t+p) - m)] \qquad (1)$$

where X(t) is the value of the parameter (here TDS) at time t, m is the mean value of X(t), and p is a displacement in time called the lag. The autocovariance function indicates the degree to which the variance in

the time series at some time t is correlated to the variance at some later time (t+p). The form of $R_x(p)$ thus indicates the tendency of a given element in the time series to repeat itself. $R_x(p)$ is computed using the relationship:

$$R_x(p) = \frac{1}{n-p} \sum_{q=1}^{n-p} Xq \; Xq+p \qquad (2)$$

where p = lag = 0, 1, 2, . . . , m (m = maximum lag), n = number of data points (here 357), and Xq = value of the q^{th} value of the time series. A maximum lag of 36 months was used for these computations. The justification of this choice are given in a later section. The above equation and others in this chapter are taken from the Biomedical Computer Programs manual (Dixon 1970).

The computations of spectral analysis of a time series sort the total variance of the series into its component frequencies. Variance is basically a measure of the spread or the dispersion of recorded values about the mean value. Components of the total variance can occur either at periodic intervals or randomly. The calculated estimates of the contribution of each frequency to the total variance make up the "power spectrum" of the record. The value of the power spectrum estimate for a given frequency indicates the magnitude of the contribution of that component and the frequency indicates the period of recurrence of that contribution.

The power spectrum is the Fourier cosine transform of the auto-covariance function. If a time series is considered as a mixture of cosine waves, the total variance can be decomposed into components of

variance at the various frequencies. If this decomposition is into a continuous set of frequencies, the result is the power spectrum. The equation of the continuous form of the power spectrum is:

$$P(f) = \int_{-\infty}^{\infty} R_x(p) \cos (2\pi f u) \, du \tag{3}$$

where $R_x(p)$ is the autocovariance function, which is a function of lag p, and f is frequency. With a finite record length, the power spectrum is often preferred to the autocovariance function because the spectrum estimates at neighboring frequencies are approximately independent and thus the interpretation of P(f) may be easier than the autocovariance function. Also the power spectrum is of direct physical significance in many cases as for indicating characteristic cyclic patterns.

For computation of the estimates of the power spectrum the continuous form above is approximated by the following relation:

$$P_x(h) = \frac{2t}{\pi} \sum_{p=0}^{m} K_p \, R_x(p) \cos \frac{hp\pi}{m} \tag{4}$$

where $P_x(h)$ is the power spectral estimate of the time series at the frequency $h\pi/mt$ (h=0, 1, . . . , m), m is the maximum lag, t is the constant time interval, K_p=1 for 0<p<m and K=1/2 for p=0 or m, and $R_x(p)$ is the autocovariance function defined above. This computation smooths out some of the wide fluctuations in the autocovariance function by applying a sinusoidal weighting factor.

The power spectrum thus calculated is then smoothed by using a weighting factor which counteracts some of the distortion caused by a less than infinite sample size. This weighting is computed using:

$$SP_x(0) = 0.54\ P_x(0) + 0.46\ P_x(1) \quad (5)$$

$$SP_x(h) = 0.23\ P_x(h-I) + 0.54\ P_x(h) + 0.23\ P_x(h+1),\ 0<h<m \quad (6)$$

$$SP_x(m) = 0.54\ P_x(m) + 0.46\ P_x(m-1) \quad (7)$$

where $SP_x(h)$ is the smoothed power spectral estimate at the frequency $h\pi/mt$.

Historical TDS data has been obtained from the publication "Quality of Water-Colorado River Basin, Progress Report No. 5" by the U.S. Department of the Interior (1971). These time series are composed of monthly mean concentrations calculated for the period of January 1941 to December 1968. These mean measurements are weighted with respect to river discharge. Discharge-weighted means are computed by multiplying the average discharge for a sampling period by the concentrations of individual samples for the corresponding period and dividing the sum of these products by the sum of the discharges. Such weighted-average concentrations approximate the composition of water that would be found in a reservoir containing all the water passing a given location during the period after thorough mixing in the reservoir. The sources of raw data and the calculation method used to create missing data is presented in this report. Time series for the period January 1969 to September 1970 has been taken from USGS monthly data (U.S. Geological Survey 1971).

These time series give a total of 357 data points for each of the five river stations. Time series analysis was performed using program BMD02T (Dixon 1970) from the primary library tape and disk of the University Computer Center.

The choice of the number of lags used in the computation was made according to Wastler (1969). The first criterion was that some lag number have a corresponding recurrence period of twelve months. This is because an annual cycle was expected to be present. The equation used for calculating the recurrence period for each lag number is

$$T_r = \frac{2mt}{r} \tag{8}$$

where T_r is the period corresponding to the rth lag, t is the time interval between data points (1 month), m is the total number of lags and r is the lag number ($0<r<m$). Calculations using several values of m indicated that 12-lag, 24-lag, and 36-lag choices would give spectral estimates for a twelve month period. The twelve month spectral estimate for the 12-lag choice would be next to the long period or ∞ estimate. If any of the time series had long period or random components, these spectral estimates might overlap the twelve month estimate. Thus this choice was ruled out.

A larger number of lags gives high resolution in the estimation of power spectra. This higher resolution is at the cost of some degree of confidence in the result. To indicate the amount of error induced by using 36 rather than 24 lags, the numbers of degrees of freedom for each spectral estimate of these lag choices were calculated. The calculation method is given by Blackman and Tukey (1958). Computation for 24-lags given 29.1 degrees of freedom; 36-lags gives 19.2 degrees of freedom. This indicates that using 36-lags gives a confi-

confidence level equivalent to having the average of 20 pieces of data for each spectral estimate.

Since the numbers of degrees of freedom for each lag choice was considered adequate, the choice became somewhat subjective. The 36-lag choice was made because of better resolution and because according to Wastler (1969) a number of lags equal to about 10% of the total number of measurements (here 357) gives a good balance between resolution and precision.

The end product of spectral analysis of a single record is a spectrum showing the frequencies and magnitudes of the dominant periodic components of the record. The comparison of two records shows the phase relationship between the dominant periodic components of the two records. The parameters of interest in this study are the coherence, the lag, and the response. These parameters, along with the results of the spectral analysis, were used in evaluating the nature of changes in water quality between the river stations. Because cause-and-effect relationships are of concern, it is common in cross-spectral analysis to term one record as input and the other as output. For station pairs on the Colorado River, the upstream record will be considered as input and the downstream record will be called output.

Upstream salinity is defined here as the input of a river reach or reservoir system and downstream salinity is defined as the system output. These two time series do not arise on an equal footing because changes in the input can cause changes in the output but not visa versa. When "normal operating" records of such inputs and outputs are analyzed, relationships connecting the two time series

which fit the data may not be adequate for predicting the effect of imposed changes in the input on the output (Jenkins and Watts 1968). The importance of these indications must be considered in evaluating any model derived from this type of data series.

The computer output was to be analyzed for several factors. The power spectra of the individual time series records indicates the dominant periodic cycles that characterize each river location. The low frequency ends of these spectra will indicate the presence of long-term trends in the records. If such trends are noted and interfere with shorter periodic components, the time series records will be detrended. Using these power spectra, an effort will be made to detect and determine the natural seasonal variations in salinity. Knowledge of these natural cycles would be useful in detecting salt loading from artificial sources which have other cyclic patterns.

The crosscorrelation of two records yields several useful statistics. Lag is the lapse time between maxima or minima in the two records. This will give the time relationship between river stations. Knowledge of the time of passage can be used as a pollution control measure through the timing of releases to minimize the effects at downstream points. Calculation of crosscovariance function values was used to indicate lag between river stations.

The values of the crosscovariance function is computed by the following equations:

$$R_{xy}(p) = \frac{1}{n-p} \sum_{q=1}^{n-p} X_q \, Y_{q+p}, \; p = 0, 1, 2, \ldots, m \qquad (9)$$

$$R_{xy}(-p) = \frac{1}{n-p} \sum_{q=1}^{n-p} X_{q+p} \, Y_q, \; p = 0, 1, 2, \ldots, m \qquad (10)$$

where $R_{xy}(p)$ indicates the degree to which the variance in the input time series X at some time q is correlated to the variance in output series at some time q+p. $R_{xy}(-p)$ gives the indicated correlation if the input time series is displaced by p time units. If there is essentially no time delay between the input and the output time series, then the function has its maximum at p=0. The location of this maximum value approximate time lag between the input and the output of the system; if the function has its maximum at p=3, this indicates a lag of approximately 3 time units between the two series.

Since average monthly data is used in this study, the actual lag times indicated by the crosscovariance functions are approximations. Weekly or daily data would be required for a more accurate determination of time lag. This type of data may be more advantageous for short-term forecasting especially for constant-withdrawal users to whom day-to-day forecasts of water quality may be important. For evaluation of the general form of salinity changes, monthly data was considered adequate.

Also, it should be noted that the crosscorrelation function gives a distribution of delay times. Thus "peak" in the function plot should be interpreted as an approximation of the time lag between two time series.

Computation of the Fourier transforms of the crosscovariance functions (Equations 9 and 10) perform the same smoothing function as for the autocovariance function. The results of this calculation, given as Equations 11 and 12 below, are the cospectrum and the quadrature spectrum, respectively.

$$C_{xy}(h) = \frac{t}{\pi} \sum_{p=0}^{m} K_p [R_{xy}(p) + R_{xy}(-p)] \cos \frac{hp\pi}{m} \qquad (11)$$

$$Q_{xy}(h) = \frac{t}{\pi} \sum_{p=0}^{m} K_p [R_{xy}(p) - R_{xy}(-p)] \sin \frac{hp\pi}{m} \qquad (12)$$

The values h, p, K_p, t were defined earlier. The spectra are smoothed using the weighting process shown in Equations 5-7. The numerical values of the sine and cosine functions are equal for angles which are 90 degrees out of phase with one another. Taking the Fourier cosine transform of one crosscovariance and the sine transform of the other results in two spectra which are 90 degrees out of phase with each other. These two spectra are components of the output spectrum. The geometrical analogy presented by Wastler (1969) is shown in Figure 2.

Coherence is a dimensionless statistic with magnitude ranging from 0.0 to 1.0. Coherence indicates how closely two records are linearly related. This "closeness" may be in both magnitude of variation and in correspondence of frequencies. It is often interpreted as the fraction of the variance in the output that is related to similar variance in the input. Its value reflects the confidence which one may put in the period of recurrence (of some indicated cyclic event).

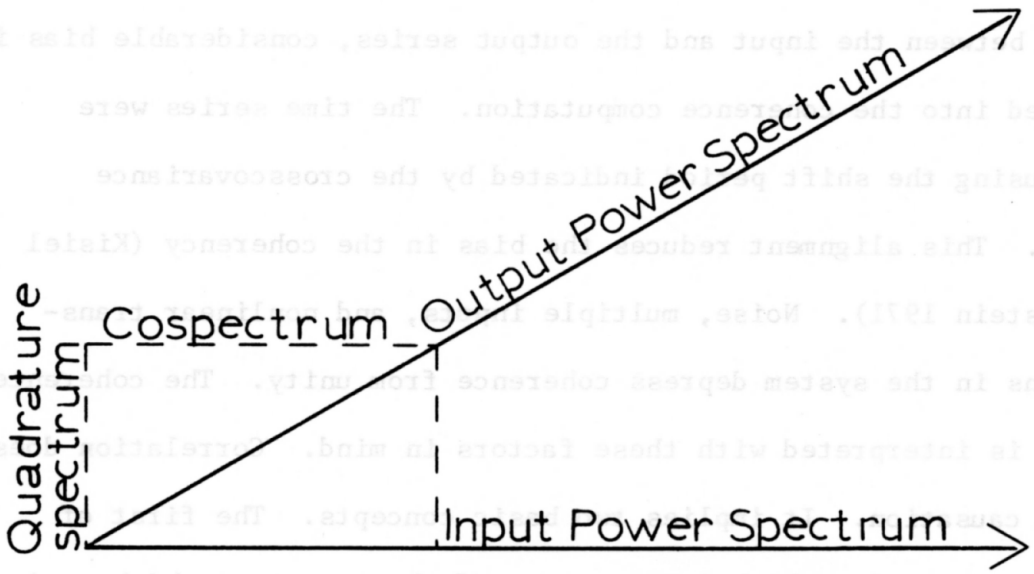

Figure 2. Geometric analogy of components of output spectrum.

Coherence measures the validity of using a linear model to describe a river reach system with the upstream salinity as the input and downstream salinity as output. A linear system with a single input function has a coherence of one at all frequencies. Several factors influence the computed values of coherence. Where there is a lag time between the input and the output series, considerable bias is introduced into the coherence computation. The time series were aligned using the shift period indicated by the crosscovariance function. This alignment reduces the bias in the coherency (Kisiel and Duckstein 1971). Noise, multiple inputs, and nonlinear transformations in the system depress coherence from unity. The coherence spectrum is interpreted with these factors in mind. Correlation does not mean causation. It implies two basic concepts. The first of these is covariation which is a measure of the extent to which variations in the input parameter are paralleled by variations in output. Correlation also defines the usefulness of a predictor (Sterling and Pollack 1968). In this instance, the degree of correlation (which is analogous to coherence) will indicate the usefulness of upstream water quality records in predicting water quality downstream. Coherence is computed according to the relation:

$$H_{xy}(h) = \frac{[C_{xy}(h)]^2 + [Q_{xy}(h)]^2}{[SP_x(h)]\ [SP_y(h)]} \qquad (13)$$

where $SP_y(h)$ is the smoothed power spectral estimate for the output series Y and the other components are defined above.

The response function gives what the output spectrum would be if the input record were the only parameter dominating it. It is interpreted the same as the power spectrum of an individual record but it is more advantageous in that it also reflects the phase relation between the two records. Frequently, where impoundments or other damping factors are present within a system, all but a single cyclic variation are damped-out. Such a situation would yield a response spectrum with a strong response at one frequency and a lack of response at other periods. This form of response spectrum also indicates a highly deterministic relationship between the input and the output. The response function spectrum is defined by:

$$R(h) = H_{xy}(h) \times SP_y(h) \tag{14}$$

The response spectrum is used to determine the degree to which concentrations at the upstream station determine concentrations at the downstream station. This is being accomplished by calculation of response or overall unit response (Wastler 1969). This statistic is calculated by taking the square root of the ratio of the sum of the response spectrum values to the sum of the input spectrum values.

$$U = \sqrt{\frac{\sum_{h=0}^{m} R(h)}{\sum_{h=0}^{m} SP_x(h)}} \tag{15}$$

This parameter can be used assuming that the input and output records have similar frequency distributions and are statistically similar. Response will have the units of ppm downstream/ppm upstream.

As an illustration, the response value indicates if the salinity of the water released downstream from Hoover Dam is predominately determined by the salinity of Colorado River water introduced into Lake Mead at South Cove or if other inputs (the Virgin River, Las Vegas Wash, etc.) are more influential.

Use of Statistical Parameters

The above statistical analysis which is outlined in the following flow chart (Figure 3) was used to evaluate the time series records of the following river station sets: Lee Ferry-Grand Canyon, Grand Canyon-below Hoover Dam, below Hoover Dam-Parker Dam, and Parker Dam-Yuma. This analysis offers the possibility of further insight into:

1. Time lag for salt movement through the reservoir systems and river reaches.
2. Changes in salinity across the entire Lower Colorado system and across each segment of the system.
3. The effect of reservoir surface area, depth, and volume on lag time and on water quality.
4. The presence and extent of salt loading in the river basin.
5. The possibility of using information about lag times and relationships between water quality at different stations in detecting additional pollution of the Colorado River.

Given the lag time between river stations and some expected salinity change between stations, the sampling program to detect pollution of the system would proceed by taking a sample and comparing

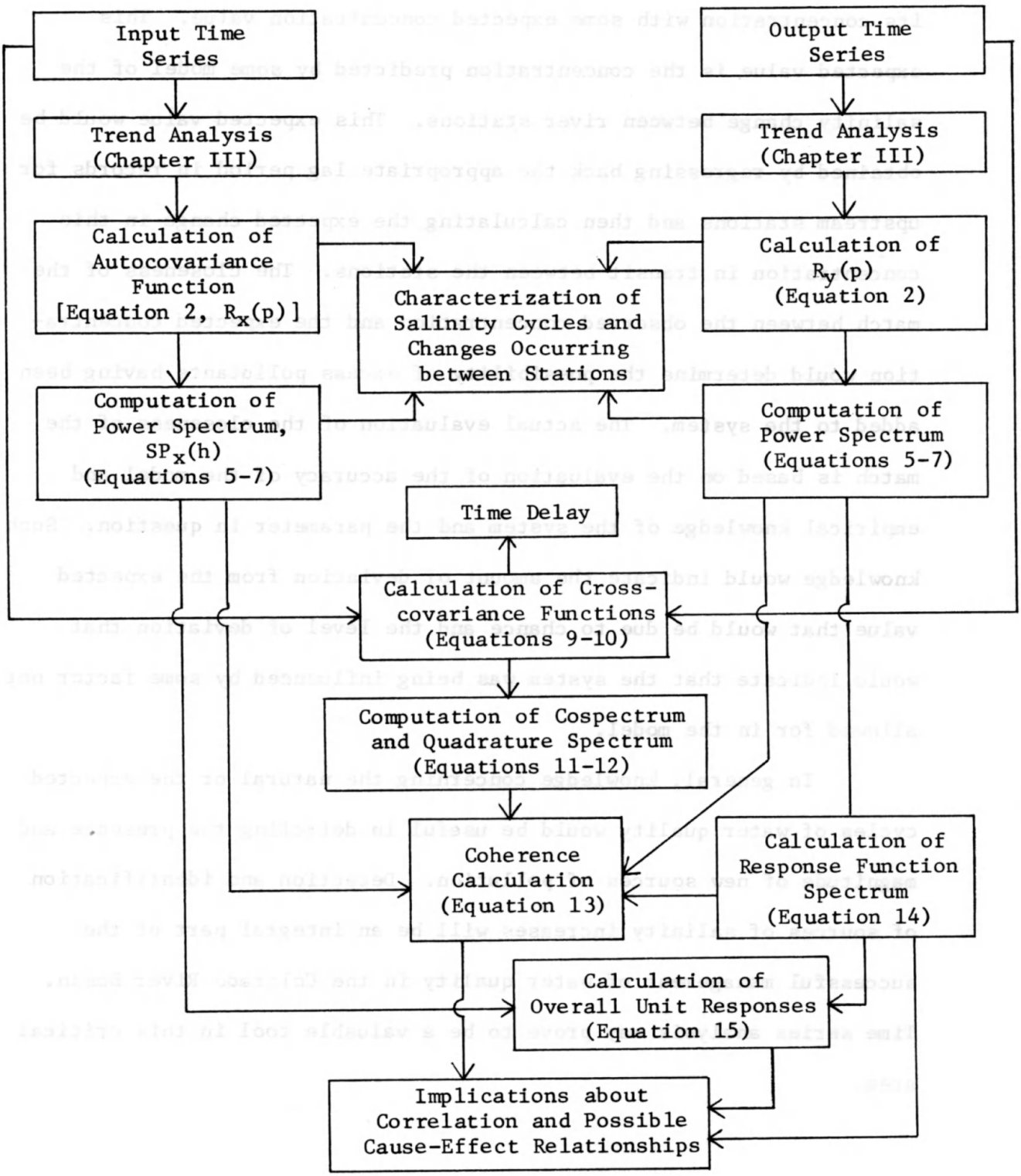

Figure 3. Flow chart of method of analysis.

its concentration with some expected concentration value. This expected value is the concentration predicted by some model of the salinity change between river stations. This expected value would be obtained by regressing back the appropriate lag period in records for upstream stations and then calculating the expected change in this concentration in transit between the stations. The closeness of the match between the observed concentration and the expected concentration would determine the possibility of excess pollutants having been added to the system. The actual evaluation of the closeness of the match is based on the evaluation of the accuracy of the model and empirical knowledge of the system and the parameter in question. Such knowledge would indicate the amount of deviation from the expected value that would be due to chance and the level of deviation that would indicate that the system was being influenced by some factor not allowed for in the model.

In general, knowledge concerning the natural or the expected cycles of water quality would be useful in detecting the presence and magnitude of new sources of pollution. Detection and identification of sources of salinity increases will be an integral part of the successful management of water quality in the Colorado River Basin. Time series analysis may prove to be a valuable tool in this critical area.

CHAPTER III

ANALYSIS OF LEE FERRY TO GRAND CANYON REACH

Analysis of the Time Series

The purpose of the analysis of salinity in the river reach between Lee Ferry and Grand Canyon was to examine the effects of salt loading from natural sources. It has been noted in other studies that the TDS concentration increases between Lee Ferry and the Grand Canyon due to salt loading from the Little Colorado River (Blue Springs) and other tributaries within the reach. If some factor or function can be found which characterizes this salt introduction, then salinity data taken at Lee Ferry can be used to predict salinity at Grand Canyon. This prediction capability would lead to optimization of sampling procedures and probably a reduction in sampling frequency at the Grand Canyon station.

Figures 4 and 5 are the time series plots for the Lee Ferry and Grand Canyon stations, respectively. Visually the time series are nearly identical. Since maxima and minima in TDS concentration in the two series coincide in time, the time lag between the two stations is less than one month. The actual time of transit is probably on the order of one week. The crosscovariance function for this station set (Figure 6) has its maximum value at the zero lag without any shifting of the time series and thus supports the conclusion of the short time lag.

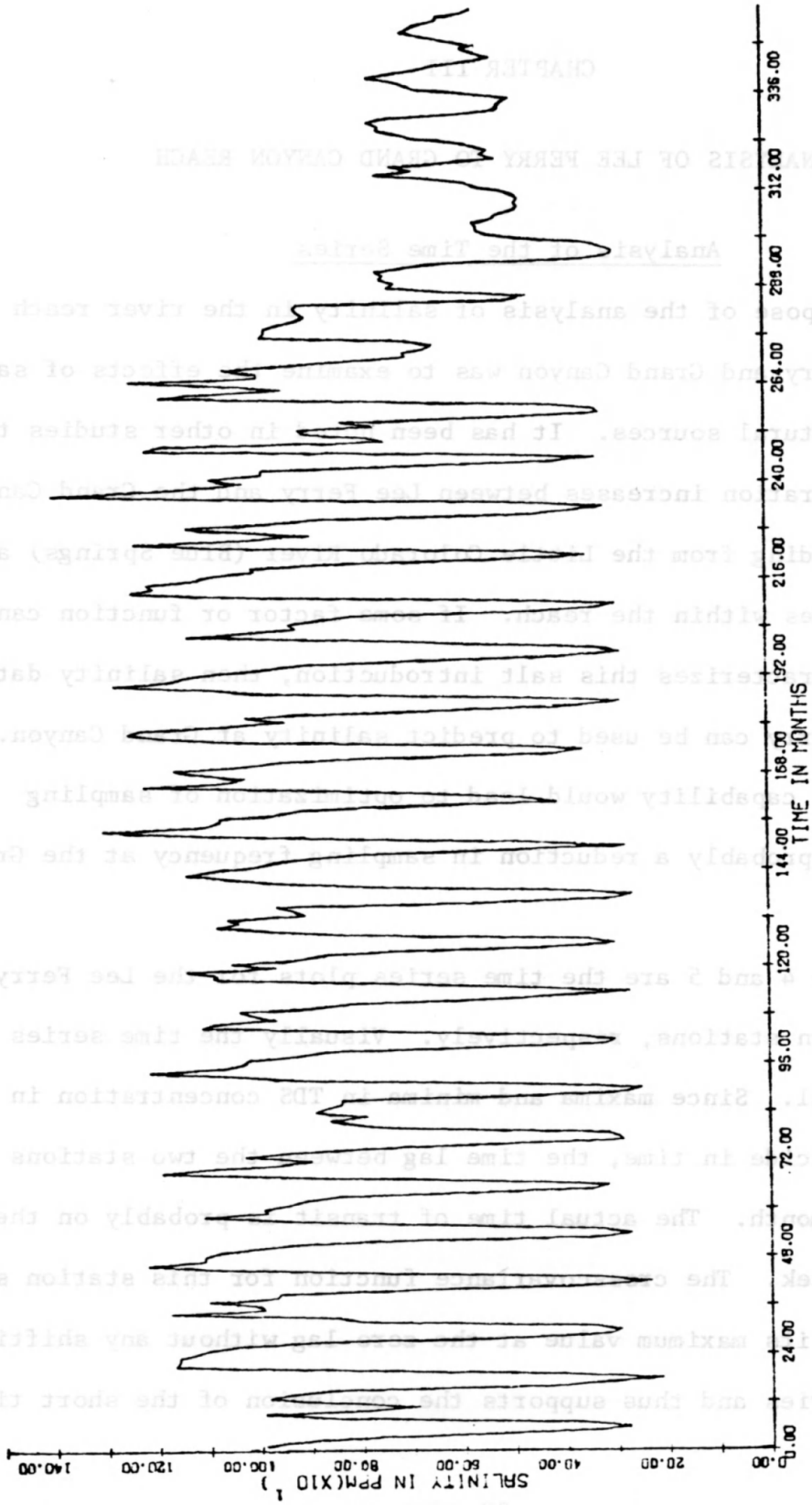

Figure 4. Lee Ferry TDS time series (1941-70).

The time axis indicates the number of months from January 1941. The divisions mark twelve month periods.

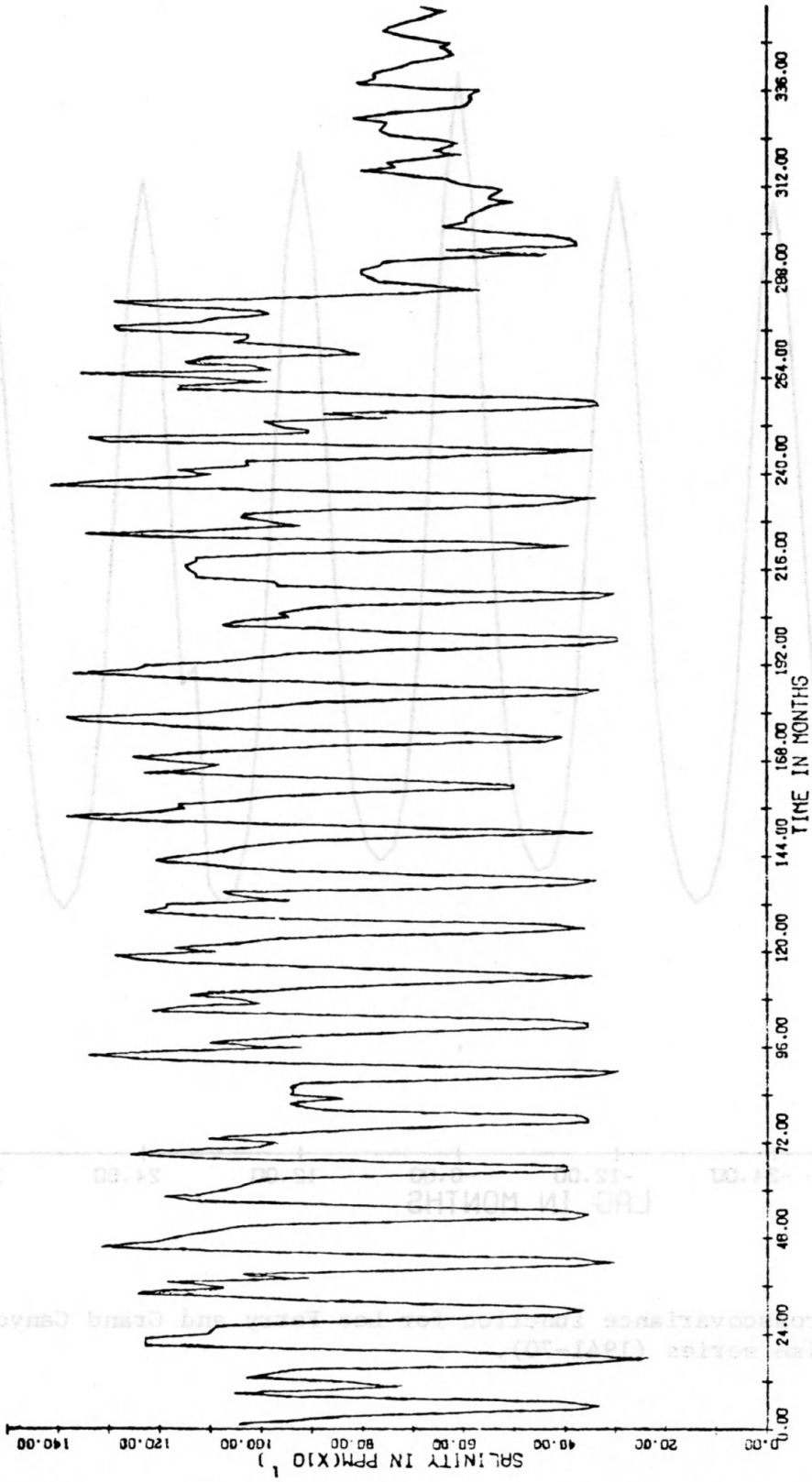

Figure 5. Grand Canyon TDS time series (1941-70).

The time axis indicates the number of months from January 1941. The divisions mark twelve month periods.

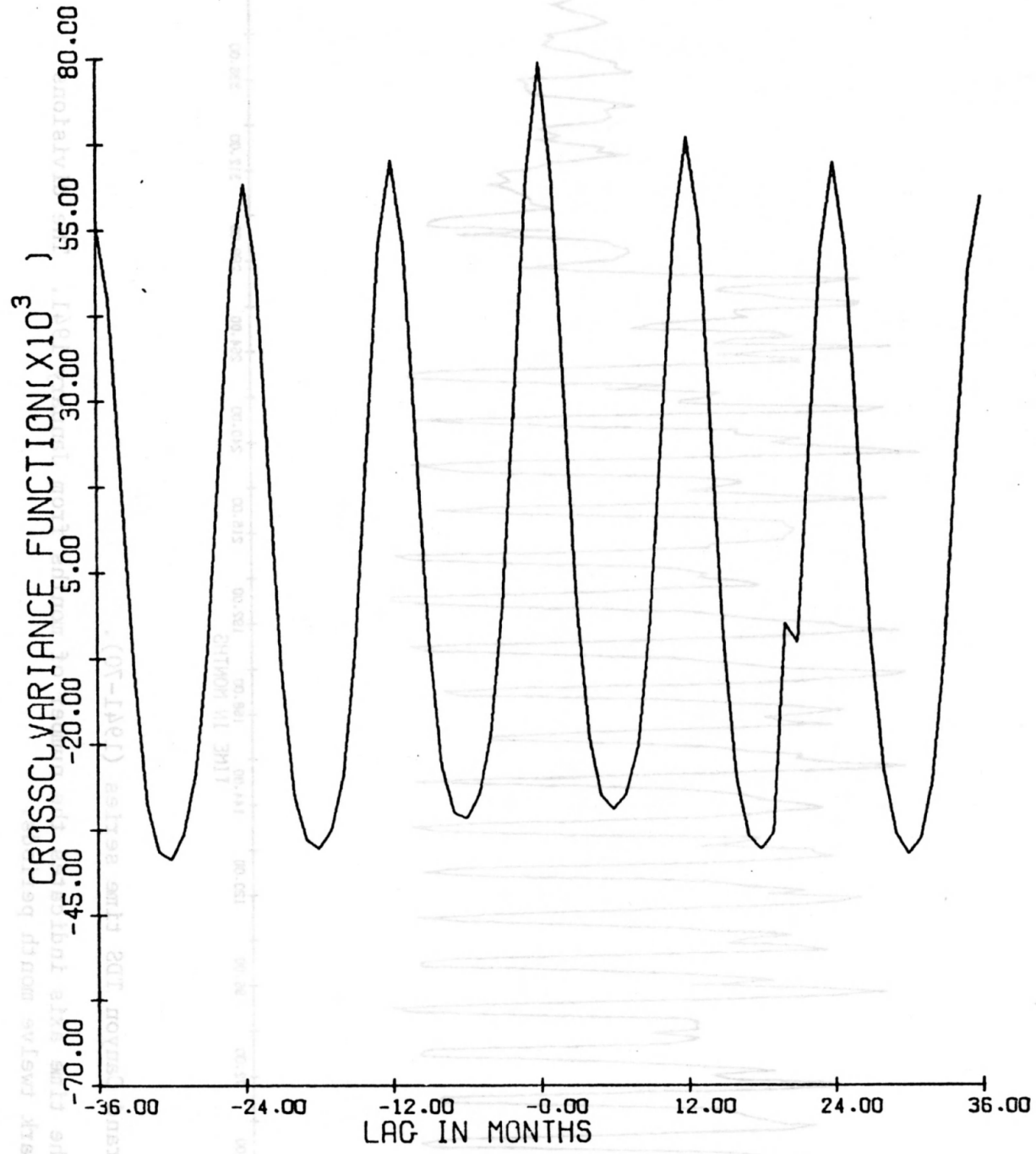

Figure 6. Crosscovariance function for Lee Ferry and Grand Canyon time series (1941-70).

The time series plots show a large minimum in TDS concentration in June of each year up to 1963 when the influence of Lake Powell became a factor. The 1941-1963 series also shows a weak minimum in the winter months (November, December, or January) of each year. These cycles are functions of streamflow. Increased discharge due to snow melt, summer rains, and winter rains caused the summer minima and the weak winter minima. Snow melt probably caused the summer minimum concentration to occur in June rather than later in the summer.

After 1963, the TDS concentration cycle shows changes induced by the filling of Lake Powell. The year 1964 appears to be a transition period. After 1964 an annual cycle in TDS concentration is still visible but its form is different from the pre-1963 cycles. For this shorter time series, there is only one annual minimum concentration and this occurs late in the year from September to December. One impact of Lake Powell is that before the construction of Glen Canyon Dam, low TDS concentrations were associated with high flows while after 1964 high flows are associated with high concentrations. This new discharge-salinity relationship may be a transient phenomenon since the major impact of the filling of Lake Powell is the damping of the salinity cycles. The initial damping is very evident and inspection of the 1964-1970 time series indicates that the annual oscillations are continuing to decrease in amplitude with time. This damping effect also explains the shift in annual minimum salinity concentration from June in the pre-1964 time series to late in the year in the post-1964 series. As the Colorado River flows into

Lake Powell, the seasonal fluctuations in salinity are compressed and the lower velocity movement in the reservoir shifts the downstream impact of snow melt and summer rains from late spring-early summer to late in the year.

Because of the great similarity between the Lee Ferry and the Grand Canyon time series, the following discussion of statistical analysis deals only with the Lee Ferry time series. The analysis of the Grand Canyon time series leads to the same conclusions. The graphs of the autocovariance function and power spectrum of the Grand Canyon times series are included in Appendix B.

Figure 7 is the graph of the autocovariance function at Lee Ferry. Peaks occur at lags of zero and at integer multiples of twelve months. This is evidence of the dominant annual cycle shown in the time series plot. The slight decline in peak height from lag zero to lag of 36 months indicates the presence of a slight trend in the time series.

Figure 8 shows the power spectrum of the Lee Ferry time series. The dominent annual cycle is noted by the peak at the 0.083 cycle/month frequency. The peak at 0.167 cycle/month shows the six month cycle caused by the combination of summer and winter rains. There is also a peak at the 0.0 cycle/month frequency. Such a peak can be caused by random fluctuations, long period cycles, or a trend.

Since the autocovariance function indicated a slight trend might be present, the time series was detrended using a least squares linear detrending computation according to $Y=X-(A+BI)$. Here X is the

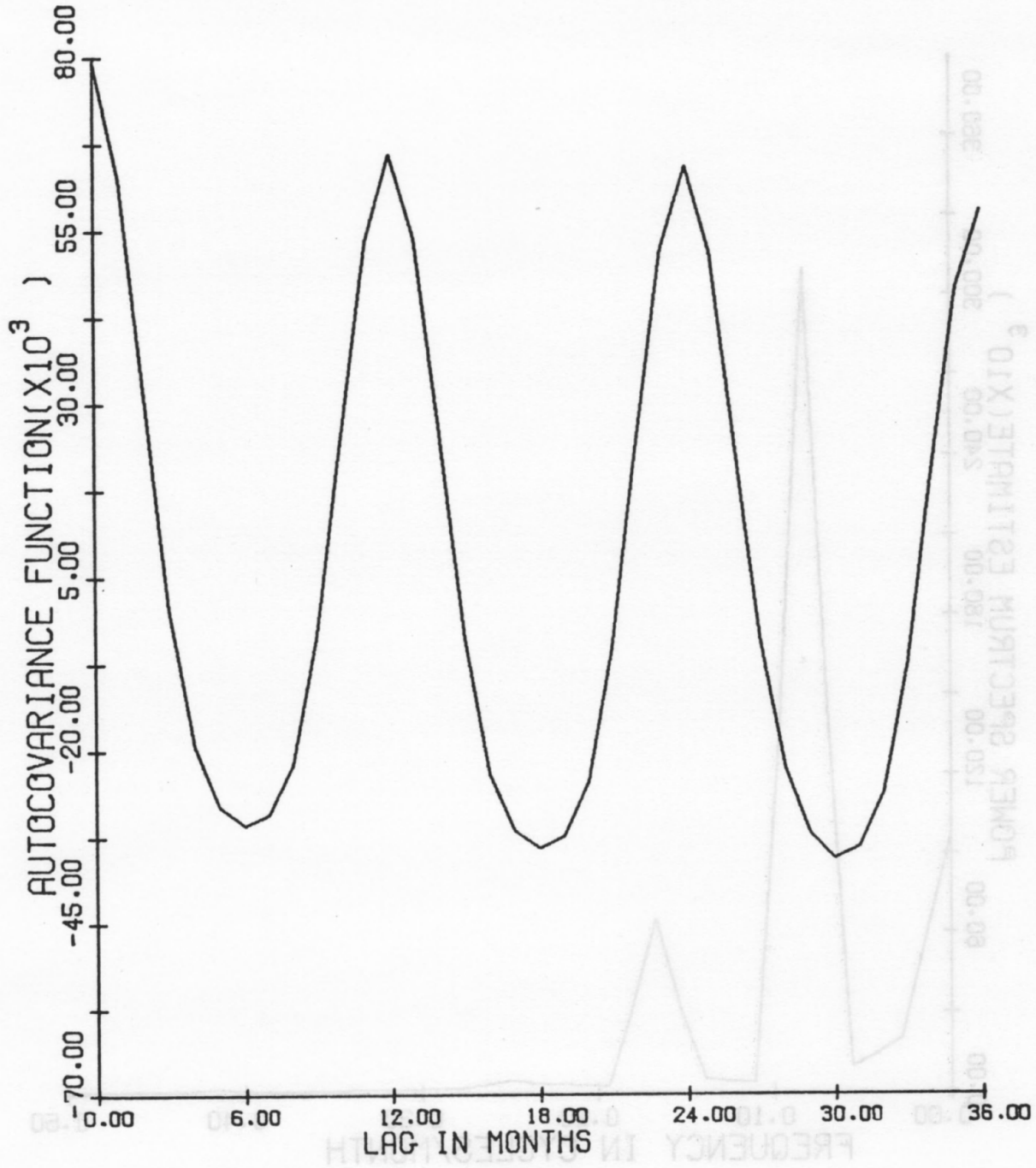

Figure 7. Autocovariance function for Lee Ferry time series (1941-70).

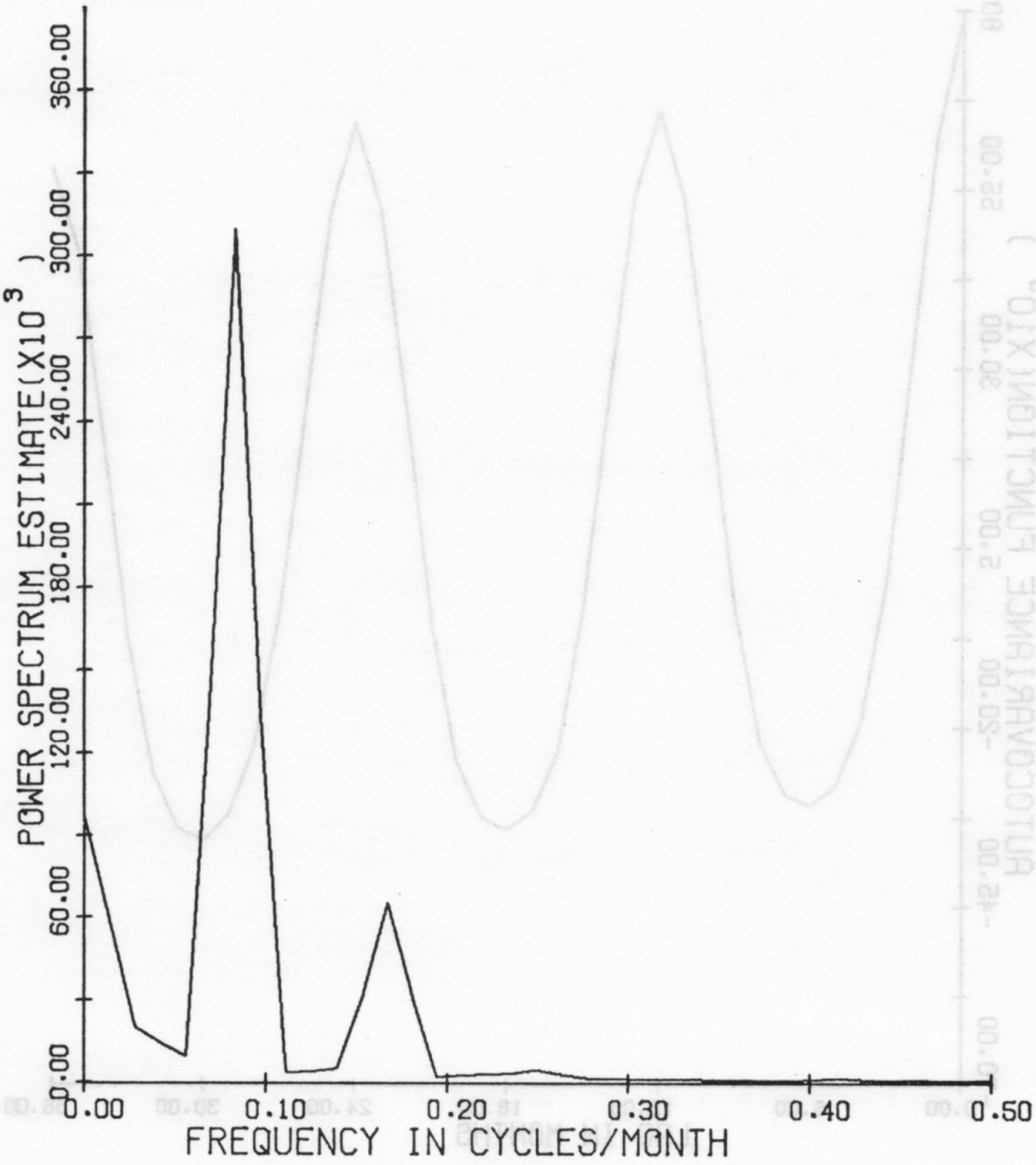

Figure 8. Power spectrum of Lee Ferry time series (1941-70).

value before detrending, Y is the value after detrending, I is the location of X on the time series (1, 2, 3, . . . , 357), and A and B are constants. For detrending the Lee Ferry time series, the values A=833.11 and B=-0.36 were used.

The form of the power spectrum of the detrended time series (Figure 9) is the same as before detrending. The only change was an 18% decline in the peak height at the 0.0 cycles/month frequency. Thus most of this frequency component is due to random and/or long period wave components.

As noted above, the construction of Glen Canyon Dam had a significant impact on the seasonal TDS cycle at Lee Ferry. The 1941 to 1964 time series was detrended as above using A=758.20 and B=-0.35. Figure 10 shows the power spectrum calculated for this 1941-1964 detrended time series. The spectral estimate at the 0.0 cycle/month frequency has become insignificant. The low frequency component of the 1941-1970 time series is caused by the construction of Glen Canyon Dam and the filling of Lake Powell.

The coefficient B used in detrending these time series is an indicator of the magnitude and direction of any trends present. A negative value for B indicates a declining trend line; values of the parameter tend to decrease with time. Positive values of B indicate an increasing trend in the time series. Changes in the coefficient A shift the time series with respect to the vertical axis; if A decreases the detrended curve is shifted in the positive direction. The coefficient A is equivalent to the Y-intercept of the "best line" drawn through the time series.

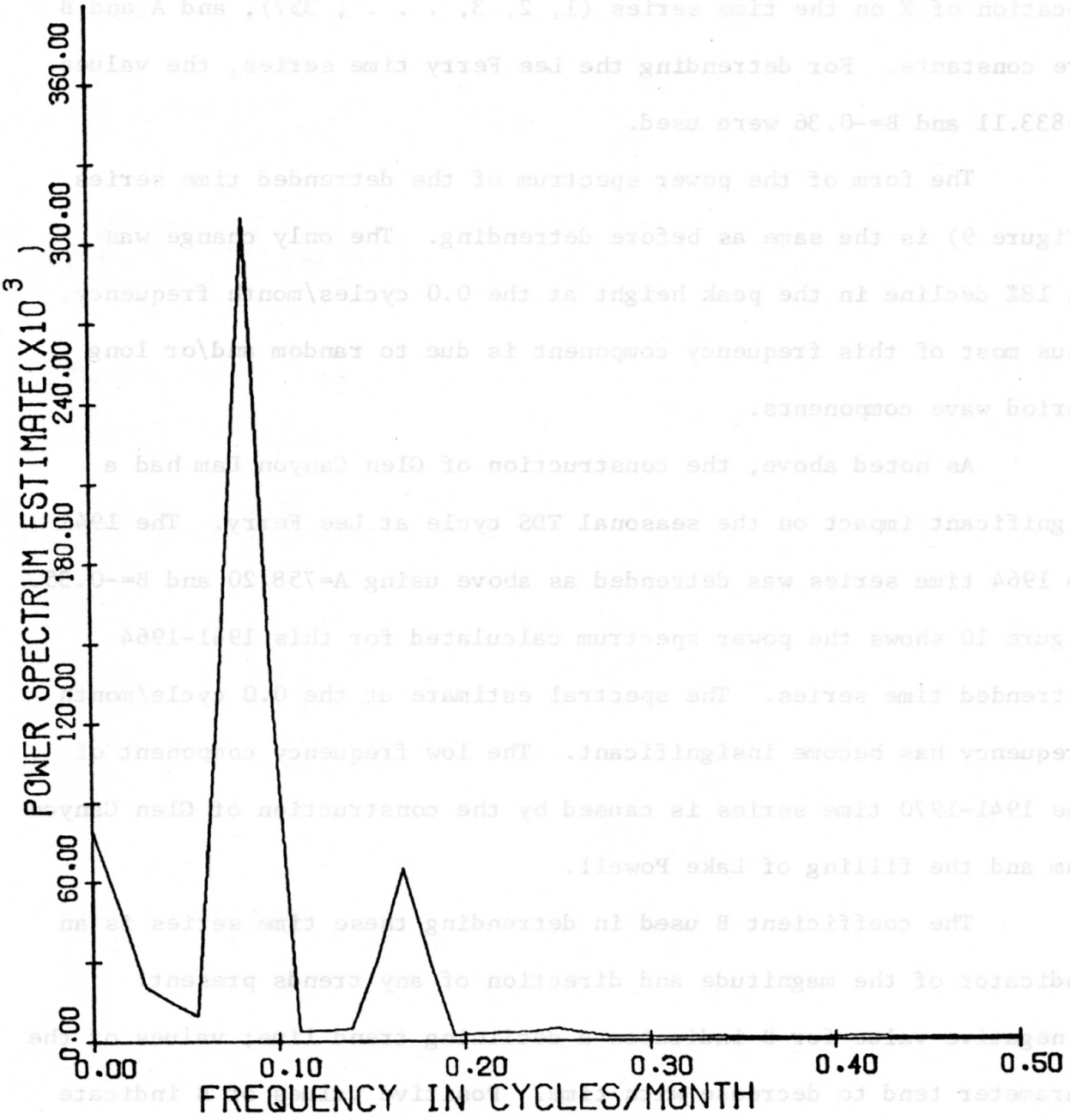

Figure 9. Power spectrum of detrended Lee Ferry time series (1941-70).

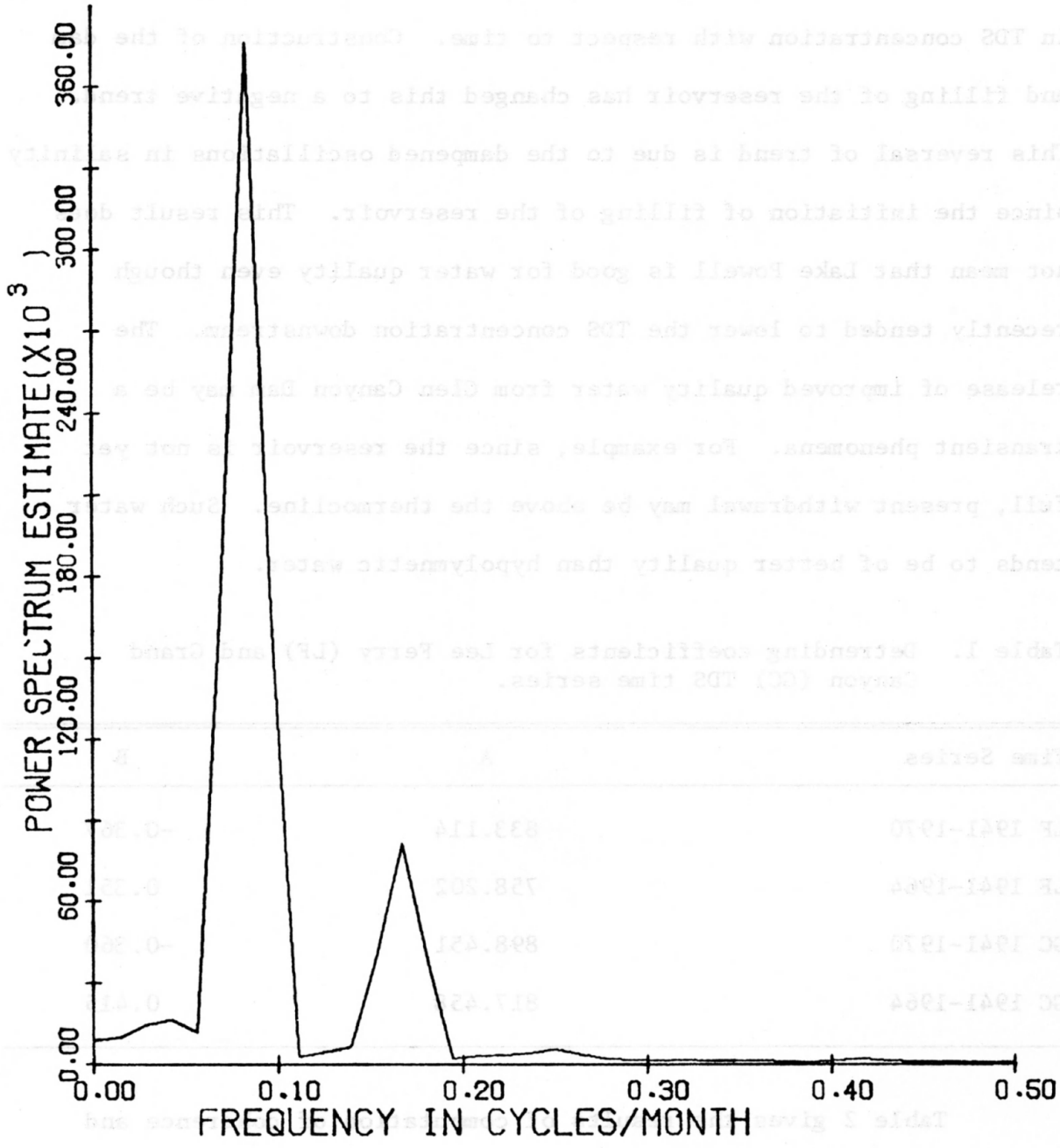

Figure 10. Power spectrum of the 1941-64 Lee Ferry time series.

The detrending coefficients shown in Table 1 indicate that before the construction of Glen Canyon Dam there was a positive trend in TDS concentration with respect to time. Construction of the dam and filling of the reservoir has changed this to a negative trend. This reversal of trend is due to the dampened oscillations in salinity since the initiation of filling of the reservoir. This result does not mean that Lake Powell is good for water quality even though recently tended to lower the TDS concentration downstream. The release of improved quality water from Glen Canyon Dam may be a transient phenomena. For example, since the reservoir is not yet full, present withdrawal may be above the thermocline. Such water tends to be of better quality than hypolymnetic water.

Table 1. Detrending coefficients for Lee Ferry (LF) and Grand Canyon (GC) TDS time series.

Time Series	A	B
LF 1941-1970	833.114	-0.367
LF 1941-1964	758.202	0.351
GC 1941-1970	898.451	-0.360
GC 1941-1964	817.458	0.415

Table 2 gives the results of computation of coherence and response function spectrum for the Lee Ferry-Grand Canyon station set. The fairly high coherence values at all frequencies shows the approximate linearity of the transfer between these two data stations.

Table 2. Coherence and response function spectrum for Lee Ferry-Grand Canyon reach.

Frequency (Cycles/Month)	Coherence	Response Function Spectrum
0.000	.899	73944.891
.014	.907	57709.429
.028	.905	30440.992
.042	.818	12263.669
.055	.822	6415.264
.069	.987	139738.230
.083	.992	312333.074
.097	.982	133519.947
.111	.610	2110.181
.125	.724	2520.687
.139	.855	5367.187
.153	.973	34662.363
.167	.988	70261.142
.181	.983	31227.600
.194	.756	1729.350
.208	.769	2711.680
.222	.814	3060.403
.236	.899	3779.900
.250	.929	4635.074
.264	.853	2378.564
.278	.757	1493.334
.292	.618	1347.652
.306	.593	877.134
.319	.779	1161.758
.333	.702	766.861
.347	.445	457.388
.361	.363	579.473
.375	.391	351.208
.389	.513	243.561
.403	.683	675.432
.417	.818	1405.082
.431	.740	827.516
.444	.570	516.175
.458	.627	638.244
.472	.432	276.807
.486	.519	438.617

The coherency is depressed at higher frequencies probably due to the inputs from saline springs within the reach. These springs have been shown to significantly affect the salinity of the Colorado River in this reach. The effect of multiple inputs on coherence is discussed in Chapter II. The response function spectrum is shown in Figure 11. This graph is almost identical to the power spectrum plot for the Grand Canyon time series (see Appendix B). The overall unit response for these two time series was 1.00 ppm downstream per ppm upstream. These results indicate that fluctuations in salinity at Lee Ferry determine the TDS concentration at the Grand Canyon station.

Description and Evaluation of Model

Due to the highly deterministic nature of this river reach system and the great similarity of the two time series, a simple model is proposed for predicting salinity at the Grand Canyon station using data collected at Lee Ferry. The components of the model are the TDS data at Lee Ferry and a salt loading factor which characterizes the impact of salt loading from the Little Colorado River.

To estimate this salt loading factor (SLF), the differences between corresponding points of the two TDS time series were computed.

The difference values tend to oscillate about some constant value and that no definite cyclic pattern was noted. The SLF for the model was computed as the arithmetic mean of the difference values and is equal to 66.6 ppm.

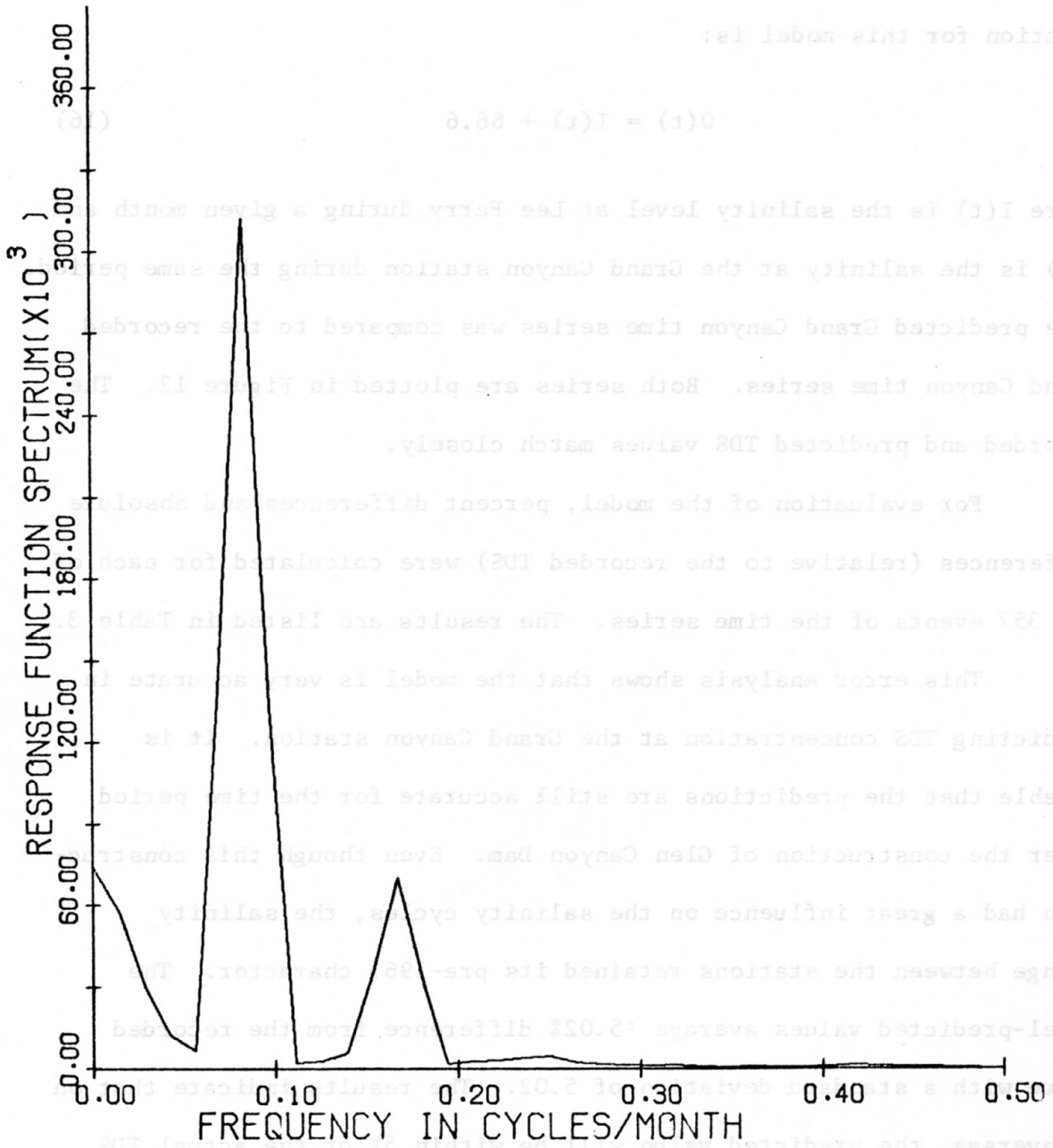

Figure 11. Response function spectrum from analysis of Lee Ferry and Grand Canyon time series.

A model-predicted time series was computed by adding 66.6 ppm to each data point of the recorded TDS time series for Lee Ferry. The equation for this model is:

$$O(t) = I(t) + 66.6 \qquad (16)$$

where I(t) is the salinity level at Lee Ferry during a given month and O(t) is the salinity at the Grand Canyon station during the same period. This predicted Grand Canyon time series was compared to the recorded Grand Canyon time series. Both series are plotted in Figure 12. The recorded and predicted TDS values match closely.

For evaluation of the model, percent differences and absolute differences (relative to the recorded TDS) were calculated for each of the 357 events of the time series. The results are listed in Table 3.

This error analysis shows that the model is very accurate in predicting TDS concentration at the Grand Canyon station. It is notable that the predictions are still accurate for the time period after the construction of Glen Canyon Dam. Even though this construction had a great influence on the salinity cycles, the salinity change between the stations retained its pre-1963 character. The model-predicted values average $\pm$5.02% difference from the recorded value with a standard deviation of 5.02. The results indicate that on an average, the predicted value will be within 5% of the actual TDS concentration. The probability of being within 10% is 0.68; within 15% is 0.95; and within 20% is 0.99. Since it has been shown that salinity at the Grand Canyon station can be fairly accurately predicted

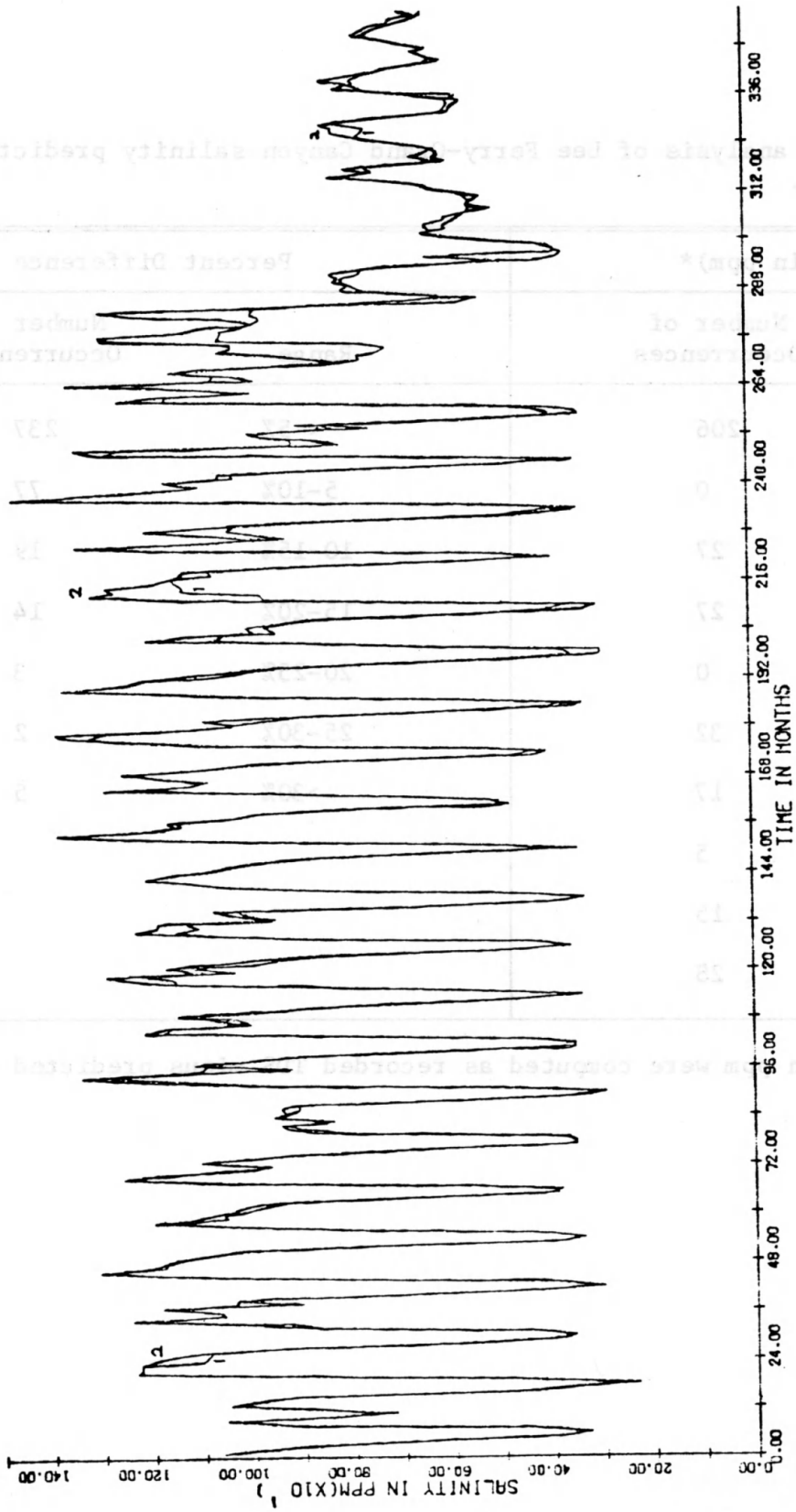

Figure 12. Recorded and model-predicted Grand Canyon time series (1941-70).

Line 1 is the recorded time series. Line 2 is the model time series. The time axis indicates the number of months from January 1941. The divisions mark twelve month periods.

Table 3. Error analysis of Lee Ferry-Grand Canyon salinity prediction model.

Difference (in ppm)*		Percent Difference	
Range	Number of Occurrences	Range	Number of Occurrences
< 0	206	< 5%	237
0- 5	0	5-10%	77
5-10	27	10-15%	19
10-15	27	15-20%	14
15-20	0	20-25%	3
20-30	32	25-30%	2
30-40	17	>30%	5
40-50	5		
50-60	15		
>60	28		

* Differences in ppm were computed as recorded TDS minus predicted TDS.

from data collected at Lee Ferry it should be possible to decrease the sampling frequency at the Grand Canyon Station.

In establishing a monitoring program, the first objective must be to define the state of the system. Here state refers to the normal or the expected salinity (TDS concentration, EC, etc.) in the Colorado River. This expected value will be defined by some model. To determine whether or not a sample or a series of samples indicates an abnormal change in salinity, it is compared to this expected value. The salt concentration predicted for a given time and place defines the state when the system is "in control." Significant deviations from this predicted value indicates that the system is "out of control." This situation would call for more extensive and/or frequent sampling to determine the cause of the unexpected change in salinity.

Here the important events would be when the actual TDS concentration is greater than that predicted by the model. The error analysis indicates that this type of event might be expected to occur 42.3% of the time. The actual TDS concentration is expected to be less than the predicted value 57.7% of the time. The probability of the actual TDS value being between the predicted concentrations and 20 ppm greater than the predicted value is 0.15. For the range 20 ppm over the predicted value to an excess of 50 ppm the probability is also 0.15. The probability of occurrence of an event when the real concentration is greater than 50 ppm over the predicted value is 0.12. These estimated probabilities are derived from the comparison of the model-predicted and the recorded TDS values above.

The following example is an illustration of how a sampling policy would be established and the parameters that must be evaluated in the process of making the policy. For this example only one level of acceptability is set: 50 ppm greater than the model-predicted TDS concentration. If a given sample is less than 50 ppm over the predicted value, the delay time to the next sample will be two months. If the sample is greater than 50 ppm over the predicted concentration, the system will be considered out of control and samples will be taken the next month. From the above discussion of probabilities:

P(actual TDS < 50 ppm greater than the predicted TDS) = 0.88

and

P(actual TDS > 50 ppm greater than the predicted TDS = 0.12

These probabilities are estimated from the error analysis in Table 3 and thus are approximations of the actual probabilities associated with these occurrences.

In the preceding paragraph, the first three steps in establishing a sampling policy is outlined. Levels of acceptability must be defined. Here there are two levels: (1) less than 50 ppm greater than the predicted concentration, and (2) greater than 50 ppm. Probabilities of occurrence are associated with each level of acceptability and a delay time is associated with each probability. Normally, in water quality sampling, higher probabilities of occurrence will be associated with longer delay periods because these events are being described by the prediction model.

Using the procedure outlined by Arnold (1970) the expected number of samples per year for the example policy was calculated. For this illustration, the number of sample-months per year would be 6.20. Using this over-simplified sampling policy, the sampling frequency could be reduced by about 50%. From the accuracy of the model predictions, delay periods of three or four months when the system was in control would not be unrealistic.

Another factor which would have to be considered in establishing a sampling policy is the probability of delaying a given number of time units before taking the next sample. This is equivalent to the probability of sampling once within the given time period. This probability is required in deciding whether or not, for a given sampling delay, the system can go out of control and this condition go undetected. For this example the calculation shows that:

P(sampling within 1 month) = .14

P(sampling within 2 month period) = 1.0

The sampling program outlined above is used as an example to illustrate the proceedure. Other sets of acceptance levels probabilities and their associated delay times would give different expected number of samples per year and probabilities of sampling within a given period. In establishing a sampling program many sets of levels of acceptance would be evaluated in the above manner. With these calculated parameters, along with consideration of economic feasibility, convenience, etc., a sampling policy would be established.

CHAPTER IV

LAKE MEAD MODEL

Analysis of the Time Series

The purpose of the Lake Mead portion of this study was to examine the movement of dissolved solids concentrations in the reservoir and to evaluate the several inputs into the system as to their effect on the quality of the waters released from Hoover Dam. An understanding of the impact and interaction of these inputs is essential for the management of the water quality in the lake and downstream from Hoover Dam.

Visually, the time series plots for the Grand Canyon station (Figure 5) and below Hoover Dam (Figure 13) show no striking similarities. The Hoover Dam releases do show a tendency to have peak concentrations early in the year and minimum concentrations in the last few months of each year. A similar pattern is noted in the Lee Ferry and Grand Canyon time series after the closure of Glen Canyon Dam. These fluctuations reflect variations in salinity of the reservoir inputs with the size and time of occurrence of the fluctuations being modified by the damping effects of the reservoir.

The peak in TDS concentration in the mid-1950's was due to the initiation of filling of Lake Powell. It is notable that these abnormally high concentrations are not evident in the Grand Canyon

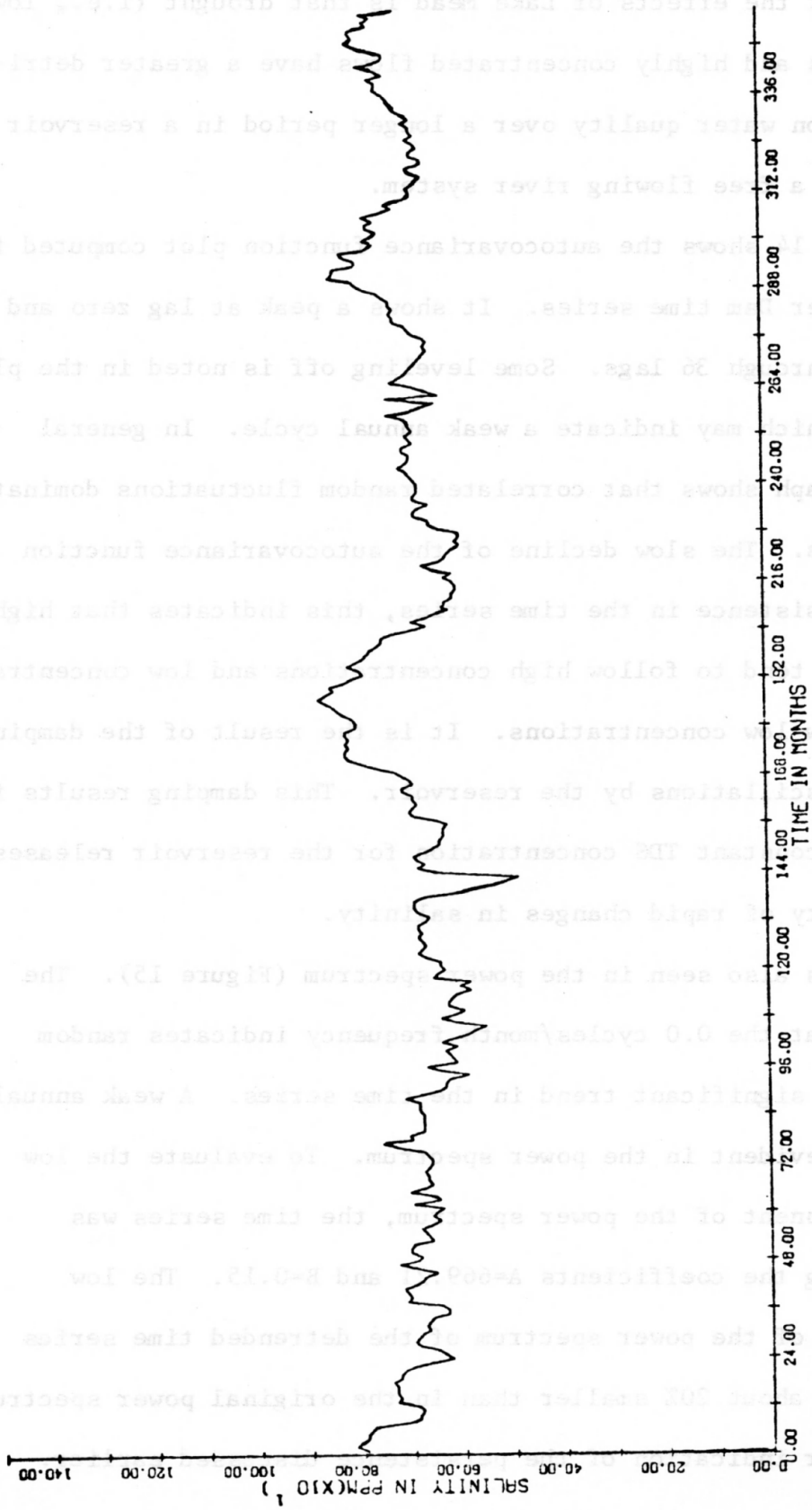

Figure 13. Below Hoover Dam time series (1941-70).

The time axis indicates the number of months from January 1941. The divisions mark twelve month periods.

series. One of the effects of Lake Mead is that drought (i.e., low inflow) periods and highly concentrated flows have a greater detrimental impact on water quality over a longer period in a reservoir system than in a free flowing river system.

Figure 14 shows the autocovariance function plot computed for the below Hoover Dam time series. It shows a peak at lag zero and a slow decline through 36 lags. Some leveling off is noted in the plot about lag 12 which may indicate a weak annual cycle. In general though, the graph shows that correlated random fluctuations dominate the time series. The slow decline of the autocovariance function shows some persistence in the time series, this indicates that high concentrations tend to follow high concentrations and low concentrations to follow low concentrations. It is the result of the damping of the input oscillations by the reservoir. This damping results in a more nearly constant TDS concentration for the reservoir releases and the scarcity of rapid changes in salinity.

This is also seen in the power spectrum (Figure 15). The dominant peak at the 0.0 cycles/month frequency indicates random variation or a significant trend in the time series. A weak annual cycle is also evident in the power spectrum. To evaluate the low frequency component of the power spectrum, the time series was detrended using the coefficients A=669.21 and B=0.15. The low frequency peak of the power spectrum of the detrended time series (Figure 16) is about 20% smaller than in the original power spectrum. This is another indication of the persistence discussed earlier.

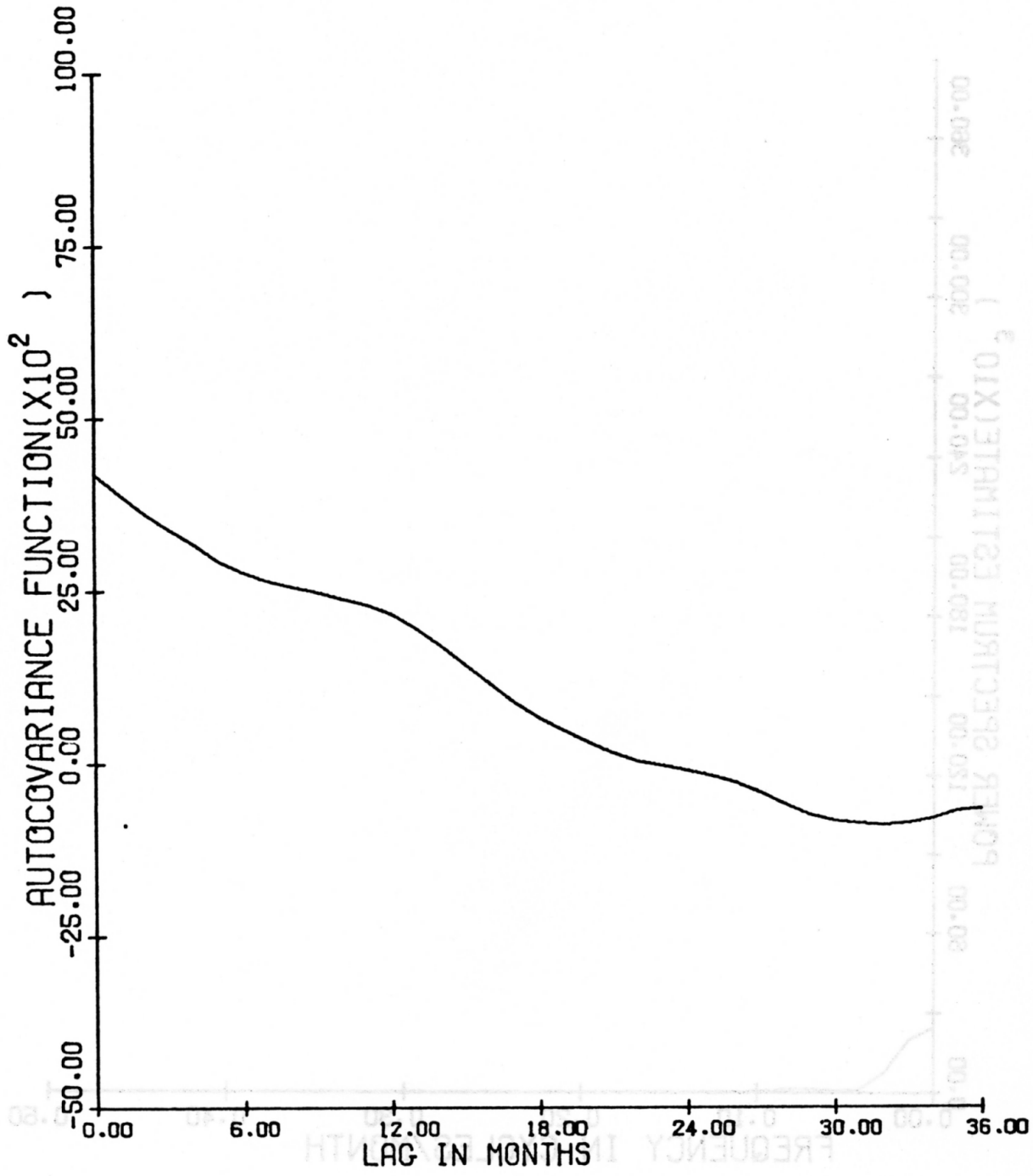

Figure 14. Autocovariance function for below Hoover Dam time series (1941-70).

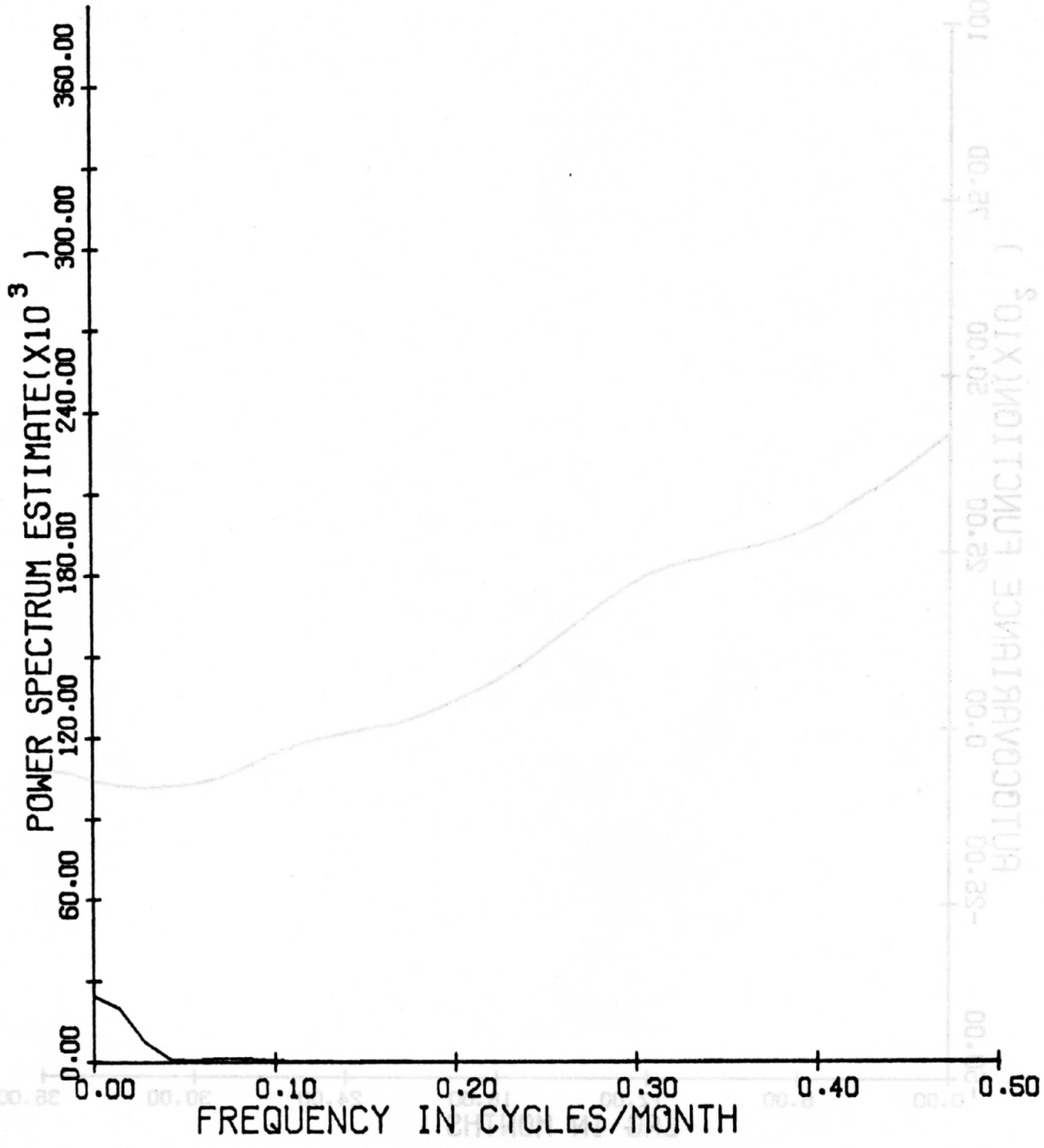

Figure 15. Power spectrum of below Hoover Dam time series (1941-70).

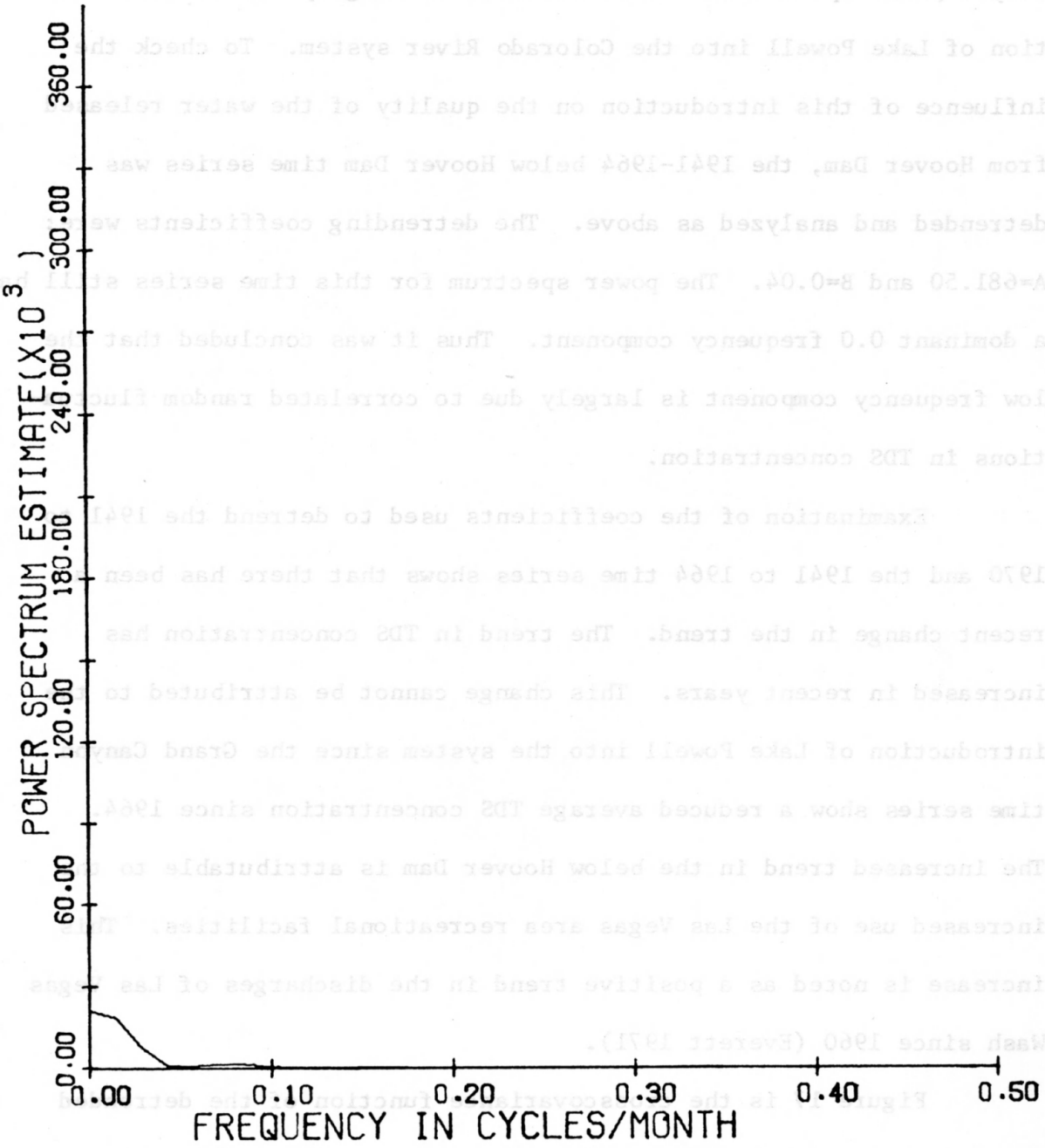

Figure 16. Power spectrum of detrended below Hoover Dam time series (1941-70).

The low frequency components in the Lee Ferry and the Grand Canyon power spectra have been shown to be largely due to the introduction of Lake Powell into the Colorado River system. To check the influence of this introduction on the quality of the water released from Hoover Dam, the 1941-1964 below Hoover Dam time series was detrended and analyzed as above. The detrending coefficients were: A=681.50 and B=0.04. The power spectrum for this time series still has a dominant 0.0 frequency component. Thus it was concluded that the low frequency component is largely due to correlated random fluctuations in TDS concentration.

Examination of the coefficients used to detrend the 1941 to 1970 and the 1941 to 1964 time series shows that there has been a recent change in the trend. The trend in TDS concentration has increased in recent years. This change cannot be attributed to the introduction of Lake Powell into the system since the Grand Canyon time series show a reduced average TDS concentration since 1964. The increased trend in the below Hoover Dam is attributable to the increased use of the Las Vegas area recreational facilities. This increase is noted as a positive trend in the discharges of Las Vegas Wash since 1960 (Everett 1971).

Figure 17 is the crosscovariance function of the detrended Grand Canyon and below Hoover Dam time series. Since the maximum value of the crosscovariance function is not at zero, a significant (i.e., greater than 1 month) time lag is indicated. The maximum crosscovariance is at +17 months which would indicate a lag of 17 months

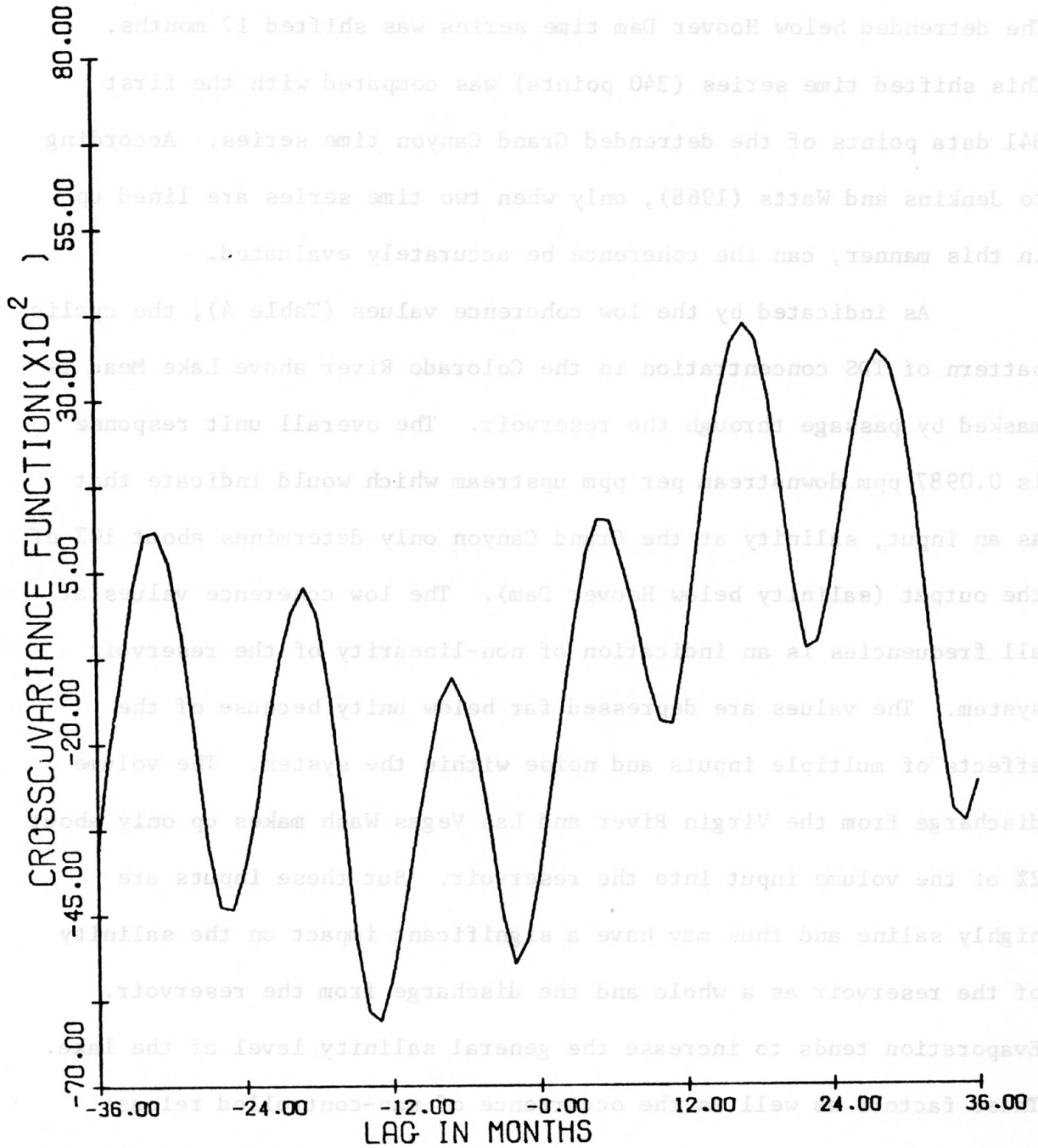

Figure 17. Crosscovariance function for Grand Canyon and below Hoover Dam time series (1941-70).

between the Grand Canyon station and the below Hoover Dam station. The detrended below Hoover Dam time series was shifted 17 months. This shifted time series (340 points) was compared with the first 341 data points of the detrended Grand Canyon time series. According to Jenkins and Watts (1968), only when two time series are lined up in this manner, can the coherence be accurately evaluated.

As indicated by the low coherence values (Table 4), the cyclic pattern of TDS concentration in the Colorado River above Lake Mead is masked by passage through the reservoir. The overall unit response is 0.0987 ppm downstream per ppm upstream which would indicate that as an input, salinity at the Grand Canyon only determines about 10% of the output (salinity below Hoover Dam). The low coherence values at all frequencies is an indication of non-linearity of the reservoir system. The values are depressed far below unity because of the effects of multiple inputs and noise within the system. The volume discharge from the Virgin River and Las Vegas Wash makes up only about 2% of the volume input into the reservoir. But these inputs are highly saline and thus may have a significant impact on the salinity of the reservoir as a whole and the discharge from the reservoir. Evaporation tends to increase the general salinity level of the lake. These factors as well as the occurrence of man-controlled release cycles may be acting to increase the noise in the system, thus leading to the depressed coherency.

To examine the changes in salinity between the Grand Canyon and Hoover Dam, the differences between corresponding points on the

Table 4. Coherence and response function spectrum for Grand Canyon and below Hoover Dam time series.

Frequency (Cycles/Month)	Coherence	Response Function Spectrum
0.000	.096	1906.041
.014	.229	4047.414
.028	.324	2381.745
.042	.049	46.137
.056	.228	116.016
.069	.213	206.244
.083	.523	655.506
.097	.432	328.373
.111	.123	52.470
.125	.098	22.470
.139	.013	2.370
.153	.046	9.282
.167	.133	21.217
.181	.103	10.708
.194	.127	14.746
.208	.139	14.613
.222	.179	21.332
.236	.065	8.763
.250	.141	21.406
.264	.064	9.086
.278	.122	12.254
.292	.126	11.168
.306	.135	13.724
.319	.001	.154
.333	.036	2.665
.347	.134	8.442
.361	.033	1.599
.375	.015	.553
.389	.047	1.730
.403	.243	6.771
.417	.141	5.459
.431	.028	1.706
.444	.044	2.890
.458	.182	9.402
.472	.198	9.855
.486	.121	5.293

Grand Canyon and shifted below Hoover Dam time series were computed. The differences show a strong annual fluctuation similar to the Grand Canyon time series but the difference time series shows maxima where the Grand Canyon series shows minimum concentrations; the two series appear as inverses of one another.

River flows having low TDS concentrations at the Grand Canyon undergo great increases in concentration by the time it is released from Hoover Dam. River flows with high TDS concentrations show smaller changes or even become more dilute. As the relatively dilute river flows pass through the more saline water of Lake Mead, exchange of salt occurs between the two water bodies. This exchange process is the damping effect of reservoirs on salinity cycles shown in the Lee Ferry and Grand Canyon time series after construction of Glen Canyon Dam. This damping mechanism as well as the relatively long residence time in Lake Mead causes the above statistical parameters to show only a slight causal relationship between the Grand Canyon and the below Hoover Dam time series. Since the Colorado River constitutes 98% of the flow into Lake Mead, the impact of this input should be larger than is indicated above.

The response function is not shown because the low coherence values and the dissimilarities between the autocovariance functions and the power spectra of the two time series indicated that the condition of statistical similarity (see Chapter II) could not be met. Thus the response function spectrum and the overall unit response were concluded to give unreliable indications. The distortion of the input

cycles caused by the damping during transit through the reservoir may be the mechanism resulting in false statistical indications.

Description of the Model

The three major inputs into Lake Mead are the Colorado River, the Virgin River, and Las Vegas Wash. Variations in the salinity and volume of these inputs plus physical factors like evaporation, precipitation, and biological activity determine the variations in salinity of the water released from Hoover Dam. If the impact of each of the inputs are superimposed in time and added together, the result should be the output releases from the reservoir. Conversely, if the sum of the inputs is subtracted from the output, the residual should be nearly a straight line.

To evaluate this procedure, the 1970 water year releases from Hoover Dam were analyzed. The impact of the major inputs and the output data was standardized by weighting the TDS concentrations with respect to the volume of the input or output discharge. The standardizing computation was:

$$\frac{(\text{TDS in ppm}) \times (\text{Discharge for month in acre-feet})}{(\text{Lake volume in acre-feet})}$$

This standardization was used to put the salinity time series in a form such that the TDS concentrations in each of the input series could be compared to one another. The above computation is a scaling function to put the recorded salinities on the same scale with the values relative to the impact of the discharges on the salinity of the reservoir. The input series were shifted in time so that they

corresponded to the output of the 1970 water year. When the time lags computed using the crosscovariance function were used to make these shifts, the residual after subtracting the sum of inputs from the output had a cyclic pattern with no physical explanation. Examination of the input impact series suggested that the use of a 24 month (rather than 17 month) time lag between the Grand Canyon and the below Hoover Dam series might give better results. Samples of standardized data series are listed in Table 5. The justification for using an average 24 month time lag between the Grand Canyon and the below Hoover Dam time series can be seen by the similarity of the two standardized data series shown in Figure 18. From Figure 18, it can be seen that variations in the standardized input from the Colorado River are reflected in variations two years later below Hoover Dam. During the summer and fall, the figure indicates that salinity has increased more between input and discharge than for other periods. Given the 24 month time lag from the Grand Canyon to Hoover Dam, this increase is due to evaporation. Figure 19 shows an average annual evaporation cycle computed by taking the averages evaporation of each month for water years 1966 to 1970. The monthly evaporation losses used were computed by the U.S. Geological Survey using methods outlined in Geological Survey Professional Paper 298 (Harbeck, Kohler, Koberg, and others 1958). The figure shows that peak evaporation occurs from June through October. These periods would have the greatest impact on the salinity of water flowing through the lake. From Figure 19, evaporation probably has a negligible effect on salinity

Table 5. Standardized time series data for Lake Mead model.

Month	Grand Canyon (1968 Water Year)	Virgin River (Feb. 1968-Jan. 1969)	Las Vegas Wash (1970 Water Year)	Hoover Dam (1970 Water Year)
Oct.	17.58	1.46	0.90	22.50
Nov.	18.30	1.15	0.82	20.07
Dec.	23.93	1.36	0.79	21.79
Jan.	29.61	1.36	0.81	29.45
Feb.	24.74	.63	0.70	25.74
Mar.	41.30	.94	0.76	36.52
Apr.	48.98	1.93	0.82	56.52
May	48.26	.48	0.75	49.76
June	42.44	.91	0.58	42.52
July	35.84	.95	0.61	44.23
Aug.	27.97	1.37	0.59	39.43
Sept.	24.07	4.21	0.80	25.66

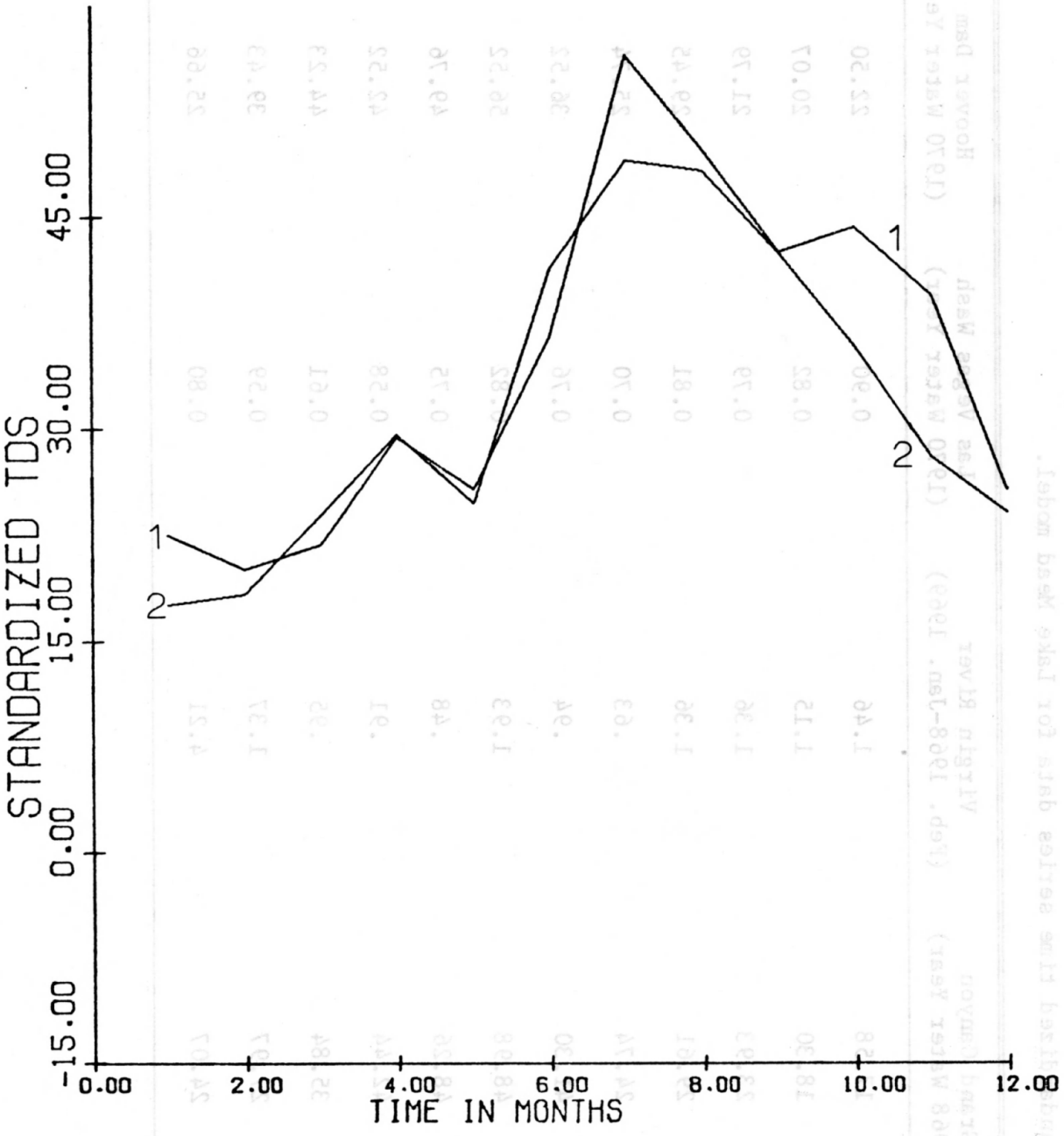

Figure 18. Standardized TDS data series for Grand Canyon (1968) and below Hoover Dam (1970).

The time axis indicates months of water year: 1 = October, 2 = November, . . . , 12 = September. Line 1 is the Hoover Dam series. Line 2 is the Grand Canyon series.

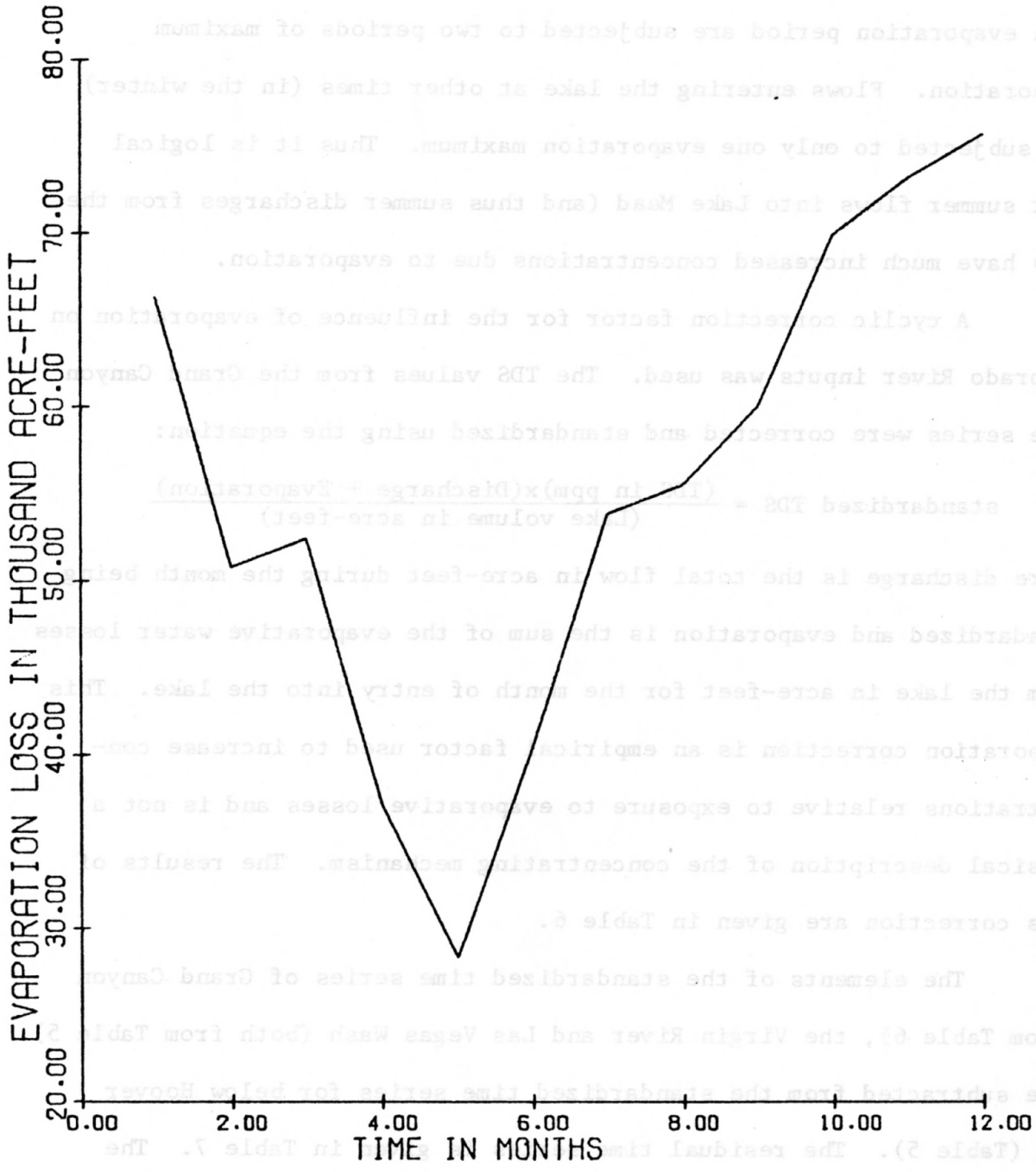

Figure 19. Average evaporation loss cycle for Lake Mead.

The time axis indicates months of water year: 1 = October, 2 = November, . . . , 12 = September.

during other parts of the year. Flows entering the reservoir during a high evaporation period are subjected to two periods of maximum evaporation. Flows entering the lake at other times (in the winter) are subjected to only one evaporation maximum. Thus it is logical that summer flows into Lake Mead (and thus summer discharges from the dam) have much increased concentrations due to evaporation.

A cyclic correction factor for the influence of evaporation on Colorado River inputs was used. The TDS values from the Grand Canyon time series were corrected and standardized using the equation:

$$\text{standardized TDS} = \frac{(\text{TDS in ppm}) \times (\text{Discharge} + \text{Evaporation})}{(\text{Lake volume in acre-feet})}$$

where discharge is the total flow in acre-feet during the month being standardized and evaporation is the sum of the evaporative water losses from the lake in acre-feet for the month of entry into the lake. This evaporation correction is an empirical factor used to increase concentrations relative to exposure to evaporative losses and is not a physical description of the concentrating mechanism. The results of this correction are given in Table 6.

The elements of the standardized time series of Grand Canyon (from Table 6), the Virgin River and Las Vegas Wash (both from Table 5) were subtracted from the standardized time series for below Hoover Dam (Table 5). The residual time series is given in Table 7. The standardized Hoover Dam time series and the residuals from Table 7 are shown in Figure 20.

Table 6. Standardized and evaporation corrected TDS input from Grand Canyon time series 1968 water year.

Month	Grand Canyon Input
Oct.	20.31
Nov.	23.66
Dec.	26.30
Jan.	31.14
Feb.	25.65
Mar.	42.99
Apr.	50.97
May	51.17
June	45.43
July	40.36
Aug.	30.32
Sept.	26.59

Table 7. Residual standardized time series for 1970 water year discharge from Lake Mead.

Month	Residuals
Oct.	.23
Nov.	-5.77
Dec.	-6.66
Jan.	-3.13
Feb.	-1.55
Mar.	-9.16
Apr.	4.25
May	-3.07
June	-4.44
July	3.90
Aug.	4.32
Sept.	-3.18

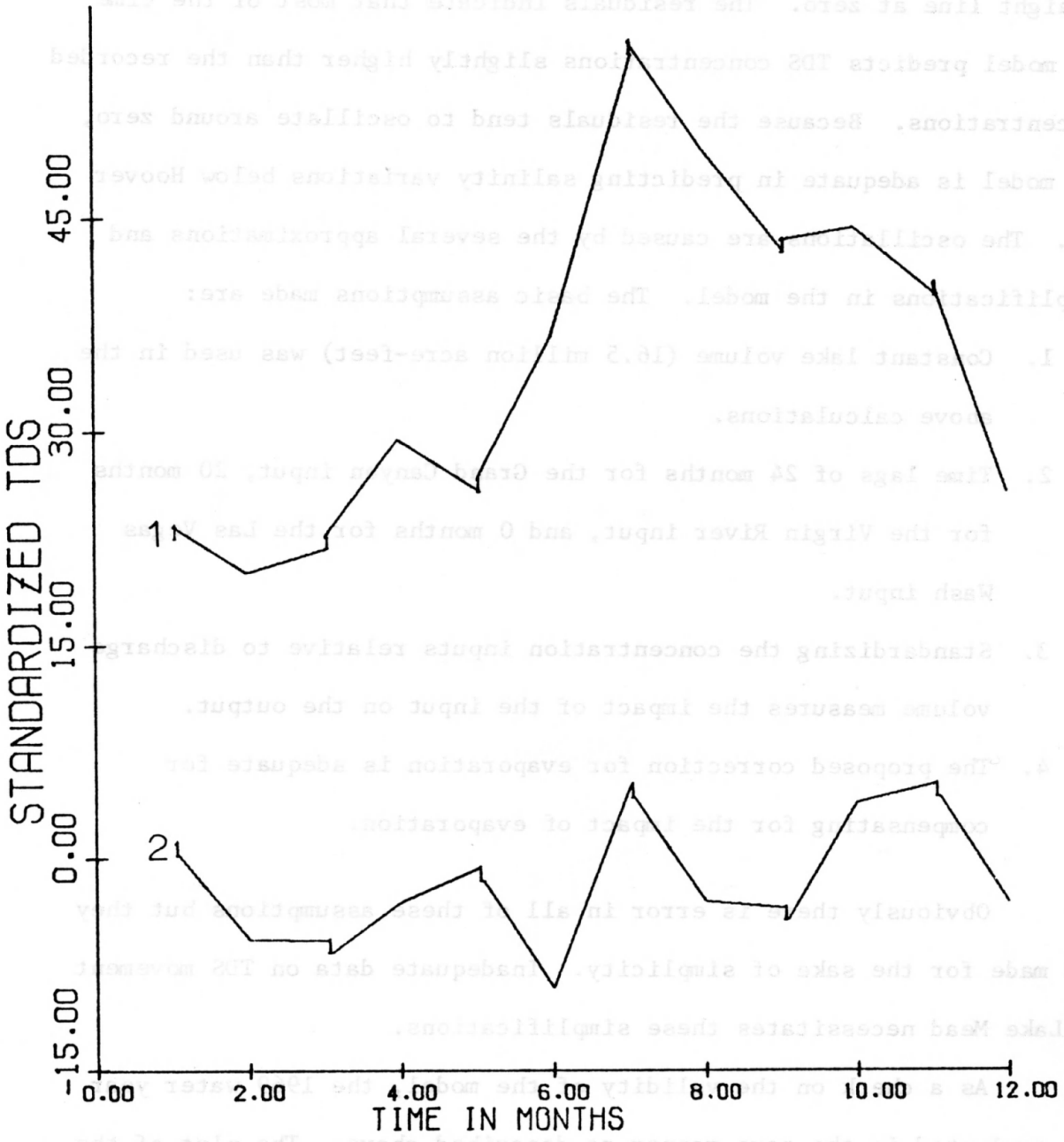

Figure 20. Standardized below Hoover Dam series (1970) and Residuals (1970).

Line 1 is the below Hoover Dam series. Line 2 is the residual series. The time axis indicates months of water year: 1 = October, etc.

Evaluation of the Model

Theoretically, the residual plot in Figure 20 should be a straight line at zero. The residuals indicate that most of the time the model predicts TDS concentrations slightly higher than the recorded concentrations. Because the residuals tend to oscillate around zero, the model is adequate in predicting salinity variations below Hoover Dam. The oscillations are caused by the several approximations and simplifications in the model. The basic assumptions made are:

1. Constant lake volume (16.5 million acre-feet) was used in the above calculations.
2. Time lags of 24 months for the Grand Canyon input, 20 months for the Virgin River input, and 0 months for the Las Vegas Wash input.
3. Standardizing the concentration inputs relative to discharge volume measures the impact of the input on the output.
4. The proposed correction for evaporation is adequate for compensating for the impact of evaporation.

Obviously there is error in all of these assumptions but they are made for the sake of simplicity. Inadequate data on TDS movement in Lake Mead necessitates these simplifications.

As a check on the validity of the model, the 1969 water year was evaluated in the same manner as described above. The plot of the residuals is shown in Figure 21. The figure shows a pattern similar to that obtained in the calibration of the model for 1970 water year.

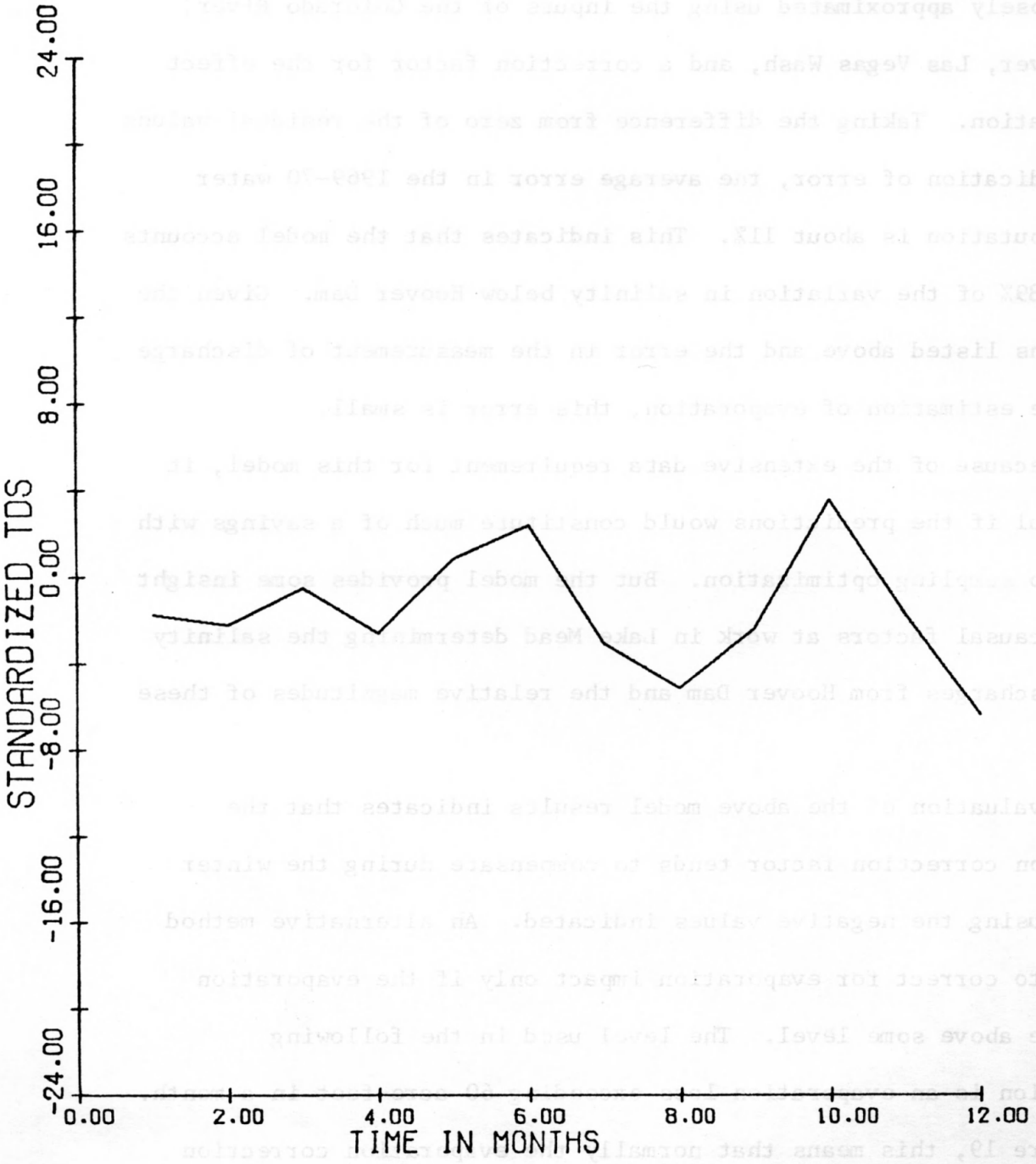

Figure 21. Residuals computed for 1969 water year.

The time axis indicates months of water year: 1 = October, etc.

It has been shown that variations in salinity at Hoover Dam can be closely approximated using the inputs of the Colorado River, Virgin River, Las Vegas Wash, and a correction factor for the effect of evaporation. Taking the difference from zero of the residual values as the indication of error, the average error in the 1969-70 water years computation is about 11%. This indicates that the model accounts for over 89% of the variation in salinity below Hoover Dam. Given the assumptions listed above and the error in the measurement of discharge and in the estimation of evaporation, this error is small.

Because of the extensive data requirement for this model, it is doubtful if the predictions would constitute much of a savings with respect to sampling optimization. But the model provides some insight into the causal factors at work in Lake Mead determining the salinity of the discharges from Hoover Dam and the relative magnitudes of these factors.

Evaluation of the above model results indicates that the evaporation correction factor tends to compensate during the winter months causing the negative values indicated. An alternative method might be to correct for evaporation impact only if the evaporation losses are above some level. The level used in the following illustration is an evaporation loss exceeding 60 acre-feet in a month. From Figure 19, this means that normally the evaporation correction would only be applied to the summer and fall inputs into the reservoir. Figure 18 shows that these inputs show a significant change which can be attributed to evaporation. With the correction factor for

evaporation being selectively applied as indicated above, the residuals for the 1969 and 1970 water years were computed.

Seasonal or selective evaporation impact weighting is supported by the general circulation patterns as presented by Anderson and Pritchard (1951) and by Smith, Vetter, Cummings, and others (1954). As the Colorado River flows into Lake Mead, it follows one of three paths. Overflow is the spreading of inflowing water over the lake surface. This flow pattern is characteristic of the spring and summer seasons due to the relatively low salinity and/or warm temperature of the Colorado River water. Figure 22 shows the average month temperatures for the 1967-1969 water years. The annual temperature cycle shows that the highest temperature flows occur during periods of high evaporation (see Figure 20). These flows in the late spring and summer generally have an overflow pattern upon entering the reservoir. These introduced surface waters would be exposed to the period of highest evaporation losses. The concentrating effect of evaporation would result in an increase in salinity in addition to the increase from diffusion of dissolved salts from the surrounding lake water.

Interflow is a flow pattern characterized by movement at some intermediate depth in the lake. It occurs in the fall season when salinity and temperature conditions in the Colorado River are such that the river flows are more dense than the lake surface waters but less dense than the lake bottom waters. This flow pattern is the least significant of the three.

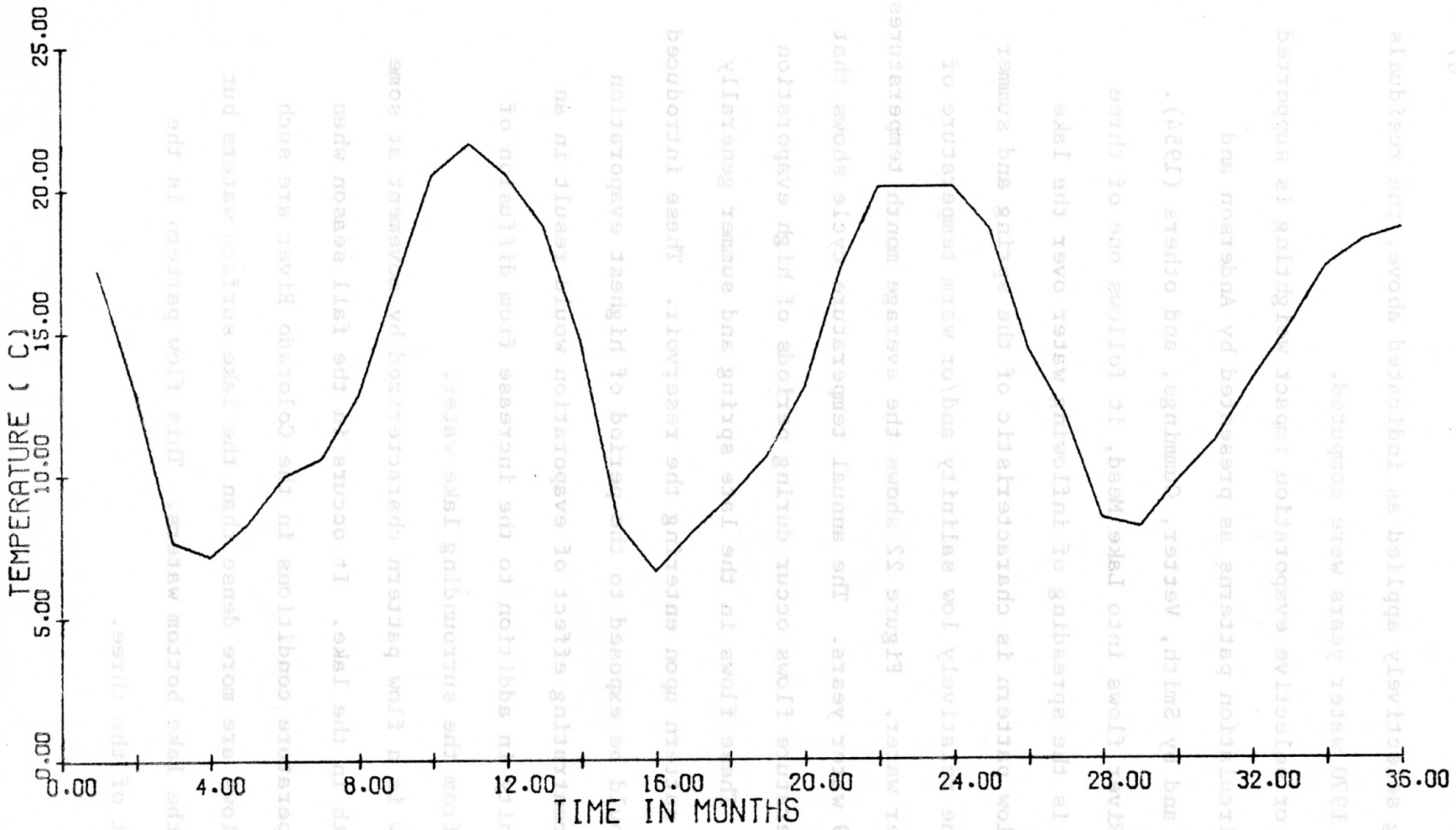

Figure 22. Temperature (°C) at Grand Canyon station (1967-69).

On the time axis, 1 = October, . . . , 36 = September.

Underflow occurs when the river inflow is more dense than the lake waters at all depths. This flow pattern along the lake bottom is characteristic of winter when low temperature and high salinity flows in the Colorado River create a period of maximum density. Such flows are not affected by evaporation at the surface are TDS changes occur only by the diffusion process.

The weighting of the Grand Canyon input with respect to the season of the input is supported by the nature of the evaporation cycle and the seasonal form of the flow patterns in Lake Mead. This evaporation correction is an empirical factor used to increase concentrations relative to exposure to evaporative losses and is not a physical description of the concentrating mechanism. The results of this correction are given in Table 8 and in Figure 23.

The modified model shows an average error of 9.80% with respect to the theoretical zero values. The mean residual for the 1969-70 water years was -0.60. The mean absolute difference from the zero line was 3.08 units with a variance of 2.20.

These results indicate the validity of relating salinity impact to discharge volume and concentration of discharge and the proposed correction factor for evaporation impact. The weighting computations are necessarily estimates and empirical in nature because of inadequate understanding of the physical mechanisms of evaporation, dilution, precipitation, sediment interaction, etc. Nevertheless, this model gives fairly good results. The form of the model (the salinity impact factors and the evaporation correction factor) appears to be valid.

Table 8. Input series from Grand Canyon weighted selectively for evaporation during summer and fall months and residuals for modified model.

Month	Grand Canyon Input	Residual
Oct.	20.78	-1.57
Nov.	18.67	-0.56
Dec.	21.00	+1.50
Jan.	24.35	-1.83
Feb.	21.62	+1.84
Mar.	30.42	+4.83
Apr.	38.35	+0.61
May	38.35	-4.13
June	32.31	+0.30
July	31.12	+3.94
Aug.	31.05	-1.65
Sept.	31.64	-6.45
Oct.	20.31	-0.18
Nov.	22.07	-3.97
Dec.	23.93	-4.29
Jan.	29.61	-2.33
Feb.	24.74	-0.32
Mar.	41.30	-6.49
Apr.	48.72	-5.06
May	48.26	-0.26
June	45.43	-4.40
July	38.36	+4.32
Aug.	30.32	+7.15
Sept.	26.59	-5.93

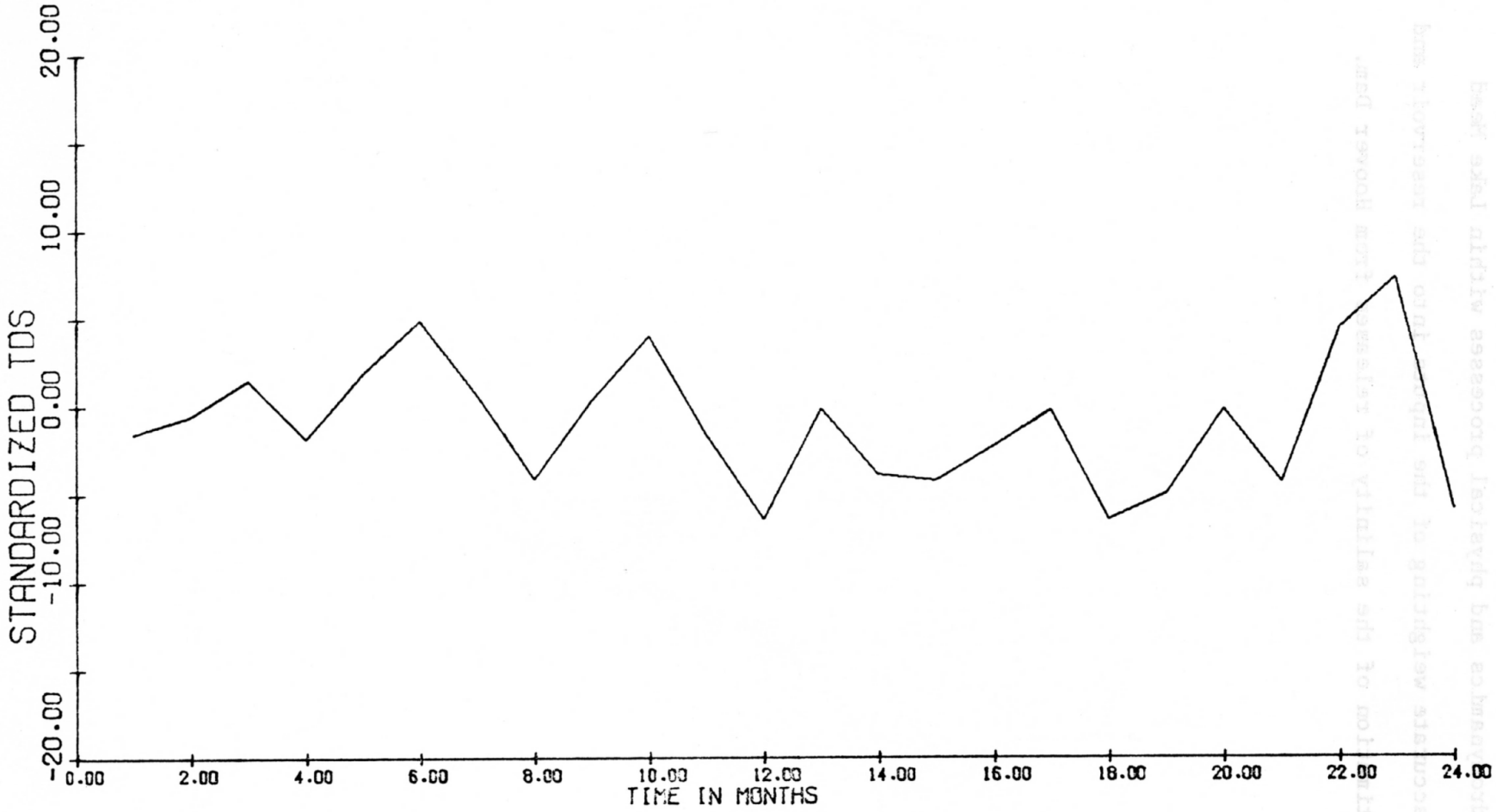

Figure 23. Residuals from selective evaporation-weighting model (1969-70).

The time axis indicates months of water years: 1 = October, 2 = November, . . . , 24 = September.

Models of the hydrodynamics and physical processes within Lake Mead will allow more accurate weighting of the inputs into the reservoir and more accurate estimation of the salinity of releases from Hoover Dam.

CHAPTER V

LAKE MOHAVE-LAKE HAVASU REACH

Analysis of the Time Series

Visual comparison of the Parker Dam and below Hoover Dam time series (Figures 24 and 13, respectively) shows that fluctuations in salinity at Hoover Dam are reflected, in variations at Parker Dam. The Parker Dam series shows the TDS concentration maximum in the mid-1950's caused by drought and the mid-1960's maximum from the beginning of the filling of Lake Powell.

Davis Dam which creates the Lake Mohave reservoir was completed in 1953. The effect of this completion on water quality is not apparent in the time series plot. Much of the impact of this new reservoir is masked by the drought-caused salinity increase during this same period. Lake Mohave has a length of 67 miles and a surface area of about 44 square miles. These dimensions indicate an average width of about 0.66 miles. The maximum width of the reservoir is about 4 miles. With this small size, the reservoir probably has a negligable effect on water quality.

Lake Havasu behind Parker Dam has a surface area of about 39 square miles and a length of 45 miles. This gives an average width of about 0.87 miles. The combined capacity of both Lake Mohave (1,818,300 acre-feet) and Lake Havasu (648,000 acre-feet) is 2,466,300 acre-feet. The average discharge from Hoover Dam for the period 1941

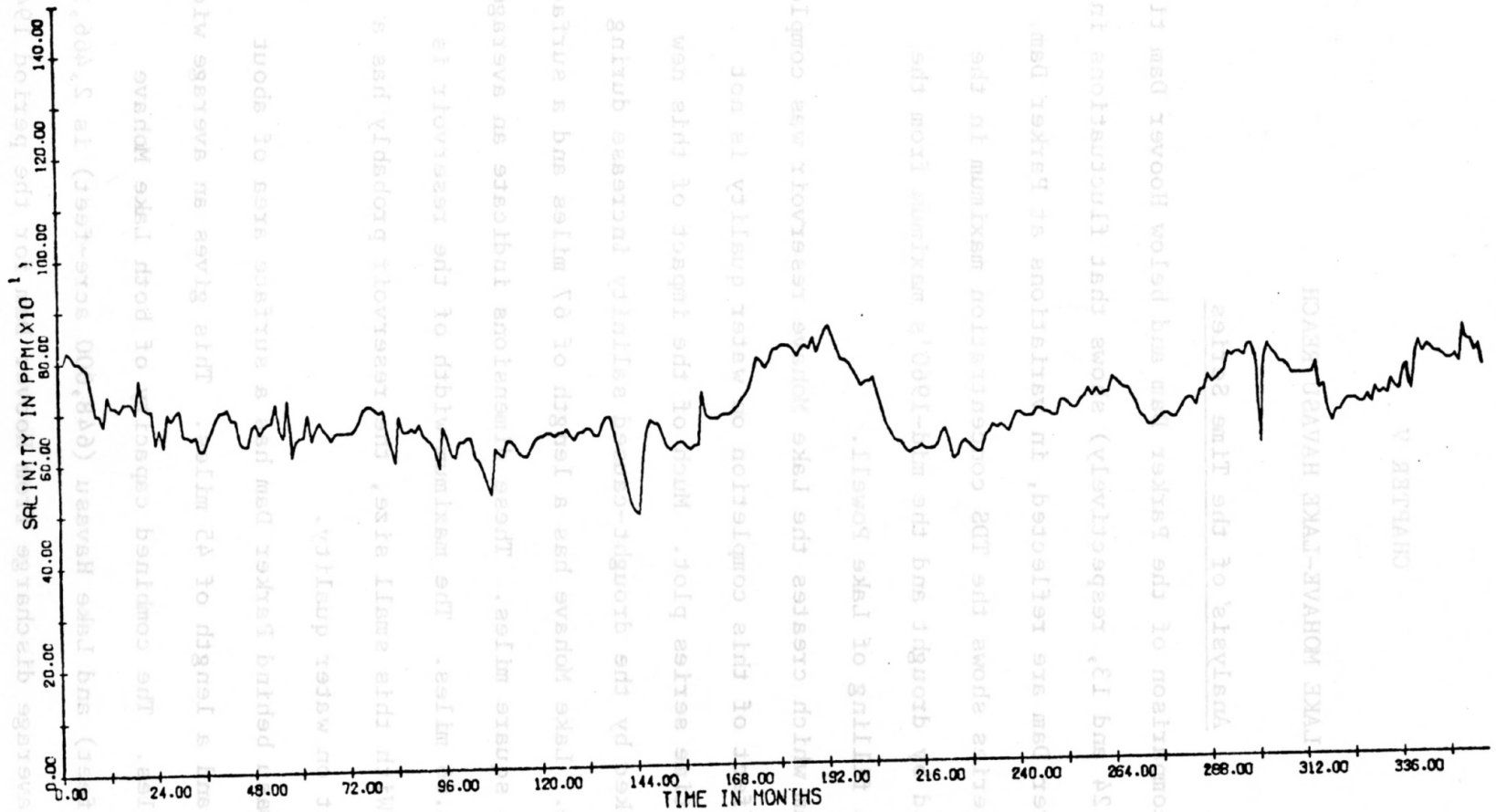

Figure 24. Parker Dam TDS time series (1941-70).

The time axis indicates the number of months from January 1941. The divisions mark twelve month periods.

to 1968 was 10,682,000 acre-feet. Comparison of capacity volume to inflow volume indicates that, even if the reservoirs were operated at full capacity, enough water enters the system to allow a complete turnover over four times each year. Due to the short residence time in the lake chain below Hoover Dam, small increases in salinity due to evaporation is a reasonable conclusion. The major input into these lakes other than the Colorado River main streams is the Bill Williams River. The effects of this tributary are discussed later.

As discussed earlier, the data for the Parker Dam time series is from the Metropolitan Water District of Southern California Pumping Station above Parker Dam. These TDS concentrations are reported as ppm calculated as the sum of constituents of the major ions. Such computed concentrations tend to be lower than the TDS concentrations obtained by weighing the residue after evaporation at 180°C. TDS concentrations reported in the other time series were obtained by this procedure. As indicated above, fluctuations in salinity at Hoover Dam are reflected in fluctuations at Parker Dam. Thus the two methods of chemical analysis cause no problems in evaluating changes in salinity patterns between the two river stations. But analysis of the magnitude of any change in TDS concentration between Hoover Dam and Parker Dam is made difficult because of the inconsistency of the data. Because of this data problem, most of the analysis of this river reach and the reach from Parker Dam to Yuma will deal with the patterns of salinity change rather than with absolute magnitudes of these changes.

Figure 25 is the plot of the autocovariance function for the Parker Dam time series. It shows the same weak correlation pattern as the below Hoover Dam time series. Random fluctuations in TDS concentration also dominate this time series. The power spectrum for the Parker Dam (Figure 26) time series also shows the dominance of this random component. A small annual cycle is shown in this power spectrum which is almost identical to the spectrum for the below Hoover Dam time series.

To examine the effect of trends in TDS concentration on the low frequency component of the power spectrum, the Parker Dam time series was detrended using the linear least squares method described above. The detrending coefficients for the 1941-1970 series were: A=654.94889 and B=0.16645. This detrending did not significantly alter the form of the power spectrum. Long period components can also contribute to the low frequency power spectrum estimate. The TDS maxima caused by the drought of the mid-1950's and the filling of Lake Powell do form such a long period wave and may thus contribute to the low frequency spectral estimate. As these are random or transient events, it is concluded that random variations create the low frequency spectrum component.

As before the time series for the period 1941-1964 was also detrended to determine any recent changes in trends in salinity. The detrending coefficients for this time series are: A=673.48 and B=0.008. This would indicate a slightly negative trend in salinity before 1964 but the closeness of B to zero indicates that this indication is

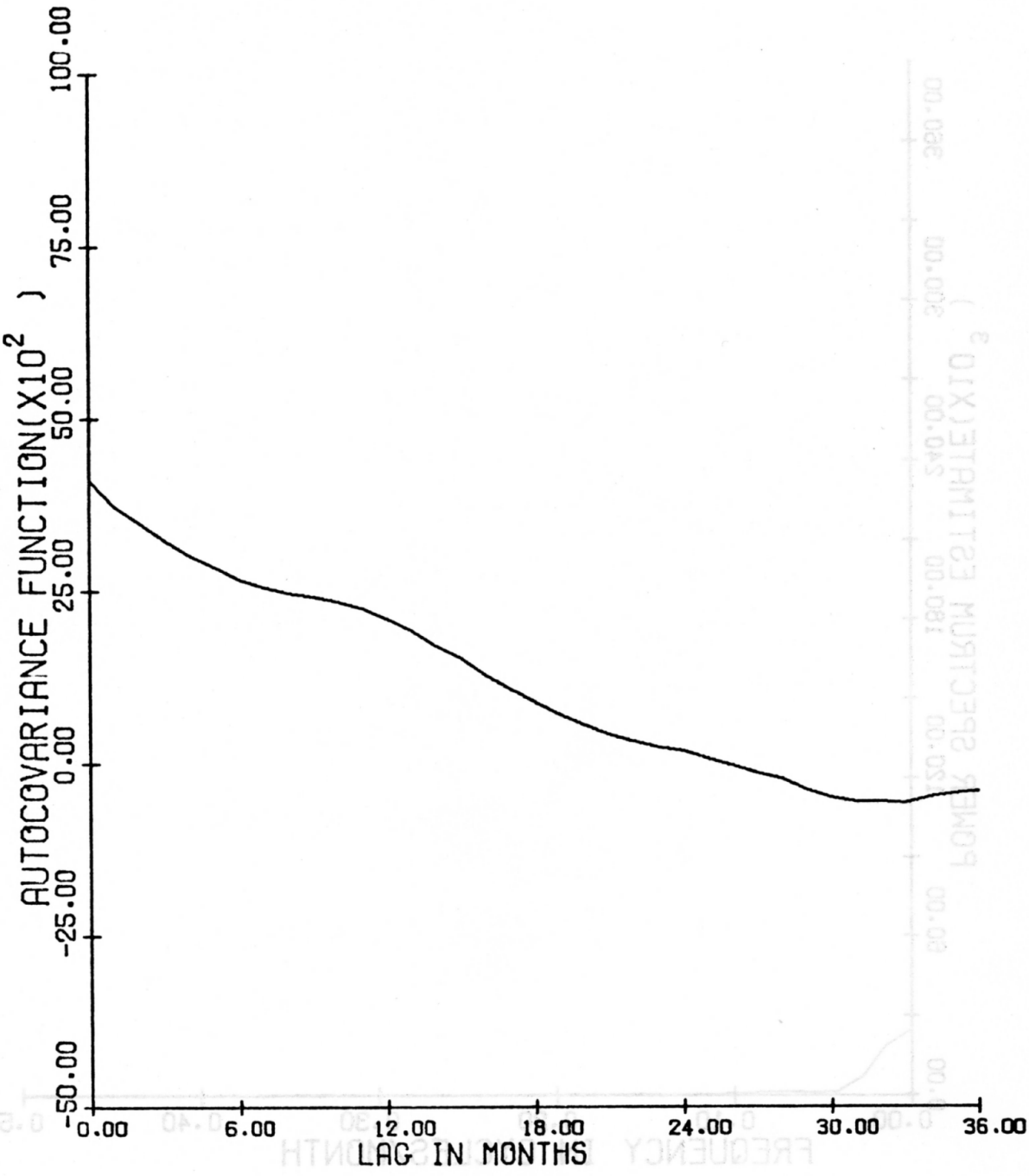

Figure 25. Autocovariance function for Parker Dam time series (1941-70).

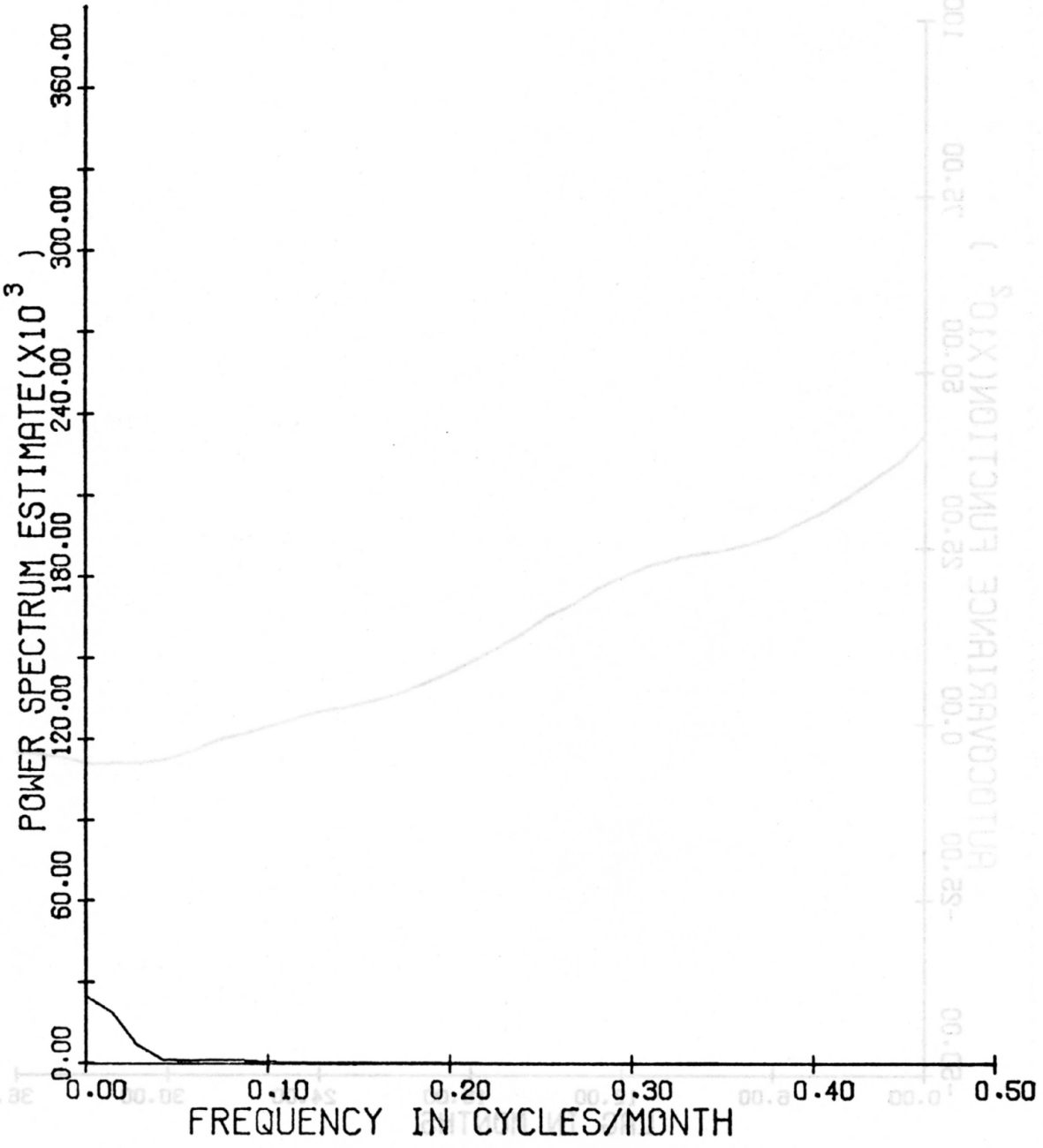

Figure 26. Power spectrum of Parker Dam time series (1941-70).

probably more a computational than a physical phenomenon. The results do indicate that in the past few years there has been a significant positive trend added to the TDS time series. From the close correspondence between changes in salinity at Hoover Dam and changes at Parker Dam, the cause of the recent increased salinity trend in the time series is due to increased discharges from Las Vegas Wash.

Figure 27 is the plot of the crosscovariance function for the below Hoover Dam-Parker Dam time series. The maximum value occurs at a lag of two months. Before the coherence and response parameters were computed, the Parker Dam time series was shifted by two months. The cross covariance function plot comparing the below Hoover Dam series to this shifted series showed the maximum at zero months. The value of the crosscovariance function of the original series at a one month lag is very close to the computated values for a two month lag. In the development of the following model it became apparent that physical explanations of fluctuations in salinity between Hoover Dam and Parker Dam are more valid in some cases if a one month time lag is used.

Visual examination of the below Hoover Dam and Parker Dam time series, and the power spectra of the two series demonstrated the similarities between salinity at these two stations. The short lag time indicated that salinity increases due to evaporation losses would be negligible. The Bill Williams River is the only other input into the two lake system but normally its influence is small.

Table 9 shows the coherence and the response spectrum for this station's set. The high coherence value at the zero frequency is

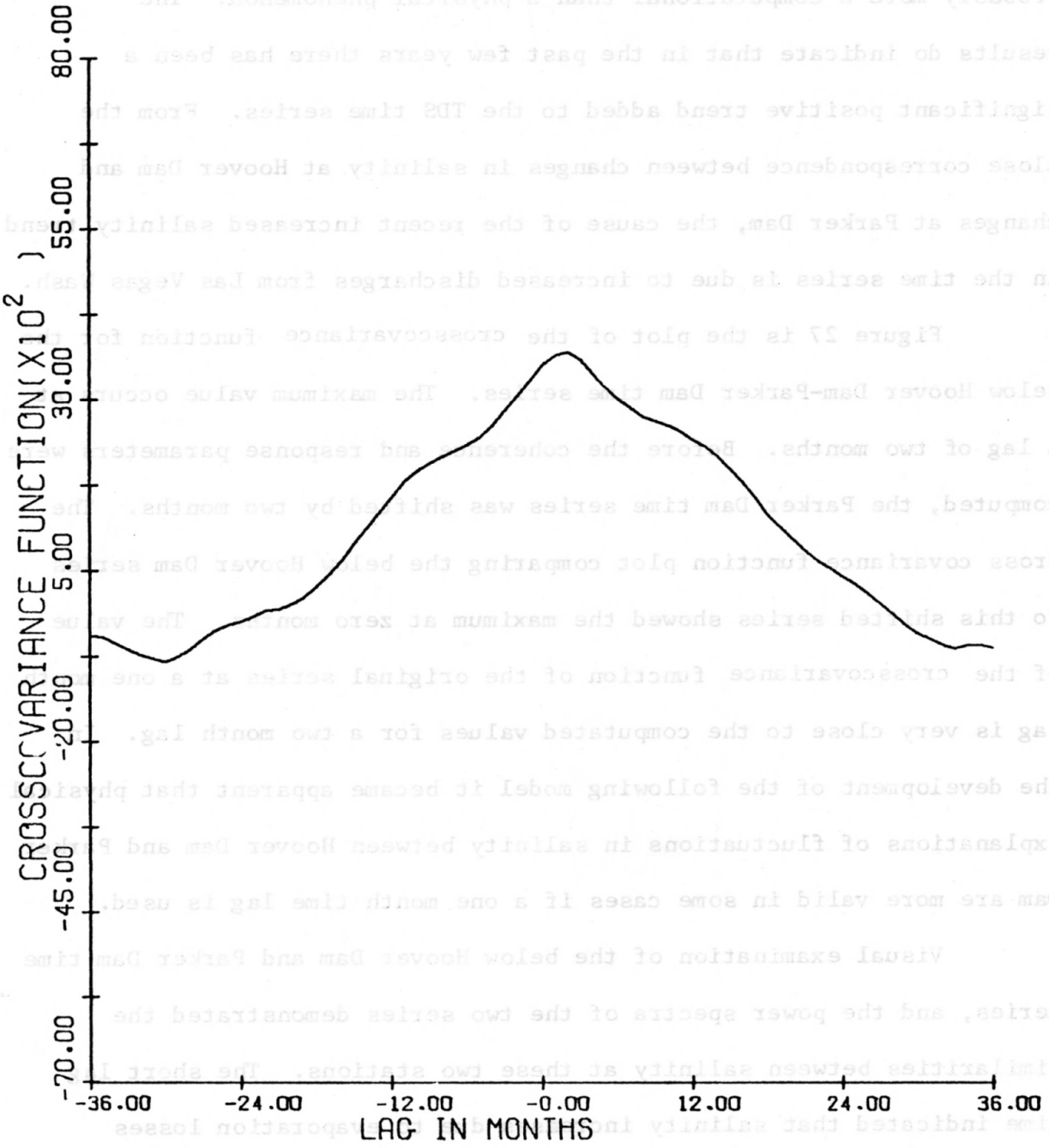

Figure 27. Crosscovariance function for below Hoover Dam and Parker Dam time series (1941-70).

Table 9. Coherence and response function spectrum for the Hoover Dam to Parker Dam river reach.

Frequency (Cycles/Month)	Coherence	Response Function Spectrum
0.000	.950	18999.648
.014	.944	15730.503
.028	.908	5997.724
.042	.719	763.240
.056	.654	493.135
.069	.676	778.510
.083	.679	884.653
.097	.585	433.578
.111	.472	235.595
.125	.518	192.674
.139	.288	64.806
.153	.218	35.252
.167	.297	57.472
.181	.100	17.834
.194	.039	6.086
.208	.231	37.772
.222	.258	38.091
.236	.252	33.914
.250	.162	21.830
.264	.087	8.165
.278	.028	2.572
.292	.111	12.428
.306	.013	1.122
.319	.011	1.091
.333	.012	1.430
.347	.069	7.798
.361	.144	11.924
.375	.068	5.423
.389	.021	2.253
.403	.112	14.269
.417	.223	23.075
.431	.027	2.021
.444	.089	8.184
.458	.118	14.855
.472	.054	5.406
.486	.093	5.142

probably the result of the trend in the time series and the absence at the complex lateral inputs of the Lake Mead system. There rapid decline of the coherency with increasing frequency is possibly due to the occasionally significant inputs from the Bill Williams River as well as to noise which may be introduced by the operation of the dam. The overall unit response was 0.9 ppm downstream per ppm upstream. This computation, with the relatively high coherence and good agreement between the salinity of Hoover Dam releases and releases from Parker Dam the following month. Since fluctuations in salinity at Hoover Dam almost totally determine variations at Parker Dam, the Hoover Dam salinity cycles were used as the main input for a model to predict salinity at Parker Dam.

Differences were computed between the TDS concentrations of the below Hoover Dam time series and the corresponding TDS values of the Parker Dam series shifted one and two months. The differences using the one month shift had smaller oscillations than did those computed with the two month shift. This indicated that the differences between the two time series was less when the Parker Dam series was shifted only one month. Since no great trend or pattern was noted in these differences, a model similar to that used for the Lee Ferry-Grand Canyon river reach was used here. The average of the differences between corresponding elements of the Hoover Dam and the shifted Parker Dam time series was computed. This average is the salt loading factor (SLF) used in the Grand Canyon reach model. Here the SLF was -6.54 ppm. This factor is a product of the inconsistency of the data

series of these river stations. It is not interpreted as a decrease in salinity between Hoover Dam and Parker Dam. The Bill Williams River flows into Lake Havasu near Parker Dam. Generally only extreme high or low flows have a significant impact on the salinity of the releases from Parker Dam. These impacts are discussed later in the evaluation of the model results.

Description and Evaluation of the Model

A model time series for Parker Dam was computed by adding -6.54 ppm to each element of the Hoover Dam time series. Figure 28 shows the plot of the recorded and the model predicted time series for the Parker Dam data station. In general the predicted time series is close to the recorded series. It is notable that occasionally the recorded series shows a peak in TDS concentration significantly exceeding the model predicted salinity level. Examples of these occurrences are November 1941, July 1942, December 1942, February 1943, and May 1943. Figure 29 shows the monthly discharge of the Bill Williams River for the period September 1941 to August 1943. As indicated by the arrows in the figure, the occurrence concentrations much higher than the predicted values closely coincides with periods of low inflow from the Bill Williams River. Very high discharges from this stream have created concentrations much lower than the predicted values. The best example of this is December 1965, when the discharge totaled 121,900 acre-feet. The dilution effect of this high flow is clearly seen in Figure 24. In an uncontrolled river concentration tends to be inversely related to discharge. Thus high flows from the

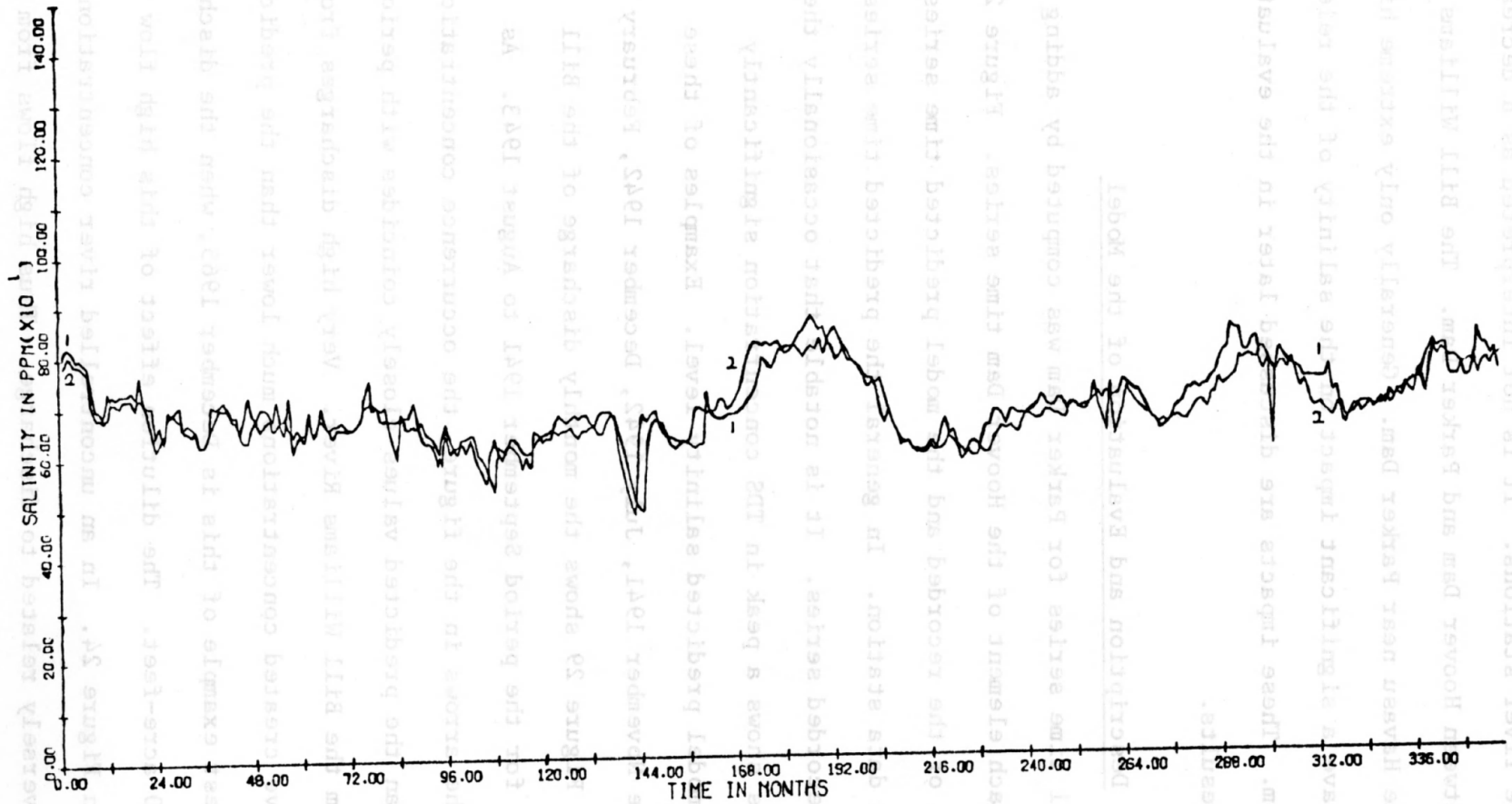

Figure 28. Recorded and model-predicted Parker Dam time series (1941-70).

Line 1 is the recorded time series. Line 2 is the model time series. The time axis indicates the number of months from January 1941. The divisions mark twelve month periods.

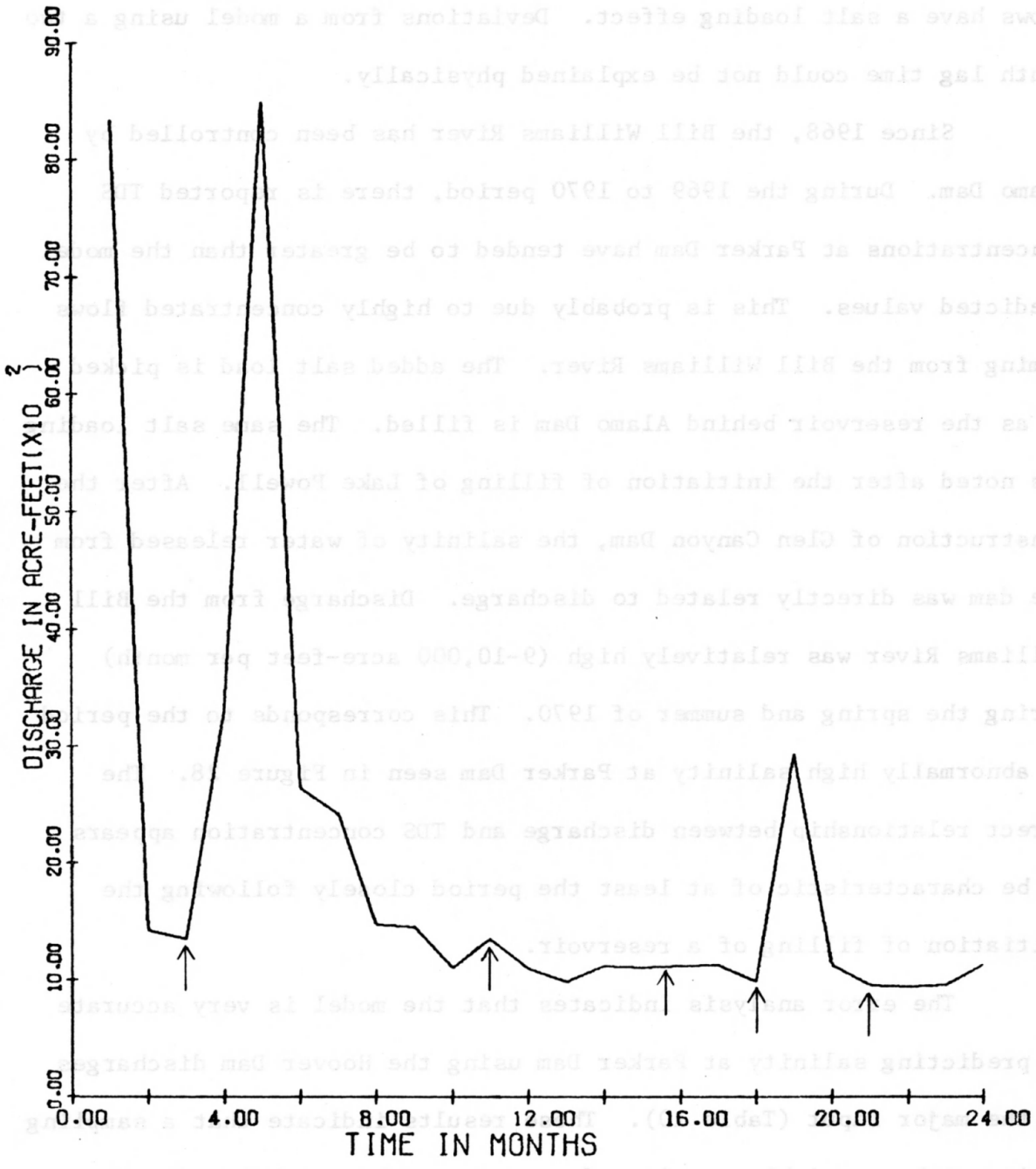

Figure 29. Monthly discharges from Bill Williams River near Alamo, Arizona.

On the time axis: 1 = September 1941, 2 = October 1941, . . . , 24 = August 1943.

Bill Williams Rover has a dilution impact on Lake Havasu water and low flows have a salt loading effect. Deviations from a model using a two month lag time could not be explained physically.

Since 1968, the Bill Williams River has been controlled by Alamo Dam. During the 1969 to 1970 period, there is reported TDS concentrations at Parker Dam have tended to be greater than the model predicted values. This is probably due to highly concentrated flows coming from the Bill Williams River. The added salt load is picked up as the reservoir behind Alamo Dam is filled. The same salt loading was noted after the initiation of filling of Lake Powell. After the construction of Glen Canyon Dam, the salinity of water released from the dam was directly related to discharge. Discharge from the Bill Williams River was relatively high (9-10,000 acre-feet per month) during the spring and summer of 1970. This corresponds to the period of abnormally high salinity at Parker Dam seen in Figure 28. The direct relationship between discharge and TDS concentration appears to be characteristic of at least the period closely following the initiation of filling of a reservoir.

The error analysis indicates that the model is very accurate in predicting salinity at Parker Dam using the Hoover Dam discharges as the major input (Table 10). These results indicate that a sampling policy with a variable sampling frequency can be established. The procedure is that outlined in Chapter II.

Table 10. Error analysis of prediction model for salinity at Parker Dam.

Difference (in ppm)		Percent Differences	
Range	Number of Occurrences	Range	Number of Occurrences
< 0	223	< 5%	284
0- 5	0	5-10%	59
5-10	39	10-15%	11
10-15	36	15-20%	0
15-20	1	20-25%	0
20-30	24	25-30%	1
30-40	9	>30%	1
40-50	7		
50-60	12		
>60	5		

Probabilities for possible choices of levels of acceptability are given below. These probabilities are estimated from the error analysis of the model predictions.

Let X be the TDS concentration predicted for Parker Dam for a given month. Let Y be the actual salinity level.

$$P(Y<X) = 0.626$$

$$P(X<Y<X + 20 \text{ ppm}) = 0.214$$

$$P(X + 20 \text{ ppm} <Y<X + 50 \text{ ppm}) = 0.112$$

$$P(Y>X + 50 \text{ ppm}) = 0.048$$

Noting that most of the occurrences of observed concentrations being much greater than the predicted TDS level can be explained by the input of the Bill Williams River, it is reasonable that this model can be very useful in lowering the sampling frequency significantly. The model-predicted values average $\pm 3.39\%$ difference from the recorded values with a standard deviation of 3.40. These results indicate that on an average, the value predicted by this model will be within 3.4% of the actual TDS concentration. The probability of the predicted value being within 6.8% is 0.68, within 10.2% is 0.95, and within 13.6% is 0.99.

CHAPTER VI

PARKER DAM TO YUMA REACH

Analysis of Time Series

The Parker Dam and Yuma TDS time series (Figures 24 and 30, respectively) were analyzed to detect the impact of agricultural development of the salinity of the Colorado River. Visual comparison of the two time series indicates that salinity at Yuma closely follows the pattern at Parker Dam up until the mid-1950's. The changed pattern during and after this period is probably due to agricultural development. Changes in the general salinity condition during the mid-1950's was aided by a drought.

The crosscovariance function shown in Figure 31 indicates no significant lag time between the time series. The actual time of transit is probably on the order of a week. Thus no shifting of the time series was required for analysis.

The power spectra of these two time series (Figures 26 and 32) indicate that both time series have similar cyclic components. The coherence and response spectrum given in Table 11 show a close relationship between the two time series. The overall unit response was nearly 1.0 ppm downstream per ppm upstream which means that the salinity at Yuma is to a large degree determined by salinity at Parker Dam. The high coherence at the zero frequency is a result of the large

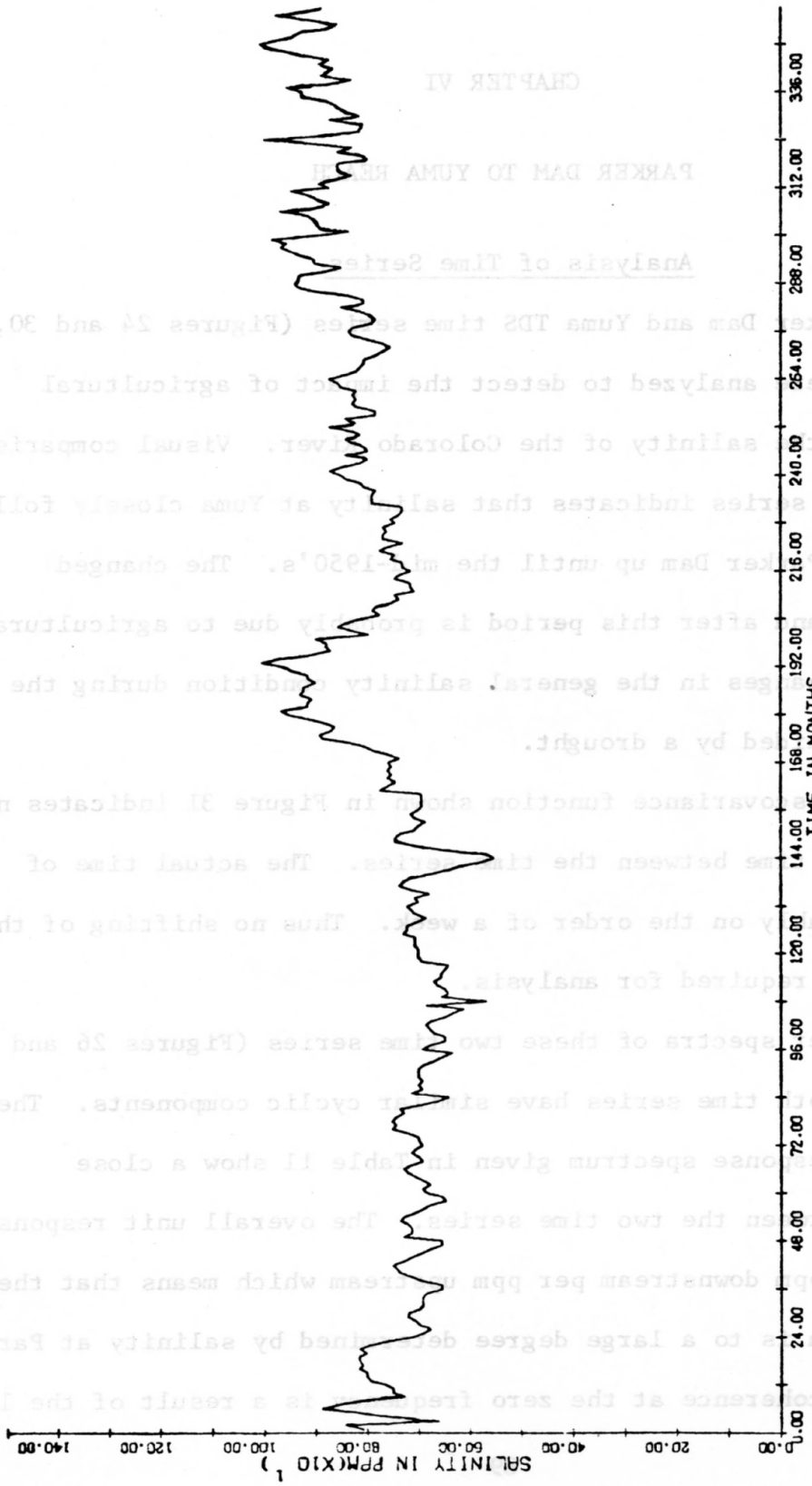

Figure 30. Yuma TDS time series (1941-70).

The time axis indicates the number of months from January 1941. The divisions mark twelve month periods.

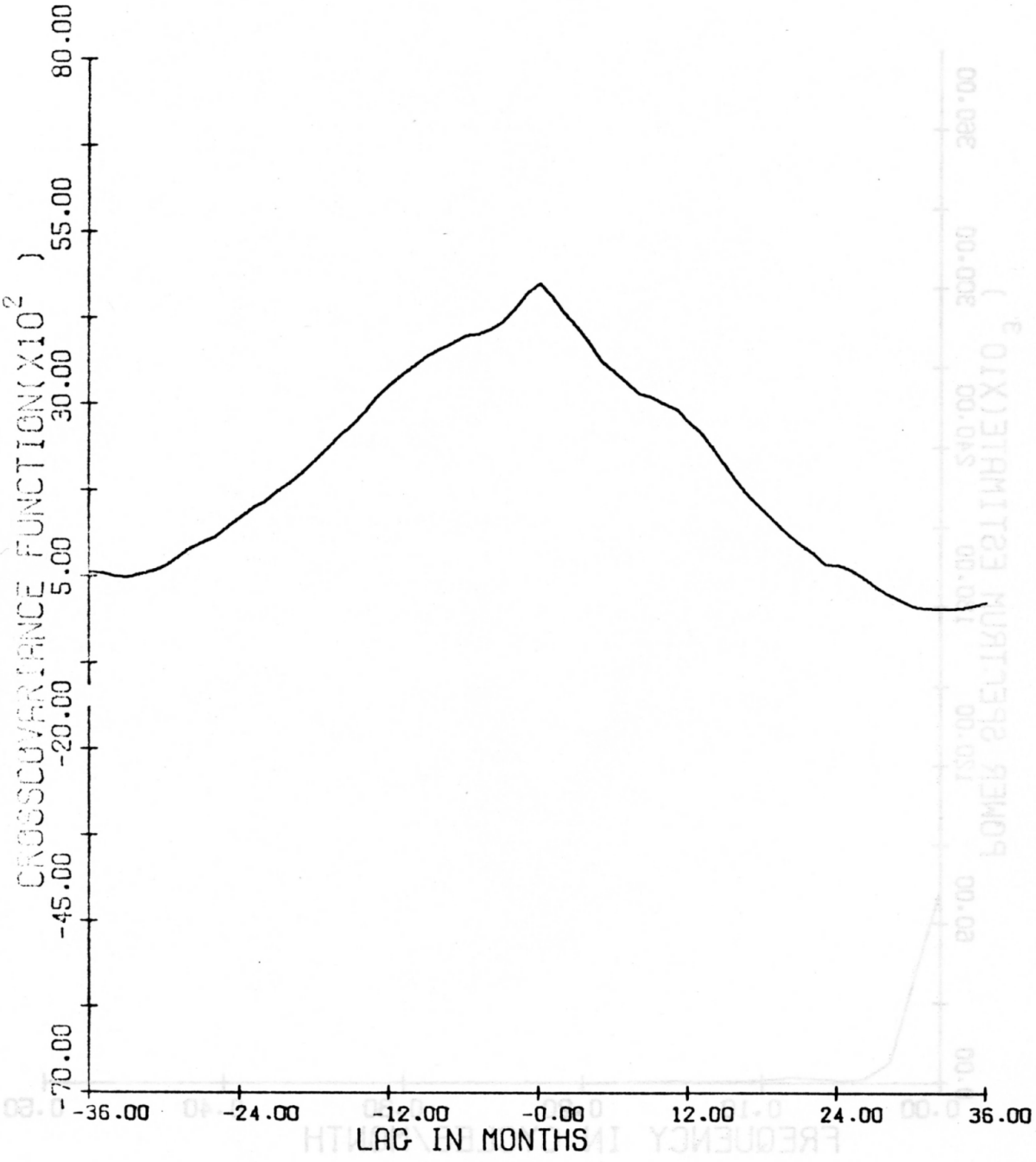

Figure 31. Crosscovariance function for Parker Dam and Yuma time series (1941-70).

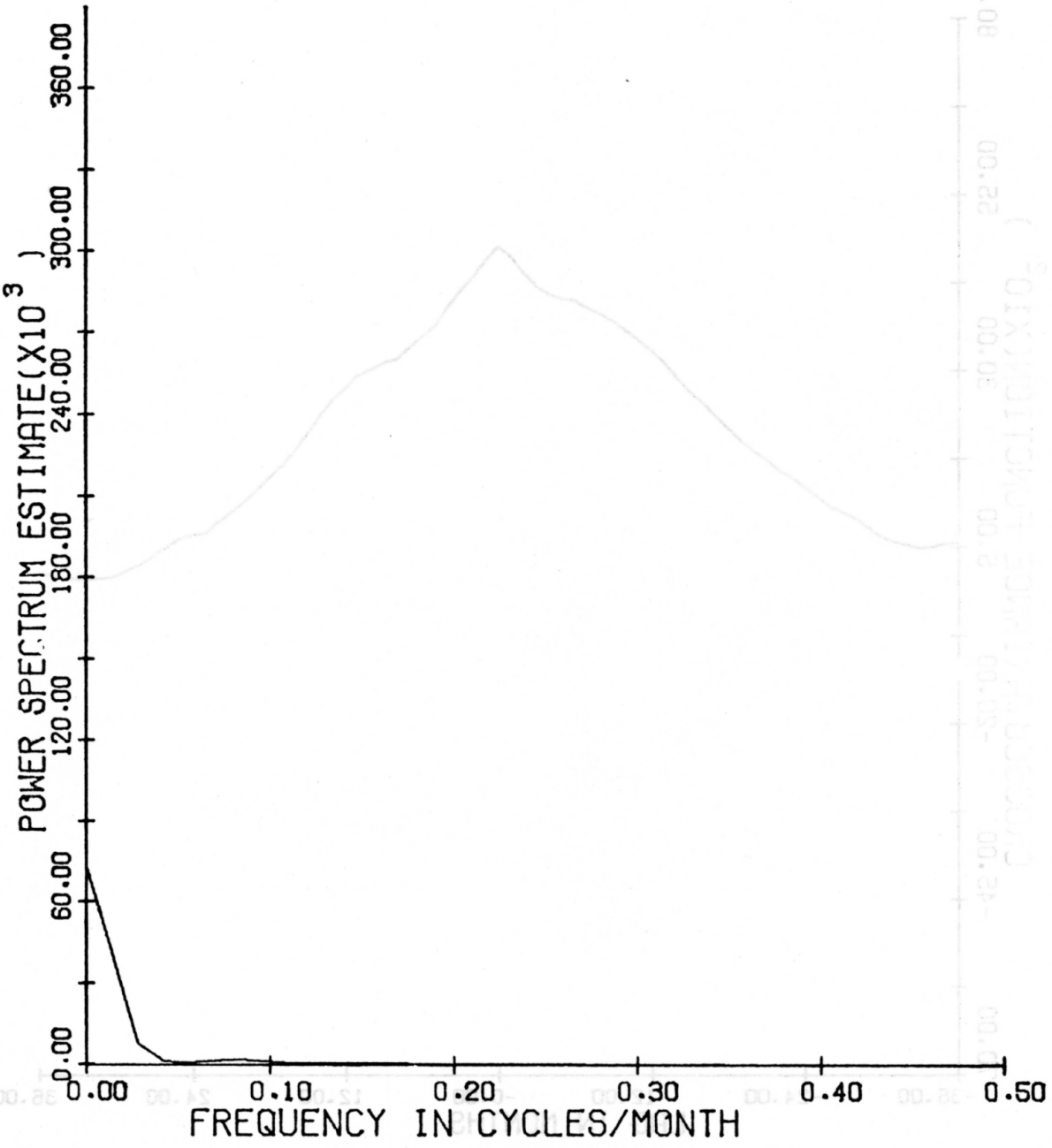

Figure 32. Power spectrum of Yuma time series (1941-70).

Table 11. Coherence and response function spectrum for Parker Dam to Yuma river reach.

Frequency (Cycles/Month)	Coherence	Response Function Spectrum
0.000	.924	24380.048
.014	.918	19183.417
.028	.863	6789.970
.042	.635	802.702
.056	.651	522.170
.069	.444	685.507
.083	.346	706.156
.097	.429	501.556
.111	.548	335.993
.125	.428	192.212
.139	.383	170.073
.153	.418	267.859
.167	.334	235.774
.181	.311	143.300
.194	.371	107.644
.208	.243	57.507
.222	.199	49.446
.236	.167	36.389
.250	.142	31.007
.264	.201	44.913
.278	.276	49.591
.292	.347	50.211
.306	.379	41.229
.319	.420	57.333
.333	.339	49.118
.347	.146	17.790
.361	.085	12.047
.375	.090	11.893
.389	.003	.383
.403	.037	2.935
.417	.006	.419
.431	.023	1.806
.444	.169	19.533
.458	.196	20.816
.472	.191	15.485
.486	.012	.096

trend in the Yuma time series. The coherence at other frequencies is depressed because of the inputs from agriculture. Because of the indicated similarities between the two time series, the model form used for upstream station pairs exhibiting this statistical similarity was used for the Parker Dam-Yuma reach.

The Impact of Irrigation Farming

The differences between corresponding points of the two time series were computed. The differences showed the above indicated changes in salinity during the mid-1950's. Since the general increase in salinity change between the two river stations does not recover to its pre-1950 level, it was concluded that the increased salt load was due to agricultural activity. The Palo Verde Diversion Project below Parker Dam was completed in 1957. The agricultural development that accompanied this project is the cause of abnormal increase of about 50 ppm in TDS concentration during and after the 1950 decade. Beginning about 1960, the differences take on a definite cyclic pattern. This cyclic pattern is accompanied by a continuation of the increasing trend in salt loading that was initiated in the 1950's.

The annual cycle in salinity increase between Parker Dam and Yuma can be explained by agricultural influences. Peak increases in TDS concentration generally occur in the winter between November and January. Minor peaks occur frequently during the summer. The summer peaks are due to rapid surface return flows from irrigated fields. The winter maximum is due to slower seepage through the subsurface to the river.

Figure 33 shows the average TDS concentrations of three inputs into the Colorado River between Parker Dam and Yuma. The TDS concentrations are computed sum of constituents values for the 1969 water year. The plots in this figure show winter as well as summer salinity maxima. In the lower two curves, the winter maxima are of greater than the summer concentrations. Assuming that these inputs are due to agricultural drainage, this indicates high seepage components in salt loading. Return flow discharges are minimum during the winter and maximum late in the summer (U.S.G.S. 1969). Thus even though the concentration of return flows is relatively constant (Figure 33) in many cases the salt load carried by these flows is significantly greater during the summer. Much of the effect of the greater loads is masked by the relatively high summer flows in the Colorado River below Parker Dam.

Figure 34 shows the monthly average dissolved solids concentration (as sum of constituents) of discharges from the Wellton-Mohawk Main Outlet Drain near Yuma. Flows in this drain are discharged below the Yuma data station. This drain and the Gila River are the main sinks for irrigation return flow and seepage in the Wellton-Mohawk farming area. Comparison of Figure 34 with the salinity curve for the Gila River in Figure 33 indicates that most of the salt load introduced by the Gila River is the result of irrigation return flows while the salt load from irrigation seepage in Wellton area is carried by the Main Outlet Drain. Gila River discharges are greatest during the summer (U.S.G.S. 1969). Since this is also a period of relatively high concentrations, a tremendous

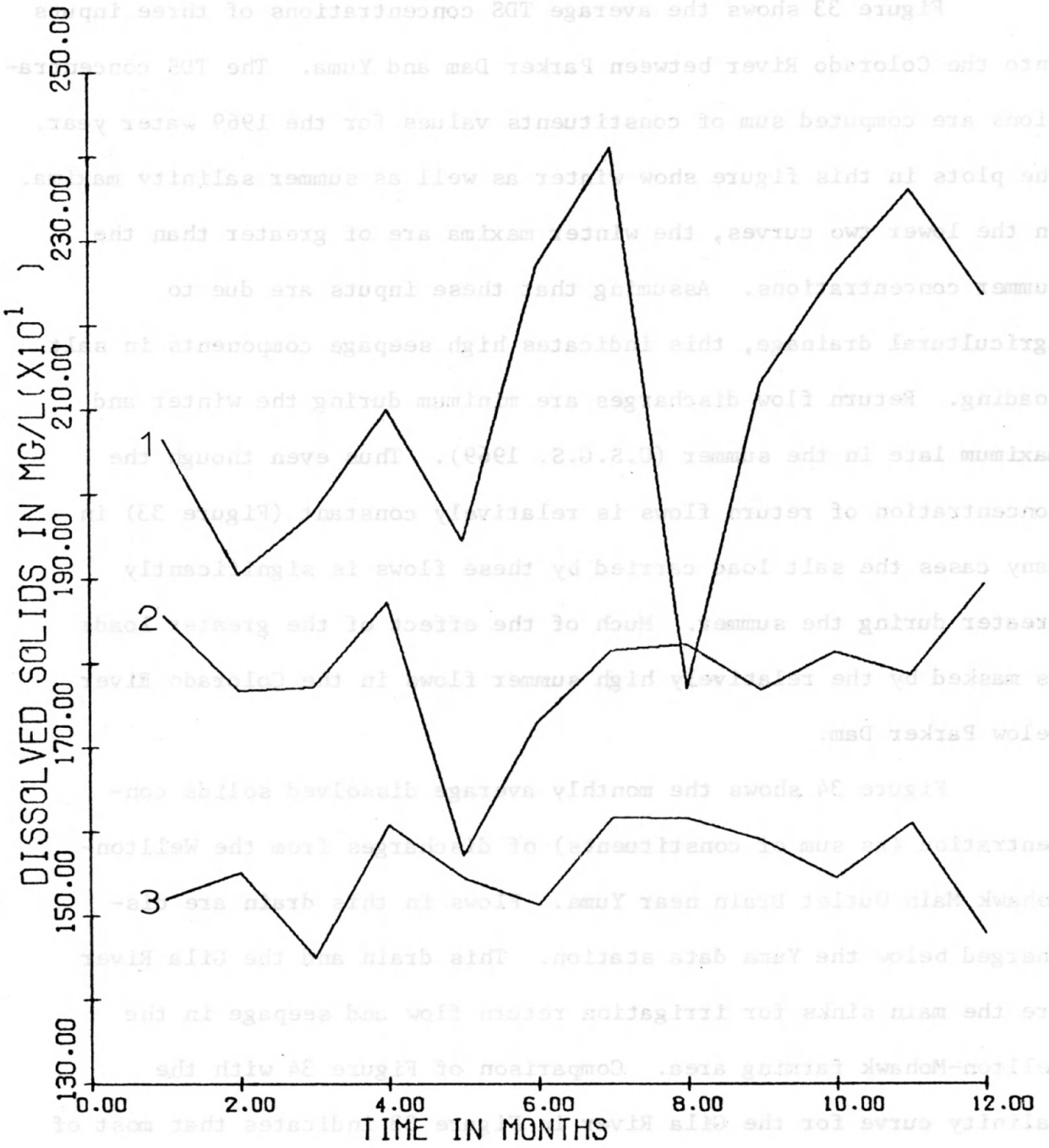

Figure 33. Three saline inputs between Parker Dam and Yuma (1969 water year).

Line 1 is average monthly TDS concentrations for the Gila River near mouth. Line 2 is for the outfall drain near Palo Verde, California. Line 3 is for the lower main drain near Parker, Arizona.

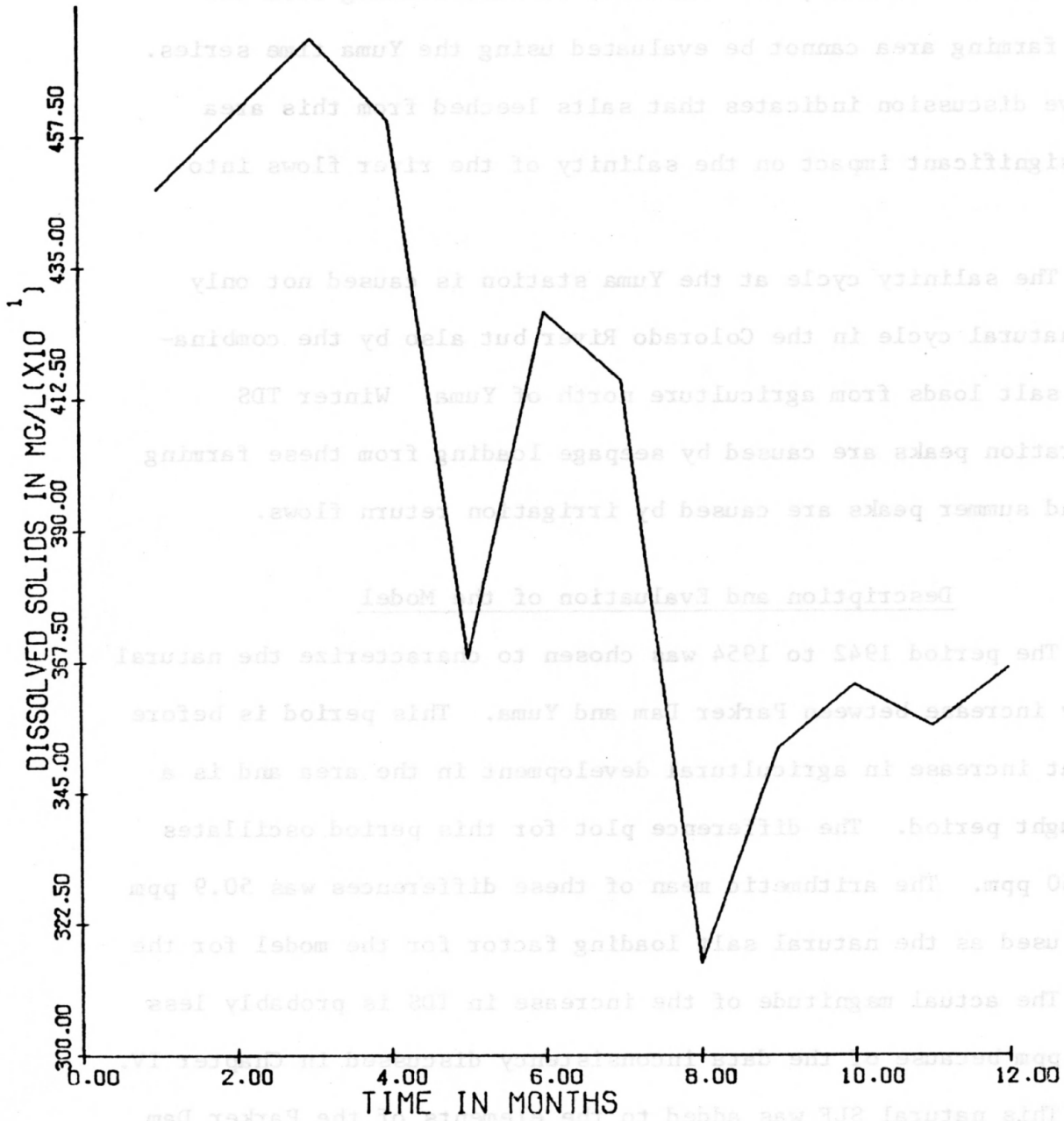

Figure 34. Average monthly salinity of discharges from Wellton-Mohawk main outlet drain (1969 water year).

salt load is introduced from this source. Because of the location of the Yuma data station, the influence of salt loading from the Wellton farming area cannot be evaluated using the Yuma time series. The above discussion indicates that salts leeched from this area have a significant impact on the salinity of the river flows into Mexico.

The salinity cycle at the Yuma station is caused not only by the natural cycle in the Colorado River but also by the combination of salt loads from agriculture north of Yuma. Winter TDS concentration peaks are caused by seepage loading from these farming areas and summer peaks are caused by irrigation return flows.

Description and Evaluation of the Model

The period 1942 to 1954 was chosen to characterize the natural salinity increase between Parker Dam and Yuma. This period is before the great increase in agricultural development in the area and is a non-drought period. The difference plot for this period oscillates around 50 ppm. The arithmetic mean of these differences was 50.9 ppm and was used as the natural salt loading factor for the model for the reach. The actual magnitude of the increase in TDS is probably less than 50 ppm because of the data inconsistency discussed in Chapter IV.

This natural SLF was added to the elements of the Parker Dam time series and this predicted time series and the recorded Yuma time series are plotted in Figure 35. As expected, the predicted TDS values agree closely with the recorded concentrations up to the mid-1950's. After this the difference between the two time series increases

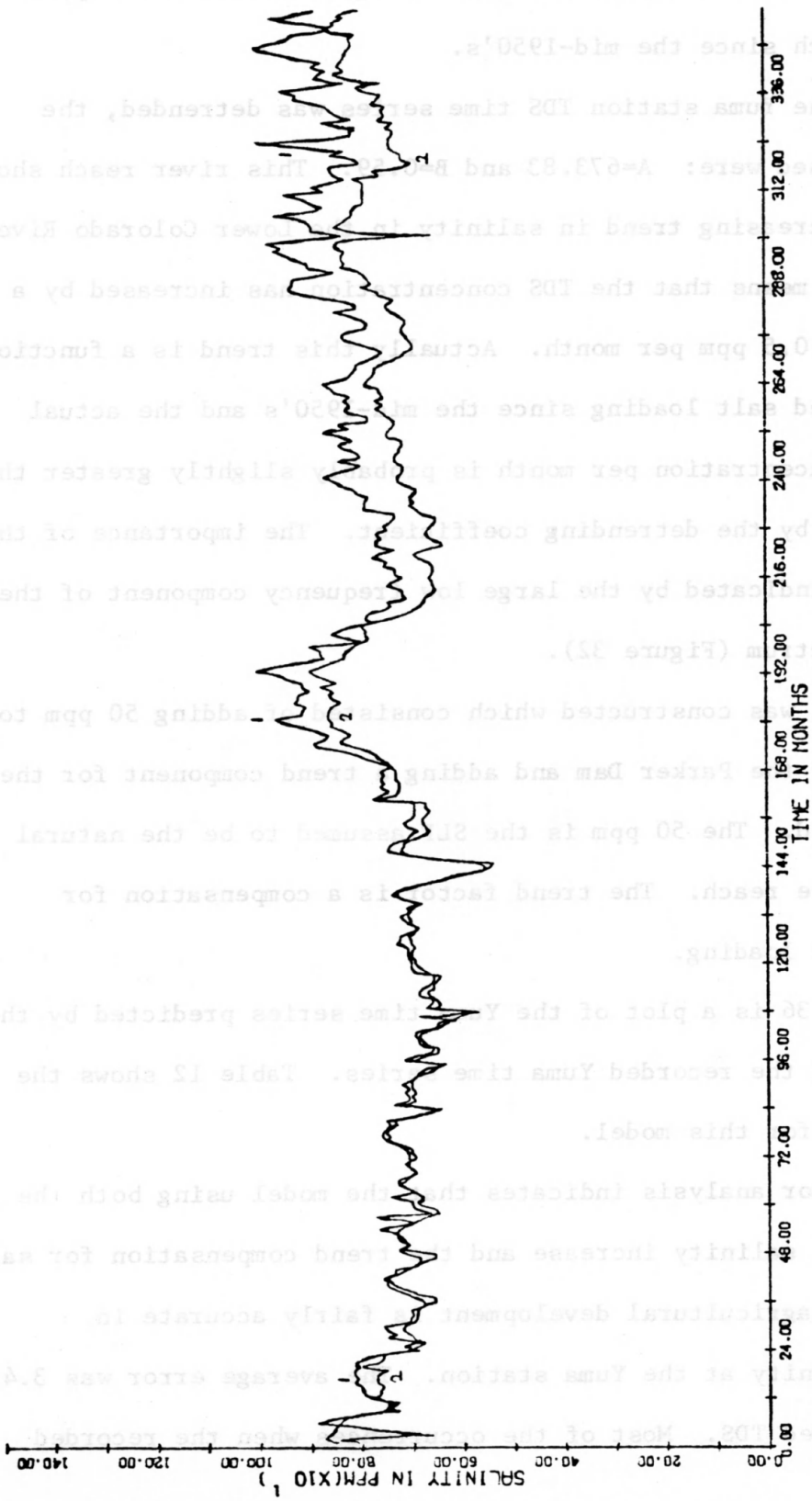

Figure 35. Recorded Yuma time series and time series predicted using simple SLF model.

Line 1 is the recorded TDS. Line 2 is the model-predicted time series. The time axis indicates the number of months from January 1941. The divisions mark twelve month periods.

steadily. This is the expected impact of agricultural development in this river reach since the mid-1950's.

When the Yuma station TDS time series was detrended, the coefficients used were: A=673.83 and B=0.59. This river reach shows the largest increasing trend in salinity in the Lower Colorado River. The value of B means that the TDS concentration has increased by a factor of over 0.5 ppm per month. Actually this trend is a function of the increased salt loading since the mid-1950's and the actual increase in concentration per month is probably slightly greater than that indicated by the detrending coefficient. The importance of this trend is also indicated by the large low frequency component of the Yuma power spectrum (Figure 32).

A model was constructed which consisted of adding 50 ppm to all elements of the Parker Dam and adding a trend component for the post-1952 period. The 50 ppm is the SLF assumed to be the natural increase for the reach. The trend factor is a compensation for artificial salt loading.

Figure 36 is a plot of the Yuma time series predicted by the above model and the recorded Yuma time series. Table 12 shows the error analysis for this model.

The error analysis indicates that the model using both the SLF for the natural salinity increase and the trend compensation for salt loading due to agricultural development is fairly accurate in predicting salinity at the Yuma station. The average error was 3.44% from the recorded TDS. Most of the occurrences when the recorded

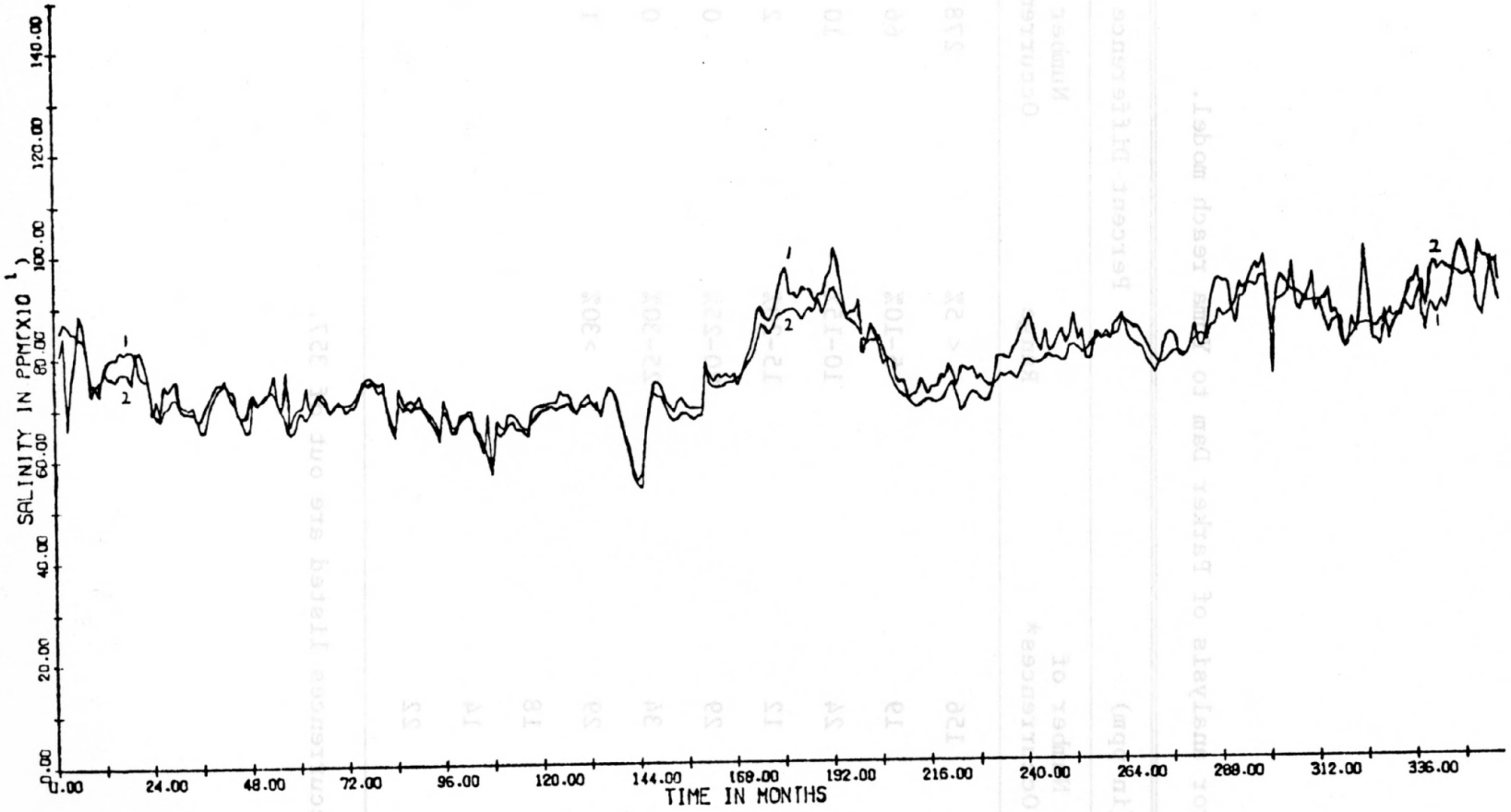

Figure 36. Recorded Yuma time series and the time series predicted using SLF model and trend compensation.

Line 1 is the recorded time series. Line 2 is the model-predicted time series. The time axis indicates the number of months from January 1941. The divisions mark twelve month periods.

Table 12. Error analysis of Parker Dam to Yuma reach model.

Difference (in ppm)		Percent Difference	
Range	Number of Occurrences*	Range	Number of Occurrences*
< 0	156	< 5%	278
0- 5	19	5-10%	66
5-10	24	10-15%	10
10-15	12	15-20%	2
15-20	29	20-25%	0
20-30	34	25-30%	0
30-40	29	>30%	1
40-50	18		
50-60	14		
>60	22		

* Number of occurrences listed are out of 357.

value significantly exceeds the model prediction are during the peak loading during the winter from seepage from farmland. During these periods of great loading, the system would (and probably should) be considered out of control.

Probabilities for possible choices of levels of acceptability are given below. These probabilities are estimated from the error analysis of the model predictions. X is the TDS concentration predicted for Parker Dam for a given month. Y is the actual salinity level.

$$P(Y<X) = 0.44$$

$$P(X<Y<X + 20 \text{ ppm}) = 0.23$$

$$P(X + 20 \text{ ppm} <Y<X + 50 \text{ ppm}) = 0.23$$

$$P(Y>X + 50 \text{ ppm}) = .10$$

From the form of the model and the nature of the major deviations from the predicted values, the model can probably be used to lower the sampling frequency at the Yuma station during the summer. But due to the erratic salt loading during the winter months the system would be considered out of control and extensive sampling would be required to access the impact of the seepage loading for a given year.

CHAPTER VII

SUMMARY AND CONCLUSIONS

The salinity increase in the Colorado River from Lee Ferry to the Mexican border is a well demonstrated fact. Table 13 lists average TDS concentrations and average annual discharge at each of the river stations for the period of January 1941 to December 1968 (U.S. Department of the Interior 1971).

Table 13. Average TDS and average annual discharge at Colorado River data stations.

Station	Discharge (10^3 ac-ft)	TDS (mg/l)	ΔTDS
Lee Ferry	10,642	552	
			+62
Grand Canyon	10,927	614	
			+73
Below Hoover Dam	10,682	687	
			-14
Parker Dam	9,758	673	
			+78
Yuma	9,120	751	

Analysis of reported data showed inconsistencies between the five stations. Magnitudes of the average TDS concentration at Parker Dam and the salinity changes between stations below Hoover Dam are misleading. Nevertheless, the table indicates that the salinity of the river increases by over 200 mg/l between Lee Ferry and Yuma.

This study has shown some of the factors involved in creating the salinity conditions and cycles at several locations in the Lower Colorado River Basin. There are two basic processes which raise the salinity of a body of water. Concentrating processes increase the salinity by removing water or by lowering the dilution capability of the river. Salt loading phenomena whether from natural salt springs, from solutioning of lake or river beds, or from man-made sources leads to increased concentrations by increasing the salt load carried by the river. These types of processes are influential in the Lower Colorado River.

The salinity increases in the Grand Canyon reach have been attributed almost entirely to salt loading from the salt springs in the reach. The major salt source here is Blue Springs located near the mouth of the Little Colorado River. The increase in TDS concentration between Lee Ferry and Grand Canyon is nearly constant throughout the year. Salinity changes in this reach remained fairly constant after Glen Canyon Dam was constructed.

Since the form of the salinity cycle of the releases from Lake Powell appears to be changing with time, the impact of salt loading from natural sources in the Grand Canyon may also change with time. Data from the last several years indicates that this change in salt loading characteristics is not likely to be great. The impact of salt loading from natural sources can thus be approximated by a constant concentration factor.

The magnitude of the salt concentration and the nature of the salinity cycles are changed significantly by the reservoirs in the Lower Colorado River Basin. The major impact of reservoirs is to dampen the amplitude of the salinity cycles which characterize uncontrolled river flows. This effect is clearly seen in the Lee Ferry and Grand Canyon time series after the construction of Glen Canyon Dam and the initiation of the filling of Lake Powell. The damping of uncontrolled salinity cycles is also seen in the visual differences between the Grand Canyon and the below Hoover Dam time series. This damping effect complicates the statistical comparison of the two time series especially with respect to the crosscovariance function, coherence, and response spectrum. This result leads to a more empirical approach for determining the factors contributing to the salinity change across Lake Mead.

The effect of the Lake Mohave-Lake Havasu chain on the salinity of this river reach is small. This is because of the small size of the reservoirs and short residence time. The impact resulting from these reservoirs shows up downstream from Parker Dam and is due to the large diversion by the Metropolitan Water District of Southern California from Lake Havasu. This diversion does not directly increase downstream salinity but it decreases the ability of the river to dilute the highly saline water from agricultural runoff in the Parker Dam-Yuma reach.

The TDS concentration between Parker Dam and Yuma increases with respect to both time and distance. This has been related to the

agricultural development of the area. The increase in salinity with time is the most important characteristic of the differences in the time series of the Parker Dam and Yuma stations. Because this time trend is caused by man's activities, it offers the opportunity of control. Examination of the two time series indicates that the salinity increase due to agriculture is presently greater than the natural increase.

As discussed in Chapter III, the concentrating effect of evaporation on the salinity of the system is a function of the flow pattern into the reservoirs. This in turn is a function of the seasonal temperature fluctuation of river inputs. The salinity of relatively warm and/or dilute inputs increases because of evaporation. More dense inputs are not appreciably affected by evaporation. Thus evaporation has a seasonal impact on salinity.

Evaporation does not have a large effect on the salinity of Lower Colorado River flows in reaches other than the Lake Mead reservoir. The residence time in the Grand Canyon and the Parker Dam to Yuma reaches is too short for significant concentrating to occur. The releases from Hoover Dam are from a depth of about 200 feet and are cold and saline (i.e., dense) with respect to the surface waters of Lake Mead. No data of the currents in Lake Mohave and Lake Havasu is available but the above indicates that underflows would probably be the dominant current pattern. As with underflows coming into Lake Mead, this flow pattern would minimize the concentrating effect of

evaporation on river flows through the two reservoirs below Hoover Dam. These reservoirs have much smaller surface areas and shorter residence times which aid in reducing the effect of evaporation.

The effects of reservoirs on the salinity of river flows are summarized below:

1. The large periodic changes in TDS concentration characteristic of an uncontrolled river system are damped out giving a more early constant salinity level to the reservoir releases.
2. Where overflow currents occur, evaporation causes increases in salinity. The magnitude of this increase is influenced by the physical dimensions of the reservoir:
   a. A larger surface area (or greater depth to surface area ratio) leads to a greater increase in TDS concentration due to evaporation.
   b. A greater volume tends to lower the turnover rate (i.e., to increase residence time) and leads to a greater opportunity for salinity changes to occur.

In this study, time series analysis was used to characterize the time series and the results of this analysis were used to characterize the changes which occur between the river stations. Computation and comparison of power spectra proved to be useful in this respect (see Figure 37). From the similarities between the power spectra of the Lee Ferry and Grand Canyon time series and between the power spectra of the below Hoover Dam station and the Parker Dam time series it was concluded that a simple relationship existed between the

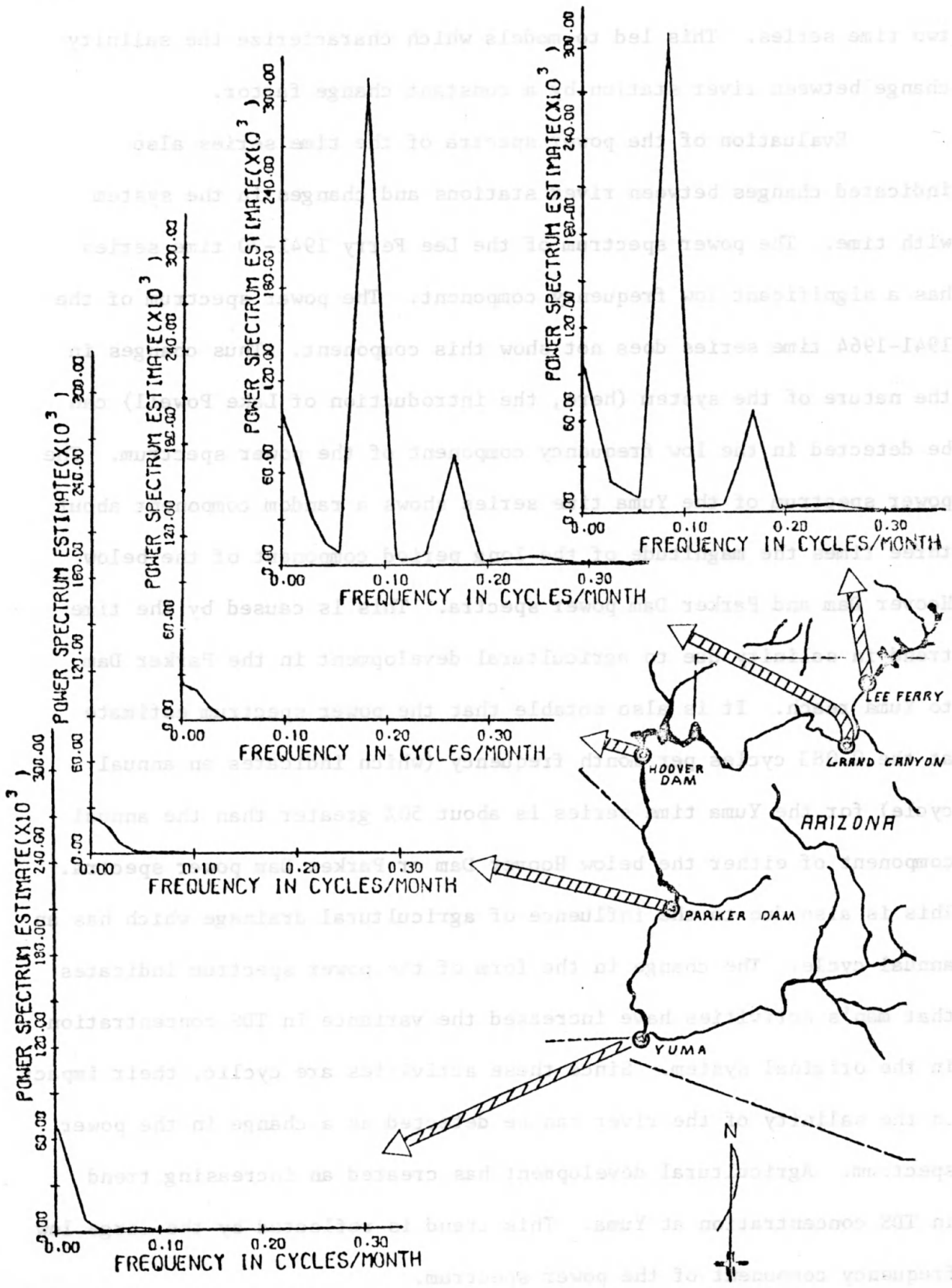

Figure 37. Power spectra of Lower Colorado River data stations.

two time series. This led to models which characterize the salinity change between river station by a constant change factor.

Evaluation of the power spectra of the time series also indicated changes between river stations and changes in the system with time. The power spectrum of the Lee Ferry 1941-70 time series has a significant low frequency component. The power spectrum of the 1941-1964 time series does not show this component. Thus changes in the nature of the system (here, the introduction of Lake Powell) can be detected in the low frequency component of the power spectrum. The power spectrum of the Yuma time series shows a random component about three times the magnitude of the long period component of the below Hoover Dam and Parker Dam power spectra. This is caused by the time trend in salinity due to agricultural development in the Parker Dam to Yuma reach. It is also notable that the power spectrum estimate at the 0.083 cycles per month frequency (which indicates an annual cycle) for the Yuma time series is about 50% greater than the annual component of either the below Hoover Dam or Parker Dam power spectra. This is also due to the influence of agricultural drainage which has an annual cycle. The change in the form of the power spectrum indicates that man's activities have increased the variance in TDS concentration in the original system. Since these activities are cyclic, their impact on the salinity of the river can be detected as a change in the power spectrum. Agricultural development has created an increasing trend in TDS concentration at Yuma. This trend is reflected by the large low frequency component of the power spectrum.

The models presented here are first approximations at quantifying the changes in salinity with respect to time and location. More accurate description of the hydrodynamics, density current phenomena, etc., will lead to a more accurate quantification of the salinity state of the system at a given time and place. This will lead to the modeling of the movement of individual ions of interest such as phosphates, nitrates, calcium, magnesium, boron, etc., as well as the total salt concentration. For many individual users of the Lower Colorado River, the knowledge of the distribution of these constituent ions is more important than the total salinity level.

Visual and statistical analysis of the time series of five stations in the Lower Colorado River Basin has lead to a qualitative description of and the quantitative approximation of the factors which influence the temporal and spatial distribution of salinity. The usefulness of time series analysis in showing spatial and temporal salinity patterns and changes in these patterns has been demonstrated. The accurate description of these patterns is needed for optimal monitoring and successful management of the water quality of the river system.

APPENDIX A

LOCATION OF DATA STATIONS

Lee Ferry: Colorado River at Lee Ferry, Arizona. Located 0.8 miles upstream from Paria River, 16 miles downstream from Glen Canyon Dam, and 61.5 miles upstream from the Little Colorado River.

Grand Canyon: Colorado River near Grand Canyon, Arizona. Located 0.4 miles upstream from Bright Angel Creek, 26 miles downstream from the Little Colorado River, 104 miles downstream from Glen Canyon Dam, and 267 miles upstream from Hoover Dam.

Below Hoover Dam: Colorado River below Hoover Dam, Arizona-Nevada (Irrigation network station). Located just downstream from gaging station in Hoover Dam powerhouse.

Parker Dam: Quality data were obtained from Metropolitan Water District of Southern California Lake Havasu intake pumping plant located just upstream from Parker Dam.

Yuma: Yuma Main Canal Below Colorado River Siphon, at Yuma, Arizona. Located 0.2 miles upstream from bridge on U.S. Highway 80 over Colorado River at Yuma and 3.5 miles downstream from siphon-drop powerplant.

Virgin River: Virgin River at Littlefield, Arizona. Located 0.4 miles downstream from Beaver Dam Wash, 0.4 miles upstream from Littlefield, and 36 miles upstream from waterline of Lake Mead at elevation 1221 feet above mean sea level.

Las Vegas Wash: Las Vegas Wash near Boulder City, Nevada. Located about 0.8 miles upstream from high-water line to Lake Mead at elevation 1221.4 feet above mean sea level.

APPENDIX B

AUTOCOVARIANCE FUNCTION AND POWER SPECTRUM OF THE GRAND CANYON TIME SERIES

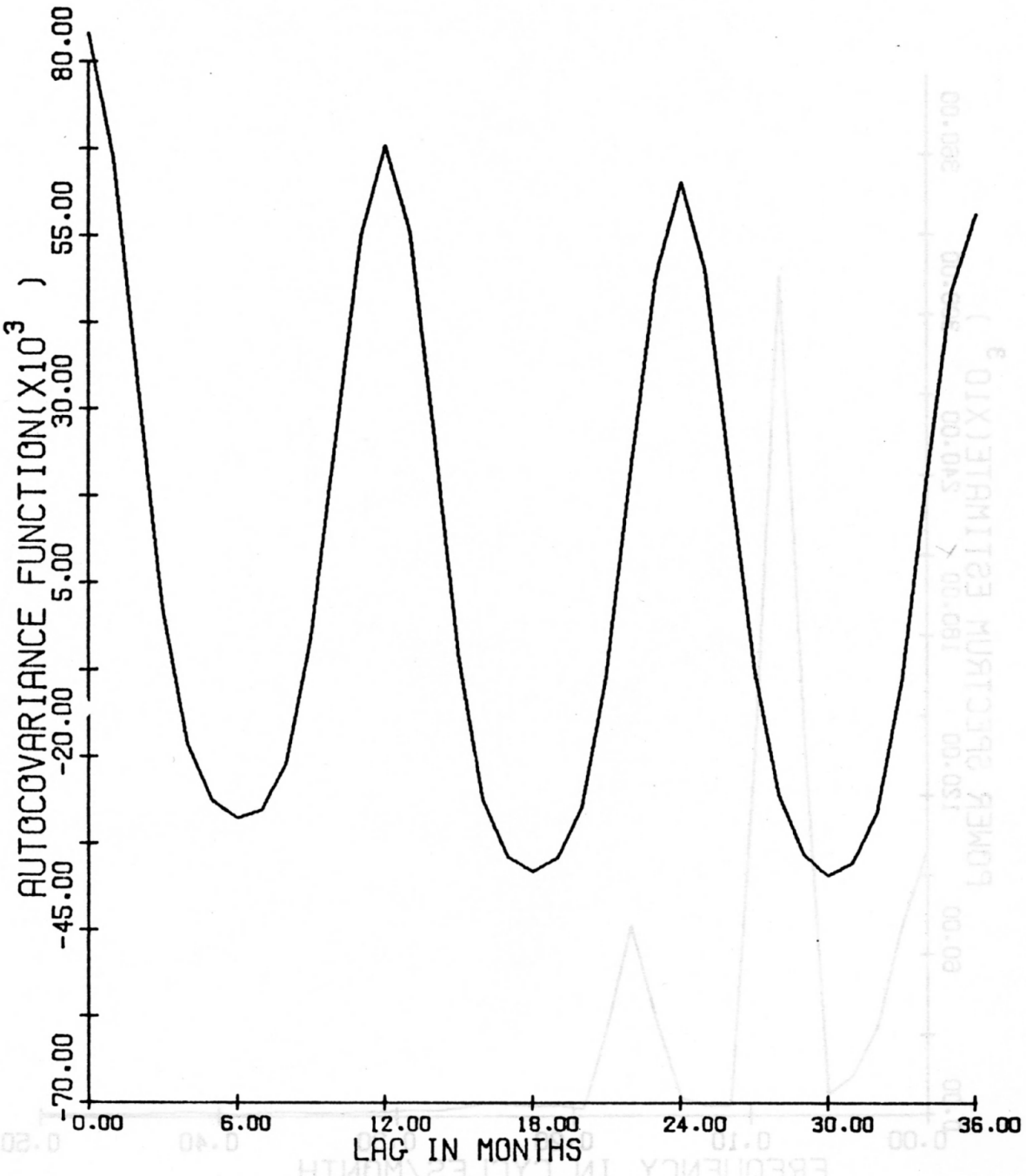

Figure B-1. Autocovariance function for Grand Canyon time series (1941-70).

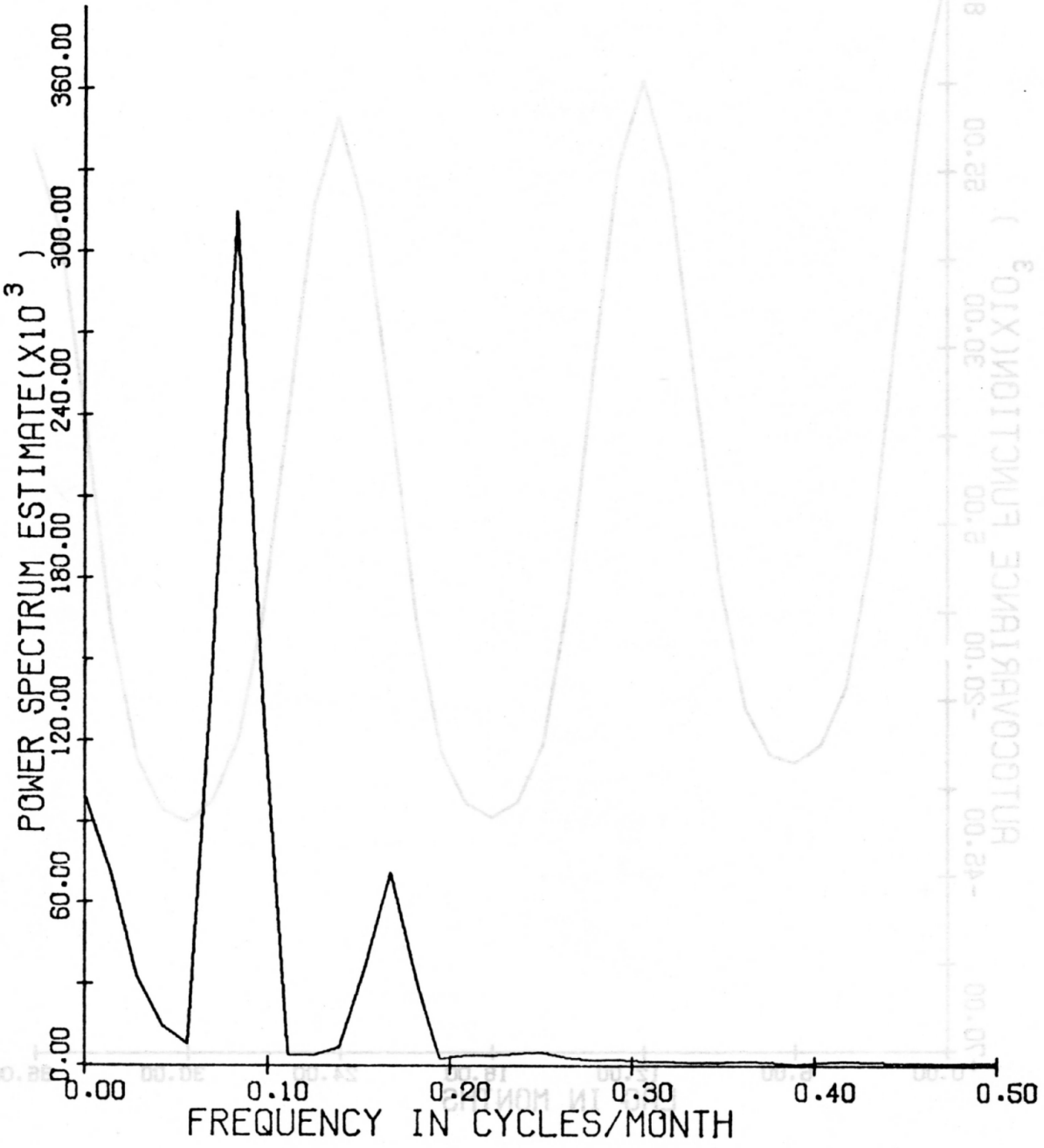

Figure B-2. Power spectrum of Grand Canyon time series (1941-70).

REFERENCES

Anderson, E. R. and D. W. Pritchard. 1951. Physical Limnology of Lake Mead. Navy Electronics Laboratory Report 258.

Arnold, J. D. 1970. A Markovian Sampling Policy Applied to Water Quality Monitoring of Streams. Biometrics. December 1970. pp. 739-747.

Blackman, R. B. and J. W. Tukey. 1958. The Measurement of Power Spectra. Dover, New York, New York.

Dixon, W. J., ed. 1970. Biomedical Computer Programs. University of California Publications in Automatic Computations, No. 2, University of California Press.

Everett, L. G. 1971. Cause-Effect Analysis of Las Vegas Wash Effluent. Submitted as report in Hydrology 343, The University of Arizona.

Harbeck, G. E., Jr., M. A. Kohler, G. E. Koberg, and others. 1958. Water-Loss Investigations: Lake Mead Studies. Geological Survey Professional Paper 298, U.S. Department of the Interior.

Jenkins, G. M. and D. G. Watts. 1968. Spectral Analysis and ts Applications. Holden-Day, Inc., San Francisco.

Kisiel, C. C. and L. Duckstein. 1971. Time and Frequency-Domain Identification of a Causal Bivariate Stochastic Process. Proceedings of International Symposium on Mathematical Models in Hydrology, Warsaw.

Qashu, H. K. and L. G. Everett. 1971. Micronutrients and Biological Patterns in Lake Mead. Final Report to Contract 14-06-300-2210 between U.S. Department of the Interior, Bureau of Reclamation and The University of Arizona.

Qashu, H. K., L. G. Everett, and R. D. Staker. 1971. A Chemical and Biological Study of the Colorado River-Grand Canyon Section, Report No. II. Submitted to National Park Service.

Smith, W. O., C. P. Vetter, G. B. Cummings, and others. 1954. Lake Mead Comprehensive Survey of 1948-49, Volume III. U.S. Department of the Interior and U.S. Department of the Navy.

Sterling, T. D. and S. V. Pollack. 1968. Introduction to Statistical Data Processing. Prentice-Hall.

U.S. Department of the Interior. 1971. Quality of Water--Colorado River Basin, Progress Report No. 5.

U.S. Environmental Protection Agency, Regions VIII and IX. 1971. The Mineral Quality Problem in the Colorado River Basin.

U.S. Geological Survey. 1964-71. Water Resources for Arizona, Part 2, Water Quality Records.

Wastler, T. A. 1969. Spectral Analysis--Applications in Water Pollution Control. FWPCA, Department of the Interior.

Water Quality of Colorado River at Lee Ferry, Grand Canyon, and Lake Havasu; and Related Hydrology. 1971. Chart prepared by the Hydrographic Engineering Branch of the Metropolitan Water District of Southern California, Los Angeles, California.